

Automatic regenerative simulation via non-reversible simulated tempering

Miguel Biron-Lattes Trevor Campbell

Alexandre Bouchard-Côté
Department of Statistics, University of British Columbia

January 26, 2024

Abstract

Simulated Tempering (ST) is an MCMC algorithm for complex target distributions that operates on a path between the target and a more amenable reference distribution. Crucially, if the reference enables i.i.d. sampling, ST is *regenerative* and can be parallelized across independent tours. However, the difficulty of tuning ST has hindered its widespread adoption. In this work, we develop a simple *nonreversible* ST (NRST) algorithm, a general theoretical analysis of ST, and an automated tuning procedure for ST. A core contribution that arises from the analysis is a novel performance metric—*Tour Effectiveness (TE)*—that controls the asymptotic variance of estimates from ST for bounded test functions. We use the TE to show that NRST dominates its reversible counterpart. We then develop an automated tuning procedure for NRST algorithms that targets the TE while minimizing computational cost. This procedure enables straightforward integration of NRST into existing probabilistic programming languages. We provide extensive experimental evidence that our tuning scheme improves the performance and robustness of NRST algorithms on a diverse set of probabilistic models.

1 Introduction

Regenerative Markov chain Monte Carlo (MCMC) is an approach to MCMC that splits the Markov chain into independent tours at *regeneration times*—steps at which the state of the chain is independent of the previous (see [Ripley, 1987](#), §6.4). There are two important advantages to regenerative

simulation: 1) computation can be trivially parallelized by running tours concurrently, and 2) it enables straightforward estimation of Monte Carlo error based on the fact that the tours are i.i.d.; indeed, regenerative MCMC is one of few ways to obtain an “honest” estimate (Jones and Hobert, 2001). Despite the benefits of regenerative MCMC, several practical difficulties have prevented its widespread adoption. First, existing methods typically require model-specific mathematical derivations to identify regeneration times. For example, many methods rely on minorization conditions on the transition kernel of the Markov chain (Mykland et al., 1995; Hobert et al., 2002), which must be derived on a case-by-case and are often difficult to obtain (Jones and Hobert, 2001). Some other approaches avoid model-specific derivations, both in the discrete time setting (Brockwell and Kadane, 2005; Minh et al., 2012; Nguyen, 2017; Douc et al., 2022), and more recently using Markov processes (Wang et al., 2021; McKimm et al., 2022), but still are not at the stage where they can be used in an automatic fashion.

The starting point of this paper is the observation that Simulated Tempering (ST) (Geyer and Thompson, 1995) can be used to automate regenerative MCMC in a large class of probabilistic programs such as BUGS (Lunn et al., 2000) and Stan (Stan Development Team, 2023) (details in Section 8.2). Given a path between a reference distribution and a target distribution of interest, ST builds an augmented Markov chain jointly on the original variable and the position along the path. As long as the reference enables i.i.d. simulation, the steps at which the sampler visits this distribution are regeneration times by construction. Past studies on ST—including recent *non-reversible* variants (Sakai and Hukushima, 2016a; Faizi et al., 2020)—have not leveraged this property. Although ST enables automated regenerative MCMC, it is not without its own drawbacks; in particular, it is difficult to tune robustly (see e.g. Mitsutake and Okamoto, 2000; Park and Pande, 2007).

In this work, we introduce several key contributions to fully realize the potential of ST as an automated regenerative MCMC method:

1. A simple non-reversible ST algorithm based on the *lifting approach* (Chen et al., 1999).
2. A diagnostic—*Tour Effectiveness (TE)*—that characterizes the performance of ST as a number between 0 and 1. In contrast to the typical MCMC notion of Effective Sample Size (ESS), the tour effectiveness can be computed without making reference to a specific test function. From the user’s point of view, TE has a “look and feel” akin to relative ESS in Sequential Monte Carlo (SMC).
3. A novel idealized model of ST algorithms that elucidates the relationship

between TE and tuning parameters of the algorithm. The model also leads to an extension of the *communication barrier*—originally developed for Parallel Tempering (Syed et al., 2022)—to ST algorithms. We show that the magnitude of the barrier is inversely related to TE.

4. A novel automated ST adaptation algorithm aimed at maximizing TE while minimizing cost, based on the aforementioned relationship between TE and tuning parameters. This tuning scheme has no free hyper-parameters and handles a wide range of problems.

We emphasize that these contributions exploit the regeneration structure of ST, which allows us to define a generic performance metric, the tour effectiveness, and then to optimize it and to formulate tuning recommendations. After these developments, we provide a variety of experiments demonstrating that our tuning procedure delivers substantial gains in efficiency for multiple reversible and non-reversible ST algorithms. Finally, we discuss the implementation of NRST in Probabilistic Programming Languages (PPLs), and provide guidance on deploying NRST to distributed systems.

2 Background

2.1 Regenerative Markov chain Monte Carlo

Markov chain Monte Carlo (MCMC) (e.g. Robert and Casella, 2004) is a standard tool for approximating integrals under an intractable probability distribution π of interest. Under certain conditions, sequentially simulating a path $\{x_n\}_{n \in \mathbb{Z}_+}$ of a Markov chain with invariant distribution π allows us to consistently estimate the expectation $\pi(h)$ of a real-valued function h via ergodic averages $m_S := \frac{1}{S} \sum_{n=0}^{S-1} h(x_n)$. In practice, however, the simulation must stop at a finite S , and assessing the *Monte Carlo error* of m_S becomes important (Flegal et al., 2008). Under further conditions (e.g. Hobert et al., 2002, Thm. 1), this error is captured by a Central Limit Theorem (CLT) $\sqrt{S}(m_S - \pi(h)) \xrightarrow{d} \mathcal{N}(0, \gamma_s^2)$, where γ_s^2 is known as the *asymptotic variance* of m_S . If a consistent estimator of γ_s is available, it is possible to construct asymptotic confidence intervals for the Monte Carlo error. This classical approach to MCMC has two important drawbacks. First, even when the conditions for the CLT hold, designing a consistent estimator for γ_s is challenging (Jones and Hobert, 2001). Second, since the Markov chain proceeds sequentially in time, it is difficult to leverage the parallelism offered by current systems (Wilkinson, 2005).

Regenerative MCMC (Mykland et al., 1995) is an alternative approach

that naturally leverages massively parallel computation and yields straightforward estimates of Monte Carlo error. Roughly, a Markov chain is regenerative if there exist stopping times $0 = r_0 < r_1 < r_2 < \dots$ with $r_k \uparrow \infty$, such that for every $k \in \mathbb{N}$, the process after r_k is independent of its past. These *regeneration times* can be used to split the sample path of the process into disjoint *tours* $x^{(k)} := \{x_n\}_{n=r_{k-1}}^{r_k-1}$, for all $k \in \mathbb{N}$. As the tours are i.i.d., they can trivially be simulated concurrently (Fishman, 1983). And at time r_k ,

$$m_{r_k} = \frac{1}{r_k} \sum_{n=0}^{r_k-1} h(x_n) = \frac{\sum_{j=1}^k s_j}{\sum_{j=1}^k \tau_j},$$

where $\tau_k := r_k - r_{k-1}$ is the length of the k -th tour, and $s_k := \sum_{n=r_{k-1}}^{r_k-1} h(x_n)$. Since $r_k \uparrow \infty$, it holds that $m_{r_k} \xrightarrow{\text{a.s.}} \pi(h)$ as $k \rightarrow \infty$. Under further conditions, the independence of the tours can be used to leverage the CLT for i.i.d. random variables to show that

$$\gamma_r^2 := \frac{\mathbb{E}[(s_1 - \tau_1 \pi(h))^2]}{\mathbb{E}[\tau_1]^2}, \quad \sqrt{k}(m_{r_k} - \pi(h)) \xrightarrow{d} \mathcal{N}(0, \gamma_r^2), \quad k \rightarrow \infty.$$

In contrast to the standard serial implementation of MCMC, γ_r^2 admits a simple and consistent estimator.

The main drawback of regenerative MCMC is the fact that finding regeneration times for Markov chains on arbitrary spaces is not straightforward. Mykland et al. (1995) provided the first attempt, exploiting the splitting technique (Nummelin, 1978) to introduce regeneration when a small set is known to exist. But finding small sets is a challenging task in general. Since then, several alternative procedures to induce regeneration in general Markov chains have been proposed (Sahu and Zhigljavsky, 2003; Brockwell and Kadane, 2005; Minh et al., 2012; Nguyen, 2017; Douc et al., 2022). In the present work, we focus on a design of Simulated Tempering (ST) Geyer and Thompson (1995) that admits regenerative structure.

2.2 Simulated tempering

Let \mathcal{X} be a set, and let π_0 be a *reference distribution* on \mathcal{X} for which i.i.d. sampling is tractable. Assume that π_0 has a density with respect to a base measure dx on \mathcal{X} ; we overload notation so that π_0 also refers to this density. Let π be a *target distribution* on \mathcal{X} with density

$$\pi(x) := \frac{\pi_0(x)e^{-V(x)}}{\mathcal{Z}}, \quad \mathcal{Z} := \int \pi_0(x)e^{-V(x)}dx < \infty. \quad (1)$$

Simulated tempering (Lyubartsev et al., 1992; Marinari and Parisi, 1992; Geyer and Thompson, 1995) aims to produce Monte Carlo samples from π by leveraging the tractability of π_0 . It does so by connecting π_0 to π with a path of distributions, and then moving draws from π_0 along the path. A common choice is the path of *tempered distributions* defined by

$$\forall \beta \in [0, 1]: \pi^{(\beta)}(x) := \frac{\pi_0(x)e^{-\beta V(x)}}{\mathcal{Z}(\beta)}, \quad \mathcal{Z}(\beta) := \int \pi_0(x)e^{-\beta V(x)} dx, \quad (2)$$

where $\mathcal{Z}(\beta)$ is the normalization constant of $\pi^{(\beta)}$. These constants are finite (Lemma C.9) but the values $\mathcal{Z}(\beta)$ are usually unknown. For example, consider the case of a Bayesian model with prior density $\varpi(x)$ and likelihood $L(y|x)$ for fixed observation y . If ϖ is proper, we can set $\pi_0 = \varpi$ and $V(x) = -\log(L(y|x))$ in Eq. (2) to obtain a valid path from ϖ to the posterior density $\pi(x) \propto \varpi(x)L(y|x)$. Note that much of the ST literature suggests choosing $\pi_0 \equiv 1$ and $V(x) = -\log(\varpi(x)L(y|x))$ (e.g. Woodard et al., 2009), but this is a valid path only in the restrictive setting where the uniform measure on \mathcal{X} is finite, thus excluding many interesting statistical problems. Another benefit of the prior–posterior path is that it can be built automatically in many probabilistic programming languages with no additional user input (see Section 8.2).

We now discretize the path to obtain a sequence of distributions $\{\pi_i\}_{i=0}^N$ to be used in computation. For $N \in \mathbb{N} := \{1, 2, \dots\}$ and $0 = \beta_0 < \beta_1 < \dots < \beta_N = 1$, define $\mathcal{P} := \{\beta_i\}_{i=0}^N$ and the sequence $\{\pi_i\}_{i=0}^N$ by $\pi_i := \pi^{(\beta_i)}$ for $i \in \{0, \dots, N\}$. ST builds a Markov chain $\{x_n, i_n\}_{n \in \mathbb{Z}_+}$ on the product space $\mathcal{X} \times \{0, \dots, N\}$ with invariant density

$$\pi_{\text{st}}(x, i) := p_i \pi_i(x), \quad (3)$$

where $\{p_i\}_{i=0}^N$ is the marginal distribution of the i component, and the conditional distribution of x given i is precisely π_i . The state of the Markov chain defined by ST is updated by alternating *exploration* and *tempering* steps. During exploration, i is fixed, so only the x component is updated. If $i = 0$, a new state $x' \sim \pi_0$ is drawn independently from the reference distribution. Otherwise, x is updated via $x'|x, i \sim K_i(x, \cdot)$, where $\{K_i\}_{i=1}^N$ is a collection of Markov kernels on \mathcal{X} such that each K_i is π_i -irreducible and π_i -invariant (e.g. Gibbs, HMC, etc). The tempering step, on the other hand, fixes x and proposes a move $i \rightarrow i'$ with a Metropolis–Hastings correction. If the proposal is symmetric, then the move is accepted with probability

$$\alpha_{i,i'}(x) = \min \left\{ 1, \frac{\pi_{i'}(x) p_{i'}}{\pi_i(x) p_i} \right\} = e^{-\max\{0, (\beta_{i'} - \beta_i)V(x) - (c_{i'} - c_i)\}}, \quad (4)$$

where $\mathcal{C} := \{c_i\}_{i=0}^N$ is a collection of real-valued tuning parameters—the *level affinities*—that are related to the p_i via

$$\forall i \in \{0, \dots, N\} : \quad p_i := \frac{\mathcal{Z}(\beta_i)e^{c_i}}{\sum_{j=0}^N \mathcal{Z}(\beta_j)e^{c_j}}. \quad (5)$$

This relationship between c_i and p_i has the effect of canceling the $\mathcal{Z}(\beta_i)$ in π_i that would otherwise appear in the Metropolis–Hastings ratio. Thus, $\alpha_{i,i'}(x)$ can be evaluated *without knowing the normalizing constants*.

As highlighted by [Geyer and Thompson \(1995\)](#), the i.i.d. draws from π_0 induce regeneration in ST: whenever the chain visits $\mathcal{X} \times \{0\}$, the next state is drawn independently of the previous one. Sets with this property are called *atoms* ([Douc et al., 2018](#), Def. 6.1.1). Indeed, if $\{t_k\}_{k \in \mathbb{N}}$ denote the times at which the chain is in the atom, then the stopping times $r_k := t_k + 1$ are regeneration times. Hence, ST allows regenerative simulation.

3 Methodology

3.1 Non-reversible simulated tempering

The effectiveness of simulated tempering can be hindered if moving between the boundaries $i = 0$ and $i = N$ is difficult. Indeed if, starting from $i = 0$, the chain returns to this level before visiting $i = N$, the tour produces no sample from the target, resulting in wasted effort. Similarly if the chain never returns to $i = 0$, then regenerations never occur. The original versions of ST have been found to exhibit this problem due to the reversibility of the tempering step ([Sakai and Hukushima, 2016a](#); [Faizi et al., 2020](#), see Section 6 for a discussion of these methods).

We therefore opt for a *non-reversible* simulated tempering method (NRST), using lifting ([Chen et al., 1999](#)) to induce momentum in the tempering dynamics and thus reduce undesirable random walk behavior. Concretely, we augment the Markov chain state $\tilde{x} := (x, i, \epsilon)$ to be in the product space

$$\tilde{\mathcal{X}} := \mathcal{X} \times \{0, \dots, N\} \times \{-1, +1\}. \quad (6)$$

The ϵ component represents the current direction of movement along $\{0, \dots, N\}$. Indeed, the new tempering step makes a deterministic proposal to move the i index one unit along the current ϵ direction; i.e., $i_{\text{prop}} = i + \epsilon$. If $i_{\text{prop}} \notin \{0, \dots, N\}$, the proposal is immediately rejected. Otherwise, it is accepted with probability $\alpha_{i, i_{\text{prop}}}(x)$, as defined in Eq. (4). If the tempering

step is rejected, the direction is reversed $\epsilon \leftarrow -\epsilon$. After tempering, NRST uses an exploration step identical to the one in simulated tempering.

In Appendix A.2 we show pseudo-code for a function that performs a full NRST step (Algorithm 2). We also detail how this function is used to run a complete NRST tour (Algorithm 3). Both the exploration and the tempering steps are invariant (Proposition C.1) with respect to the *lifted* distribution $\tilde{\pi}$ with density

$$\forall \tilde{x} \in \tilde{\mathcal{X}} : \tilde{\pi}(\tilde{x}, i, \epsilon) := \frac{1}{2} p_i \pi_i(x),$$

where $\{p_i\}_{i=0}^N$ are as in Eq. (5). As in ST, the conditional distribution of x given i (marginalizing ϵ) under $\tilde{\pi}$ is π_i . Indeed, it is not difficult to show that

$$\pi(h) = \frac{\tilde{\pi}(h(x)\mathbb{1}\{i = N\})}{\tilde{\pi}(\mathbb{1}\{i = N\})}.$$

for any $h : \mathcal{X} \rightarrow \mathbb{R}$. Moreover, NRST preserves the regenerative structure of ST: consider $\mathcal{A} := \mathcal{X} \times \{0\} \times \{-1\}$, and note that starting from any $\tilde{x} \in \mathcal{A}$, the law of the next state \tilde{x}' is

$$\nu(\tilde{x}') := \pi_0(x')\mathbb{1}\{i' = 0, \epsilon' = +1\}. \quad (7)$$

Hence, \mathcal{A} is an atom with regeneration measure ν . We use \mathbb{P}_ν to denote the law of the Markov chain with initial distribution ν , and use \mathbb{E}_ν for corresponding expectations.

The presence of the atom allows us to use the machinery of regenerative simulation to build a consistent estimator of $\pi(h)$. To this end, define the sequence of times at which the chain visits \mathcal{A} by setting $T_0 := -1$ and recursively defining

$$\forall k \in \mathbb{N} : T_k := \inf\{n > T_{k-1} : \tilde{x}_n \in \mathcal{A}\}.$$

Furthermore, for any function $f : \tilde{\mathcal{X}} \rightarrow \mathbb{R}$, define the *tour sums* of f

$$\forall k \in \mathbb{N} : s_k(f) := \sum_{n=T_{k-1}+1}^{T_k} f(\tilde{x}_n).$$

Under \mathbb{P}_ν , $\{s_k(f)\}_{k \in \mathbb{N}}$ are i.i.d. (Lemma C.5), $s_j(\mathbb{1}\{i = N\})$ is the number of visits to the top level during the j -th tour, and the length of the k -th tour is $\tau_k := s_k(1) = T_k - T_{k-1}$. Finally, let $\hat{R}_k(h)$ be an estimator of $\pi(h)$ given by

$$\hat{R}_k(h) := \frac{\sum_{j=1}^k s_j(h(x)\mathbb{1}\{i = N\})}{\sum_{j=1}^k s_j(\mathbb{1}\{i = N\})}. \quad (8)$$

$\widehat{R}_k(h)$ is consistent due to the Law of Large Numbers (LLN) for the lifted chain (Theorem 3.1). This is a known result (Thm. 6.6.2 Douc et al., 2018), but we reproduce it here for convenience (proof in Appendix C). Let $s(f)$ and τ be independent copies of $s_k(f)$ and τ_k .

Theorem 3.1. *For any $f : \widetilde{\mathcal{X}} \rightarrow \mathbb{R}$ such that $\widetilde{\pi}(|f|) < \infty$,*

$$\mathbb{E}_\nu[s(f)] = \mathbb{E}_\nu[\tau] \widetilde{\pi}(f) = \frac{2}{p_0} \widetilde{\pi}(f). \quad (9)$$

Moreover, if $g : \widetilde{\mathcal{X}} \rightarrow \mathbb{R}$ satisfies $\widetilde{\pi}(|g|) < \infty$ and $\widetilde{\pi}(g) \neq 0$, then

$$\lim_{k \rightarrow \infty} \frac{\sum_{j=1}^k s_j(f)}{\sum_{j=1}^k s_j(g)} = \frac{\mathbb{E}_\nu[s(f)]}{\mathbb{E}_\nu[s(g)]} = \frac{\widetilde{\pi}(f)}{\widetilde{\pi}(g)}, \quad \mathbb{P}_\nu\text{-a.s.}$$

Using $f(\tilde{x}) := h(x)\mathbf{1}\{i = N\}$ and $g(\tilde{x}) := \mathbf{1}\{i = N\}$ in Theorem 3.1 shows that $\widehat{R}(h)$ is a consistent estimator of $\pi(h)$. Beyond consistency, a central limit theorem (Theorem 3.2) holds for $\widehat{R}(h)$. This result is equivalent to the one given in Geyer and Thompson (1995) for ST, but we reproduce it here for convenience (proof in Appendix C).

Theorem 3.2. *Let $h : \mathcal{X} \rightarrow \mathbb{R}$ be a function with $\pi(|h|) < \infty$, and define*

$$\sigma(h)^2 := \frac{\mathbb{E}_\nu \left[s(\mathbf{1}\{i = N\})(h(x) - \pi(h))^2 \right]}{\mathbb{E}_\nu[s(\mathbf{1}\{i = N\})]^2}. \quad (10)$$

If $\sigma(h)^2 < \infty$, then $\sqrt{k} \left(\widehat{R}_k(h) - \pi(h) \right) \xrightarrow{d} \mathcal{N}(0, \sigma(h)^2)$ as $k \rightarrow \infty$.

The variance $\sigma(h)^2$ can be estimated directly from the output of the regenerative simulation; indeed, by Theorem 3.1,

$$\widehat{\sigma(h)^2}_k := \frac{k \sum_{j=1}^k s_j \left(\mathbf{1}\{i = N\} (h(x) - \widehat{R}_k(h)) \right)^2}{\left(\sum_{j=1}^k s_j(\mathbf{1}\{i = N\}) \right)^2}$$

is a consistent estimator of $\sigma(h)^2$. Then, an asymptotically valid α -confidence interval may be constructed for $\alpha \in (0, 1)$, such that

$$\mathbb{P}_\nu \left(\left| \widehat{R}_k(h) - \pi(h) \right| \leq \frac{\widehat{\sigma(h)^2}_k}{\sqrt{k}} z_\alpha \right) \xrightarrow{k \rightarrow \infty} \alpha, \quad z_\alpha := \Phi^{-1}((1 + \alpha)/2),$$

with Φ^{-1} the quantile function of a standard normal distribution.

3.2 Tour effectiveness

The asymptotic variance estimate $\widehat{\sigma(h)}_k^2$ depends on h in general; but for bounded test functions $|h| \leq 1$, we can uniformly bound $|h(x) - \widehat{R}_k(h)|$ and obtain a diagnostic for simulated tempering performance that we call the *estimated tour effectiveness*,

$$\widehat{\text{TE}} := \frac{\left(\sum_{j=1}^k s_j(\mathbf{1}\{i = N\})\right)^2}{k \sum_{j=1}^k s_j(\mathbf{1}\{i = N\})^2}. \quad (11)$$

The $\widehat{\text{TE}}$ diagnostic is a number between 0 and 1, and applies to any ST algorithm. A higher $\widehat{\text{TE}}$ indicates more efficient motion of the Markov chain along the path from the reference π_0 to the target π . Note that unlike the typical effective sample size (ESS) for MCMC algorithms, $\widehat{\text{TE}}$ does not require the choice of a test function h . $\widehat{\text{TE}}$ is more akin to the relative effective sample size (rESS) from sequential Monte Carlo (SMC) (Liu and Chen, 1995): both diagnostics exist in $[0, 1]$ and are defined in terms of ratios of the first and second moments of a nonnegative “weight” (a density ratio for rESS, and a number of target visits for $\widehat{\text{TE}}$). We will provide a more in-depth analysis of tour effectiveness in Section 4.

For any confidence level α and tolerance $\delta > 0$, we can estimate the minimum number of tours K_{\min} required to obtain an approximate α -confidence interval of half-width less than δ for all functions $|h| \leq 1$ by setting

$$K_{\min}(\alpha, \delta, \widehat{\text{TE}}) := \left\lceil \frac{4}{\widehat{\text{TE}}} \left(\frac{z_\alpha}{\delta}\right)^2 \right\rceil. \quad (12)$$

Algorithm 4 (Appendix A.2) describes how this method is used to run a parallel regenerative simulation of NRST. Of course, after obtaining the results, it is possible to produce tighter intervals by computing $\widehat{\sigma(h)}^2$ for each function of interest.

4 Theoretical analysis

4.1 The index process

We now analyze tour effectiveness and use it to characterize the performance of NRST and traditional ST. To begin, note that $\widehat{\text{TE}}$ depends only on the tempering indices, and can be computed without knowing the values of the state x . Therefore, we focus the analysis on the *index process* $\{(i_n, \epsilon_n)\}_{n \in \mathbb{Z}_+}$.

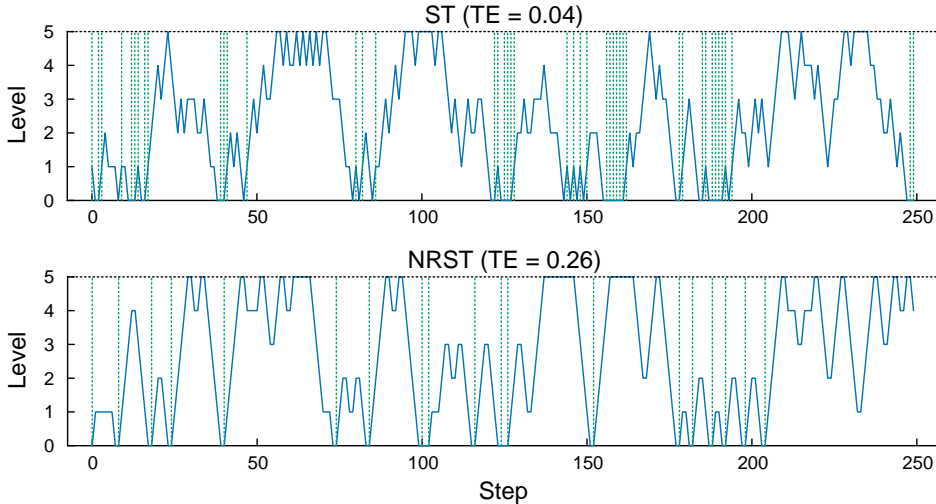


Figure 1: First 250 steps of the index processes of ST and NRST applied to a toy problem, using the same grid ($N = 6$), level affinities, and stream of pseudo-random numbers on both algorithms. The start of each tour is marked by vertical dotted lines.

Fig. 1 shows a realization of the index process for both ST and NRST applied to a toy problem (see Appendix B.1). Both algorithms use the same grid, level affinities, and pseudo-random stream. Regenerations are indicated by a vertical dotted line. Fig. 1 shows a stark difference between ST and NRST: while NRST produces tours that travel quickly between the reference and target, ST produces meandering tours that inflate the variance of Monte Carlo estimators. This difference appears in the $\widehat{\text{TE}}$ values.

Alas, studying the index process itself is hard, because it is *not* a Markov chain in general. However, the tempering step depends only on x via $V(x)$; so in cases where the exploration kernels are efficient enough that $V(x)$ appears to be i.i.d., the index process becomes Markovian. The following idealized assumption describes this condition precisely.

Assumption 4.1. *For $i \in \{1, \dots, N\}$, let $K_i(x, dv')$ be the distribution of $V(x')$ conditional on the current state $x \in \mathcal{X}$, where K_i is the i -th exploration kernel and x' is the state after exploration. There exists a probability distribution q_i on \mathbb{R} such that $K_i(x, dv') = q_i(dv')$, for π -almost all x .*

Assumption 4.1 requires that $V(x_n)$ “mixes perfectly” in one exploration step. Note that this is *not* the same as the stronger requirement that x_n itself does so during exploration (the latter would defy the point of using ST). Assumption 4.1 can be thought of as a *model*, i.e., a simplifying framework

that is not expected to hold exactly in real scenarios. However this model is *useful* in the sense that we obtain approximations allowing us to derive an adaptation scheme (Algorithm 1) that performs robustly across a variety of models—even when Assumption 4.1 does not exactly hold. For this reason, our experiments (Section 7) focus on real target distributions in which Assumption 4.1 is not satisfied. See Section 5.6 for a discussion on how one can enforce Assumption 4.1 and the practical effects of doing so. Related performance models have been used to analyze parallel tempering; see Syed et al. (2022, Sec. 3.3) for empirical examples where $V(x_n)$ mixes well but x_n does not.

We characterize the Markov index process using the acceptance and rejection probabilities under π_i , and their symmetrized versions, given by

$$\begin{aligned}\alpha_{i,i+\epsilon} &:= \mathbb{E}^{(i)}[\alpha_{i,i+\epsilon}(x)], & \rho_{i,i+\epsilon} &:= 1 - \alpha_{i,i+\epsilon} \\ \alpha_i &:= (\alpha_{i,i-1} + \alpha_{i-1,i})/2, & \rho_i &:= 1 - \alpha_i.\end{aligned}\tag{13}$$

Proposition 4.2 describes the index process using these probabilities.

Proposition 4.2. *Under Assumption 4.1, the marginal distribution of the index process for both ST and NRST is a homogeneous Markov chain on $\{0, \dots, N\} \times \{-1, +1\}$, with invariant distribution $\tilde{\pi}(i, \epsilon) := p_i/2$. Moreover, the transition kernels for NRST and ST are:*

$$\begin{aligned}\mathbf{k}_{\text{NRST}}((i, \epsilon), (i', \epsilon')) &:= \alpha_{i,i+\epsilon} \mathbb{1}\{i' = i + \epsilon, \epsilon' = \epsilon\} + \rho_{i,i+\epsilon} \mathbb{1}\{i' = i, \epsilon' = -\epsilon\}, \\ \mathbf{k}_{\text{ST}}((i, \epsilon), (i', \epsilon')) &:= (\alpha_{i,i+\epsilon'} \mathbb{1}\{i' = i + \epsilon'\} + \rho_{i,i+\epsilon'} \mathbb{1}\{i' = i\})/2.\end{aligned}$$

4.2 The Tour Effectiveness diagnostic

The aim of this section is to rigorously analyze the tour effectiveness diagnostic introduced briefly in Section 3.2. Let $v_k = s_k(\mathbb{1}\{i = N\})$ be the number of visits to level N during the k^{th} tour, and v be an independent copy of v_k from \mathbb{P}_ν . Then we define the *tour effectiveness* (TE) of a generic simulated tempering sampler as

$$\text{TE} := \frac{\mathbb{E}_\nu[v]^2}{\mathbb{E}_\nu[v^2]}.$$

Intuitively, TE describes how easy it is for the process to move between the two endpoints of $\{0, \dots, N\}$. To see this, note first that $\text{TE} \in [0, 1]$, since $\mathbb{E}_\nu[v]^2 \leq \mathbb{E}_\nu[v^2]$. When $\text{TE} = 1$, the number of visits per tour to the top level is deterministic and equal to $2p_N/p_0$ (Eq. (9) with $f \equiv 1$). At the

opposite extreme, $\text{TE} = 0$ when v has infinite second moment. Note that, since $\{v_k\}_{k \in \mathbb{N}}$ is an i.i.d. collection, the statistic $\widehat{\text{TE}}$ introduced in Section 3.1 (Eq. (11)) is a consistent estimator of TE . Theorem 4.3 shows that TE controls the ST asymptotic variance $\sigma(h)^2$ from Eq. (10), and hence is a relevant diagnostic for simulated tempering.

Theorem 4.3. $\sup_{|h| \leq 1} \sigma(h)^2 \leq 4/\text{TE}$, and under Assumption 4.1, $\text{TE} > 0$.

Theorem 4.3 shows that the more *effective* the tours are—as measured by TE —the lower (a bound on) the asymptotic variance of Monte Carlo estimators for bounded functions will be. Furthermore, Theorem 4.3 states that under Assumption 4.1, this variance is always finite. This is not guaranteed in general, as $\sigma^2(h)$ can be infinite even for bounded h .

To further understand the role of TE as a diagnostic tool, we require a better grasp of its dependence on algorithm parameters. Whenever $c_i = -\log(\mathcal{Z}(\beta_i))$, the distribution over levels is uniform (see Eq. (5)), and the average rejection/acceptance probabilities become symmetric (Lemma C.7),

$$\forall i \in \{1, \dots, N\}: \rho_{i-1,i} = \rho_{i,i-1} = \rho_i \quad \text{and} \quad \alpha_{i-1,i} = \alpha_{i,i-1} = \alpha_i. \quad (14)$$

In this setting, Theorem 4.4 provides an expression for TE in terms of the rejection probabilities (proof in Appendix C).

Theorem 4.4. Under Assumption 4.1, if $\{p_i\}_{i=0}^N$ is uniform, then the TE for NRST, TE_{NRST} , and the TE for reversible ST, TE_{ST} , satisfy

$$\text{TE}_{\text{NRST}} = \frac{1}{1 + 2 \sum_{i=1}^N \frac{\rho_i}{1-\rho_i}} > \frac{1}{4N - 1 + 4 \sum_{i=1}^N \frac{\rho_i}{1-\rho_i}} = \text{TE}_{\text{ST}}.$$

Given uniform levels and Assumption 4.1, Theorem 4.4 shows that NRST will produce more effective tours than ST, and that the difference increases as the size of the grid N grows. Additionally, Theorem 4.4 shows that TE depends on the grid \mathcal{P} only through the quantity $\sum_{i=1}^N \frac{\rho_i}{1-\rho_i}$.

4.3 Limit of infinite temperatures

Motivated by the link between TE and the rejection probabilities, we now analyze the limiting behavior of these quantities for NRST, in the hypothetical case where the grid becomes increasingly fine; i.e., when we let $\|\mathcal{P}\| := \max\{\beta_i - \beta_{i-1} : i \in \{1, \dots, N\}\}$ go to zero. We will show that the optimal grid has a finite mesh size (Section 5.5), but the asymptotic results developed here provide the basis for approximations used as a stepping stone towards

these (approximate) optimality results. To proceed, let us extend Eq. (4) to arbitrary pairs $\beta, \beta' \in [0, 1]$,

$$\alpha_{\beta, \beta'}(x) := \exp\left(-\max\left\{0, (\beta' - \beta)V(x) - [c(\beta') - c(\beta)]\right\}\right), \quad (15)$$

where $c : [0, 1] \rightarrow \mathbb{R}$ is the *affinity function*, which extends the level affinities to a continuum by setting $c_i = c(\beta_i)$. Eq. (15) induces an extension of the average acceptance and rejection probabilities (c.f. Eq. (13)), i.e., $\alpha_{\beta, \beta'} := \mathbb{E}^{(\beta)}[\alpha_{\beta, \beta'}(x)]$ and $\rho_{\beta, \beta'} := 1 - \alpha_{\beta, \beta'}$. Theorem 4.7 gives a second order approximation of the rejection probabilities between two close grid points. Let us write $V = V(x)$ and $V \sim \pi^{(\beta)}$ whenever $x \sim \pi^{(\beta)}$.

Assumption 4.5. $c(\cdot)$ is thrice continuously differentiable on $(0, 1)$.

Assumption 4.6. For all $\beta, \beta' \in (0, 1)$, $\beta \neq \beta'$, $\pi_0\left\{V = \frac{c(\beta') - c(\beta)}{\beta' - \beta}\right\} = 0$.

Theorem 4.7. Under Assumptions 4.5 and 4.6, for $0 < \beta < \beta' < 1$, $\Delta\beta := \beta' - \beta$ and $\bar{\beta} := (\beta + \beta')/2$,

$$\begin{aligned} \rho_{\beta, \beta'} &= \mathbb{E}^{(\bar{\beta})}[\max\{0, V - c'(\bar{\beta})\}]\Delta\beta - \frac{1}{2}\mathbb{E}^{(\bar{\beta})}[V - c'(\bar{\beta})]\mathbb{E}^{(\bar{\beta})}[\max\{0, V - c'(\bar{\beta})\}]\Delta\beta^2 + o(\Delta\beta^2) \\ \rho_{\beta', \beta} &= -\mathbb{E}^{(\bar{\beta})}[\min\{0, V - c'(\bar{\beta})\}]\Delta\beta - \frac{1}{2}\mathbb{E}^{(\bar{\beta})}[V - c'(\bar{\beta})]\mathbb{E}^{(\bar{\beta})}[\min\{0, V - c'(\bar{\beta})\}]\Delta\beta^2 + o(\Delta\beta^2). \end{aligned}$$

In the special case where the affinity function satisfies $c'(\beta) = \mathbb{E}^{(\beta)}[V]$, the second order error vanishes. This mimics the result obtained by Predescu et al. (2004) for parallel tempering. To better understand the implications of different choices of affinity functions, we will focus on first-order effects. To this end, define the *directional rates of rejection* as

$$\forall \beta \in (0, 1) : \rho'_+(\beta) := \lim_{\Delta\beta \downarrow 0} \frac{\rho_{\beta, \beta + \Delta\beta}}{\Delta\beta}, \quad \rho'_-(\beta) := \lim_{\Delta\beta \downarrow 0} \frac{\rho_{\beta, \beta - \Delta\beta}}{\Delta\beta}.$$

Furthermore, let the *rate of rejection* be the average of the directional rates; i.e., $\rho'(\beta) := (\rho'_+(\beta) + \rho'_-(\beta))/2$. The following result is a direct consequence of Theorem 4.7.

Corollary 4.8. Under Assumptions 4.5 and 4.6, for all $\beta \in (0, 1)$,

$$\rho'_+(\beta) := \mathbb{E}^{(\beta)}[\max\{0, V - c'(\beta)\}], \quad \rho'_-(\beta) := -\mathbb{E}^{(\beta)}[\min\{0, V - c'(\beta)\}].$$

It follows that the rejection rate is

$$\rho'(\beta) = \frac{1}{2}\mathbb{E}^{(\beta)}[|V - c'(\beta)|], \quad (16)$$

while the difference in directional rates is

$$\rho'_+(\beta) - \rho'_-(\beta) = \mathbb{E}^{(\beta)}[V] - c'(\beta). \quad (17)$$

Corollary 4.8 lets us analyze the behavior of the rejection rates given the affinity function c . We discuss two important cases. Since constants shifts in c are irrelevant, we assume without loss of generality that $c(0) = 0$.

Assumption 4.9 (Mean energy affinity). *The affinity function satisfies*

$$\forall \beta \in [0, 1] : c(\beta) = \int_0^\beta \mathbb{E}^{(\beta')} [V] d\beta'. \quad (18)$$

Differentiating the affinity function in Eq. (18) shows that $c'(\beta) = \mathbb{E}^{(\beta)} [V]$. Thus the directional rates are identical by Eq. (17). Moreover, using the thermodynamic identity (see Gelman and Meng, 1998, and Corollary C.12) $\log(\mathcal{Z}(\beta)) = -\int_0^\beta \mathbb{E}^{(\beta')} [V] d\beta'$, we see that

$$c(\beta) = -\log(\mathcal{Z}(\beta)). \quad (19)$$

Thus this choice of level affinities results in a uniform distribution over levels with symmetric rejections; the equality of the directional rates is the infinitesimal counterpart of Eq. (14). Furthermore, since $\mathcal{Z} \in \mathcal{C}^\infty((0, 1))$ (see Lemma C.11), the representation in Eq. (19) shows that this choice of affinity function is $\mathcal{C}^\infty((0, 1))$ too, and thus satisfies Assumption 4.5. Substituting c into Eq. (16), the rate of rejections is

$$\rho'(\beta) = \frac{1}{2} \mathbb{E}^{(\beta)} \left[\left| V - \mathbb{E}^{(\beta)}[V] \right| \right].$$

Compare this quantity to the corresponding rate for non-reversible parallel tempering, the *local communication barrier*, defined as (Syed et al., 2022)

$$\lambda(\beta) := \frac{1}{2} \mathbb{E}^{(\beta)} \left[|V - V'| \right],$$

where V' is an independent copy of V defined on the same probability space. Lemma C.17 shows that rejections should be lower for NRST (but not less than half).

Assumption 4.10 (Minimum rejection affinity). *Let $\text{med}^{(\beta)}(V)$ be a median of V under $\pi^{(\beta)}$. Then, the affinity function satisfies*

$$\forall \beta \in [0, 1] : c(\beta) = \int_0^\beta \text{med}^{(\beta')} (V) d\beta'. \quad (20)$$

Differentiating the affinity function in Eq. (20) shows that

$$\frac{dc}{d\beta}(\beta) = \text{med}^{(\beta)}(V). \quad (21)$$

Since $\text{med}^{(\beta)}(V)$ minimizes the absolute deviation of V , this choice of c function minimizes the rejection rate. Its value becomes

$$\rho'(\beta) = \frac{1}{2} \mathbb{E}^{(\beta)} \left[\left| V - \text{med}^{(\beta)}(V) \right| \right] \leq \frac{1}{2} \mathbb{E}^{(\beta)} \left[\left| V - \mathbb{E}^{(\beta)}[V] \right| \right],$$

where the inequality is due to the optimality of the median. Using Eq. (21) in Eq. (17) shows that the directional rates of rejection do not agree; their difference equals the difference between the mean and the median of V under $\pi^{(\beta)}$. Finally, integrating Eq. (21) and using the thermodynamic identity, the pseudo-prior corresponding to this choice of c is

$$p_i \propto \exp(\log(\mathcal{Z}(\beta_i)) + c(\beta_i)) \propto \exp \left(- \int_0^{\beta_i} (\mathbb{E}^{(\beta)}[V] - \text{med}^{(\beta)}(V)) d\beta \right).$$

Again, the marginal probability of level i depends on the cumulative effect of the skewness of the distribution of V along the path.

The rates of rejection describe the *local* behavior of the sampler, measuring how difficult it is to move between two infinitesimally close levels. However, these rates are also helpful in studying the *global* behavior of the Markov chain, revealing how hard it is to transport i.i.d. samples from the reference towards the target measure through the path $\beta \mapsto \pi^{(\beta)}$. To this end, let us define the *tempering barrier function* as the cumulative rate of rejection $\Lambda(\beta) := \int_0^\beta \rho'(b) db$. Proposition 4.13 relates $\Lambda(\beta)$ and the symmetrized rejection rates.

Assumption 4.11. For $\beta \in \{0, 1\}$, $\mathbb{E}^{(\beta)}[V^2] < \infty$.

Assumption 4.12. There exist constants $\{\bar{c}_k\}_{k=0}^3$ such that

$$\forall k \in \{0, 1, 2\}, \forall \beta \in [0, 1] : \left| \frac{d^k c}{d\beta^k}(\beta) \right| \leq \bar{c}_k.$$

Proposition 4.13. Given Assumptions 4.5, 4.6, 4.11 and 4.12, define

$$\forall \beta \in [0, 1] : \ell(\beta) := \max\{i \in \{0, \dots, N\} : \beta_i \leq \beta\}.$$

Then, for all $\beta \in [0, 1]$,

$$\lim_{\|\mathcal{P}\| \rightarrow 0} \sum_{i=1}^{\ell(\beta)} \frac{\rho_i}{1 - \rho_i} = \lim_{\|\mathcal{P}\| \rightarrow 0} \sum_{i=1}^{\ell(\beta)} \rho_i = \Lambda(\beta). \quad (22)$$

Corollary 4.14 combines Proposition 4.13 and Theorem 4.4 to understand the asymptotic behavior of the tour effectiveness in terms of the *total tempering barrier* $\Lambda := \Lambda(1)$.

Corollary 4.14. *Under Assumptions 4.1, 4.6, 4.9, 4.11 and 4.12*

$$\text{TE}^\infty := \lim_{\|\mathcal{P}\| \rightarrow 0} \text{TE}_{\text{NRST}} = \frac{1}{1 + 2\Lambda}, \quad \lim_{\|\mathcal{P}\| \rightarrow 0} \text{TE}_{\text{ST}} = 0.$$

Corollary 4.14 states that as the tempering grid becomes finer, the NRST tour effectiveness converges to a positive value depending solely on the total tempering barrier. In contrast, the standard ST TE collapses to zero in the same limit. Furthermore, Corollary 4.14 establishes that, after precisely tuning level affinities and introducing sufficiently many grid points, the tour effectiveness of NRST is controlled by the difficulty of the problem, Λ , and the precise grid \mathcal{P} becomes irrelevant. This is similar to the fundamental limit to the asymptotic round trip rate imposed by the global communication barrier in NRPT (Syed et al., 2022).

5 Adaptation algorithms

Drawing on the insights from Section 4, we present an adaptation strategy that works well in a wide range of problems and requires no user input. We will first consider a fixed-size grid, and focus on the adaptation of grid points and level affinities. The procedure requires only a “dataset” $\mathbf{V} := \left\{ \{V_n^{(i)}\}_{n=1}^{S_i} : i \in \{0, \dots, N\} \right\}$, containing ergodic samples of $V \sim \pi^{(\beta)}$ for each $\beta \in \mathcal{P}$. One way to obtain \mathbf{V} is to bootstrap NRST with an arbitrary grid and level affinities. However, when the affinities are not well-tuned, we find that ST fails catastrophically and produces no draws of V for levels even just a few steps up from the reference. Another option is to simply run the exploration kernels $\{K_i\}_{i=1}^N$ independently in parallel at each grid point; however, such independent exploration does not produce high-quality V samples when the path of distributions is even slightly complex.

We recommend instead running non-reversible parallel tempering (NRPT) (Syed et al., 2022) to generate \mathbf{V} . Notably, this requires no additional evaluations of $V(x)$ compared with running the kernels individually, but often improves the quality of the dataset of potentials considerably. Algorithm 1 gives an overview of the adaptation process that is described in this section. At each iteration, NRPT is run with a doubling computational budget to construct \mathbf{V} , which then is used to adapt both the grid and the affinities. In turn, the improved grid should result in NRPT samples of higher quality on the next iteration.

Although NRPT is used to tune NRST, NRST has key advantages over NRPT once tuned. Indeed, parallelization in NRPT is tightly linked to the

Algorithm 1 Adaptation of grid and level affinities

```
function ADAPTRNST( $N, n_{\text{max-rounds}}$ )
   $\mathcal{P} \leftarrow \{\frac{i}{N} : i \in \{0, \dots, N\}\}$ 
   $n_{\text{scan}} \leftarrow 1$ 
  # Loop adaptation with doubling effort until convergence
  while  $n_{\text{scan}} < 2^{n_{\text{max-rounds}}}$  do
     $n_{\text{scan}} \leftarrow 2n_{\text{scan}}$ 
     $\mathbf{V} \leftarrow \text{RUNNRPT}(\mathcal{P}, n_{\text{scan}})$ 
     $\mathcal{C} \leftarrow \text{ADJUSTAFFINITIES}(\mathbf{V})$  ▷ Section 5.1
     $\hat{\Lambda} \leftarrow \text{BUILDBARRIERFUNCTION}(\mathcal{P}, \mathcal{C}, \mathbf{V})$  ▷ Eq. (23) in Section 5.2
     $\mathcal{P} \leftarrow \text{OPTIMIZEGRID}(\hat{\Lambda})$  ▷ Section 5.2
    if  $\text{HASCONVERGED}()$  then break ▷ Section 5.3
  # Tune the affinities for the final grid
   $\mathbf{V} \leftarrow \text{RUNNRPT}(\mathcal{P}, n_{\text{scan}})$ 
   $\mathcal{C} \leftarrow \text{ADJUSTAFFINITIES}(\mathbf{V})$ 
   $\hat{\Lambda} \leftarrow \text{BUILDBARRIERFUNCTION}(\mathcal{P}, \mathcal{C}, \mathbf{V})$ 
  return  $\mathcal{P}, \mathcal{C}, \hat{\Lambda}$ 
```

size of the grid. Since there is an optimal value for the latter, adding more processors past this point results in diminishing gains (Syed et al., 2022, §5.3). In contrast, regenerative processes like NRST always benefit from adding more processors (Fishman, 1983). Moreover, whereas NRST requires no communication between workers, NRPT involves repeated messaging between random pairs of processors, making distributed implementations highly non-trivial (see e.g. Surjanovic et al., 2023). NRST also admits the TE diagnostic derived from its simple CLT, whereas no such diagnostic for NRPT exists. Finally, as discussed in Section 4.3, NRST exhibits a lower barrier than NRPT for any given problem.

5.1 Adjusting the affinities

We restrict attention to the two affinity settings from Section 4.3. In the **mean energy** setting, the affinity function has the closed form expression $c(\beta) = -\log(\mathcal{Z}(\beta))$. We can thus employ existing approaches for approximating log-normalizing constants (see Fournent et al., 2019, for a review). Among these, the *stepping-stone* estimator (Xie et al., 2010) is a good fit for simulated tempering algorithms. In Appendix A.1 we detail how this approach can be used to produce an estimate $\widehat{\log(\mathcal{Z}(\beta_i))}$ of the log-normalization constant at each grid point. In the **minimum rejection rate** setting, computing the minimum rejection affinity function requires numerically integrating Eq. (20).

We use a trapezoidal approximation

$$\frac{1}{2} \sum_{j=1}^i (\text{med}^{(\beta_{j-1})}(V) + \text{med}^{(\beta_j)}(V)) \Delta \beta_j.$$

$\text{med}^{(\beta)}(V)$ can then be approximated using the sample medians of \mathbf{V} .

5.2 Adapting the grid

Theorem 4.4 shows that under mild conditions, TE is maximized when $\sum_{i=1}^N \frac{\rho_i}{1-\rho_i}$ is minimized. Lemma C.20 indicates that for fixed $\sum_{i=1}^N \rho_i$ (justified by Proposition 4.13), the minimum occurs when $\forall i, \rho_i = \rho \in (0, 1)$, i.e., the grid exhibits *equi-rejection*. In order to find a grid that satisfies this condition, we adapt the tuning approach outlined in Syed et al. (2022) to ST. The idea leverages Proposition 4.13: under equi-rejection, the finite grid approximation of Eq. (22) becomes

$$\forall i \in \{0, \dots, N\} : \sum_{j=1}^i \rho_j = i\rho \approx \Lambda(\beta_i), \quad \rho \approx \Lambda/N.$$

This suggests setting $\beta_i = \Lambda^{-1}((i/N)\Lambda)$. In practice, we must use estimates of ρ_i to approximate this expression. In particular, let $r_{i,i+\epsilon}$ be the Monte Carlo estimate of $\rho_{i,i+\epsilon}$ using the \mathbf{V} dataset, and $r_i = (r_{i-1,i} + r_{i,i-1})/2$. Then we let $\hat{\Lambda}(\beta), \beta \in [0, 1]$ be a monotonic interpolation of

$$\forall i \in \{0, \dots, N\} : \hat{\Lambda}(\beta_i) := \sum_{j=1}^i r_j, \quad \hat{\Lambda}(1) = \hat{\Lambda} = \sum_{j=1}^N r_j. \quad (23)$$

Finally, we set $\beta_i = \hat{\Lambda}^{-1}\left(\frac{i}{N}\hat{\Lambda}\right)$ using a root finding algorithm.

Fig. 2 shows the result of applying the grid adaptation strategy to a selection of six models (see Appendix B.1). Note that the optimal points are far from uniformly distributed. They also do not follow a common pattern, like a logarithmic spacing concentrated at $\beta = 0$. Indeed, the optimal grid can concentrate in arbitrary parts of the unit interval, highlighting the necessity of the adaptation scheme described in this section.

5.3 Convergence detection

We propose three heuristic indicators and thresholds that, when *jointly* satisfied, signal that Algorithm 1 can be safely terminated. The first—the

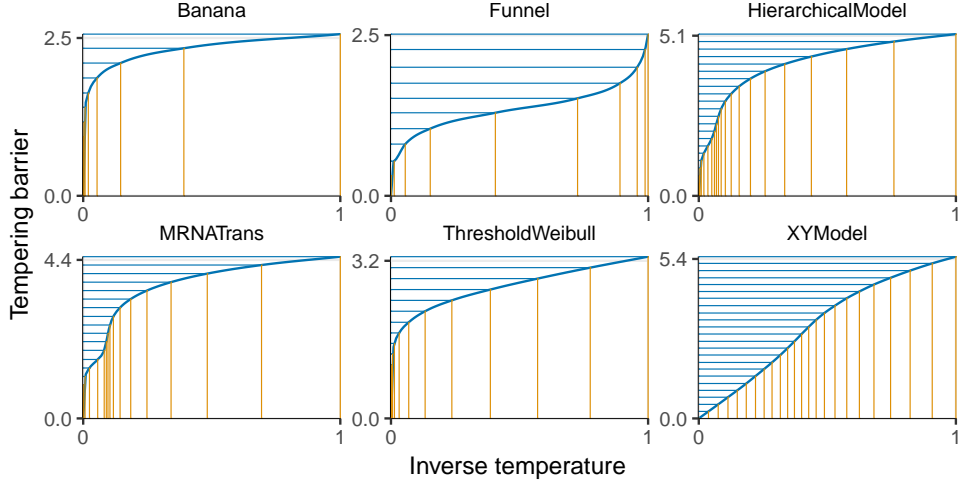


Figure 2: Monotonic interpolation of the estimated tempering barrier (Eq. (23)) for an array of six models. Vertical lines (yellow) show the grid after running Algorithm 1. Evenly-spaced horizontal lines (blue) signal that the grid satisfies equi-rejection.

ratio of the standard deviation and mean of the rejection probabilities—tracks agreement with the equi-rejection criterion. Agreement occurs when

$$\frac{\sqrt{N^{-1} \sum_{i=1}^N (r_i - \bar{r})^2}}{\bar{r}} < L_r,$$

where $\bar{r} := N^{-1} \sum_{i=1}^N r_i$. The other two indicators track the convergence in level affinities and tempering barrier, which have stabilized when

$$\frac{|c_{\text{new}}(1) - c_{\text{old}}(1)|}{c_{\text{old}}(1)} < L_c \quad \text{and} \quad \frac{|\hat{\Lambda}_{\text{new}} - \hat{\Lambda}_{\text{old}}|}{\hat{\Lambda}_{\text{old}}} < L_\Lambda.$$

Furthermore, when the mean-energy strategy is chosen for the affinity function, the difference in directional rejection probabilities is also a useful diagnostic (c.f. Eq. (14)), which we monitor via the threshold

$$\frac{\frac{1}{N} \sum_{i=1}^N |r_{i,i-1} - r_{i-1,i}|}{\bar{r}} < L_d.$$

Based on experimental evidence, we recommend setting $L_r = 0.1$, $L_c = 0.005$, $L_\Lambda = 0.01$, and $L_d = 0.05$. These thresholds do not have a theoretical grounding—they are heuristics based on extensive testing on a variety of models.

5.4 Choice of exploration kernels

The basic theory described in Section 3.1 for the correctness of NRST—particularly the Law of Large numbers (Theorem 3.1)—places minimal requirements on the collection of kernels $\{K_i\}_{i=1}^N$; only π_i -invariance and π_i -irreducibility are assumed. In practice, using different exploration kernels, each with many tunable parameters, can make the adaptation of NRST harder. This problem is further complicated by the “moving target” effect generated by the adaptation described in Algorithm 1: at each round we have a new grid and therefore a new path of distributions, which in theory requires re-tuning the explorers.

Therefore, it is convenient to rely on a single parametric family of exploration kernels that can be used without much or any tuning effort. If adaptation is required, a simple yet effective strategy is to optimize the kernel for the target distribution $\pi = \pi_N$ —which is always part of the path $\{\pi_i\}_{i=0}^N$, thus avoiding the moving target issue. In our experiments (Section 7) we opt for using the slice sampler (Neal, 2003) because it can be used without any adaptation across all the experiments we covered. Biron-Lattes et al. (2023) is a more recent example of an MCMC sampler that can be used with minimal inter-round adaptation.

5.5 Selecting the grid size

We now discuss tuning the grid size N . If N is too low, the sampler will struggle to move between endpoints due to the high probability of rejection in tempering. Increasing N , on the other hand, generally increases the cost of running a single tour. A natural candidate to capture this trade-off is the ratio of expected tour length and tour effectiveness. This ratio captures the total number of exploration steps taken to produce a result for fixed (α, δ) in Eq. (12), i.e., fixed result quality:

$$\frac{\mathbb{E}_\nu[\tau]}{\text{TE}} \propto K_{\min}(\alpha, \delta, \text{TE})\mathbb{E}_\nu[\tau].$$

Under Assumptions 4.1 and 4.9, the expected tour length is $\mathbb{E}_\nu[\tau] = 2(N + 1)$. Assuming further that equi-rejection is approximately satisfied, and further that $\rho \approx \Lambda/N$, the ratio has the form

$$\frac{\mathbb{E}_\nu[\tau]}{\text{TE}} \approx 2(N + 1) \left(1 + 2N \frac{\Lambda/N}{1 - \Lambda/N} \right) = \frac{2(N + 1)(N(1 + 2\Lambda) - \Lambda)}{N - \Lambda}.$$

Lemma C.22 shows that this expression is minimized over $N \in \mathbb{R}$, $N > \Lambda$ by

$$N^* := \Lambda \left[1 + \sqrt{1 + \frac{1}{1 + 2\Lambda}} \right]. \quad (24)$$

Note that $N^* \in (2\Lambda, (1 + \sqrt{2})\Lambda)$, so that the grid size grows linearly with the total tempering barrier. A practical way of using Eq. (24) is to estimate Λ by $\hat{\Lambda}$ during the tuning rounds in Algorithm 1. Then, if the difference between the current N and the estimated N^* is substantial, the tuning can be re-started with this new value. In practice, we use γN^* tempering levels for some $\gamma \geq 1$ to account for the various approximations and assumptions used in deriving N^* . In Appendix B.2 we show that the safety factor $\gamma = 2$ results in more robust performance without sacrificing efficiency.

5.6 Managing the serial correlation in exploration steps

Assumption 4.1 is an important condition of many findings in Section 4, and suggests that a high correlation in the potential $V(x)$ before and after an exploration step might hinder the performance of ST. One can decrease this correlation, if necessary, by composing the exploration kernels $\{K_i\}_{i=1}^N$ with themselves. Specifically, for each $i \in \{1, \dots, N\}$, let $K_i^0 := \text{Id}$ be the identity kernel, and define for $n > 1$, $K_i^n := K_i^{n-1} \circ K_i$. Under mild regularity conditions, the serial correlation in $V(x)$ can be decreased by substituting K_i in the exploration step with K_i^n for $n > 1$. The best value of n for a given inference problem will generally depend on the kernel K_i . We suggest selecting a maximum tolerable correlation $\bar{\kappa} < 1$, and then setting, for all $i \in \{1, \dots, N\}$, $n_i^* := \inf\{n \in \mathbb{Z}_+ : \kappa_i(n) \leq \bar{\kappa}\}$, where $\kappa_i(n)$ denotes the correlation $\kappa_i(n) = \text{Corr}(V(x_0), V(x_n))$ for $x_0 \sim \pi_i$ and $x_n \sim K_i^n(x_0, \cdot)$. The autocorrelation functions can be approximated, for example, by running the exploration kernels at each point in the final grid obtained in Algorithm 1. In Appendix B.2 we show that $\bar{\kappa} = 0.95$ results in the best performance.

6 Related work

Non-reversible extensions of simulated tempering have appeared previously in the literature. Sakai and Hukushima (2016a) apply the general technique described in Turitsyn et al. (2011) to transform reversible chains into non-reversible ones. Indeed, Sakai and Hukushima (2016a) start from the symmetric random walk ST and build a continuum of MCMC algorithms controlled by a parameter $\delta \in [0, 1]$. The original reversible algorithm is

recovered when $\delta = 0$. For $\delta > 0$ however, the Markov chain is non-reversible and its performance improves monotonically as δ increases. NRST is similar to the result of taking $\delta = 1$, although not exactly equal: the algorithm with $\delta = 1$ allows for the possibility of not updating neither i nor ϵ during one step, while this is impossible in our formulation. [Faizi et al. \(2020\)](#) also apply the [Turitsyn et al. \(2011\)](#) approach, but starting instead from a reversible ST algorithm that updates the temperature using the full conditional $\pi_{\text{st}}(i|x)$ corresponding to Eq. (3) ([Rosta and Hummer, 2010](#)).

There exists a vast literature describing heuristics to set the affinities (see e.g. [Park and Pande, 2007](#); [Chelli, 2010](#); [Nguyen et al., 2013](#); [Sakai and Hukushima, 2016b](#)). The mean-energy strategy is adopted (implicitly or explicitly) in all of these works, so that log-normalization constants need to be estimated. In particular, [Mitsutake and Okamoto \(2000\)](#) proposes using a preliminary run of parallel tempering with the same grid in order to estimate these constants. [Geyer and Thompson \(1995\)](#) also considers the possibility of using parallel tempering, but recommends instead an alternative method.

In contrast, less attention has been put on automatically selecting grid points. These are generally determined using either a uniformly or logarithmically spaced grid between endpoints. [Geyer and Thompson \(1995\)](#) is one of the few works that tackle this issue, aiming to obtain equi-rejection via an ad-hoc model of the acceptance rate as a function of β . Alternatively, recent work ([Gobbo and Leimkuhler, 2015](#); [Graham and Storkey, 2017](#)) has sidestepped the issue of finding a grid by working with a continuum of inverse temperatures. Furthermore, building on these developments, [Martinsson et al. \(2019\)](#) propose marginalizing-out β via averaging results for Markov processes (see e.g. [Pavliotis and Stuart, 2008](#), Ch. 17), however this line of work applies only to smooth target distributions, whereas NRST is applicable to general state-spaces.

Throughout this paper we have suggested running NRST for a fixed number of tours determined via Eq. (12) and then estimating expectations under π via Eq. (8). Nevertheless, alternative stopping criteria and estimators have been proposed in the regenerative simulation literature (see e.g. [Glynn, 2006](#), and references therein).

The coefficient of variation of the tour lengths $\{\tau_k\}_{k \in \mathbb{N}}$ is a common diagnostic used in regenerative simulation (see [Mykland et al., 1995](#), and references therein). It arises from bounding the asymptotic variance of estimates of unconditional expectations—in contrast to TE which bounds the error of estimating a conditional expectation that is specific to ST.

Regenerations allow adapting MCMC by using past information without disrupting the stationary distribution (see [Gilks et al. 1998](#) and [Lan et al.](#)

2014 for an application). Lastly, there has been work towards unifying ST with other MCMC methods aimed at sampling from finite collections of distributions—like Wang-Landau and trans-dimensional MCMC—in order to propose more efficient sampling strategies for all (Atchadé and Liu, 2010; Tan, 2017).

7 Numerical results

In this section we show experimental evidence for the effectiveness of our proposed adaptation algorithm. Moreover, we provide a numerical assessment of the closeness between the estimator $\widehat{\text{TE}}$ (Eq. (11)) and the limiting value derived in Corollary 4.14.

Since the focus of this paper is on *automatic* regenerative samplers, in the following we have excluded comparisons against non-ST regenerative samplers. As discussed in Sections 1 and 2, we have not found other regenerative MCMC methods that are as automatic as ST.¹ Hence, we restrict ourselves to ST algorithms because putatively more efficient regenerative samplers that require model specific derivations lie outside of the scope of this paper.

7.1 Evaluation of the ST adaptation algorithm

We first evaluate the effect and applicability of the adaptation algorithm in Section 5. In particular, we compare the performance of multiple ST algorithms both with and without parameters set using the proposed strategy: our novel NRST method, the original reversible simulated tempering of Geyer and Thompson (1995) (abbreviated henceforth as “GT95”), and the two non-reversible algorithms of Sakai and Hukushima (2016a) (“SH16”) and Faizi et al. (2020) (“FBDR”). When *not* using our proposed method for tuning, we default to each past method’s recommended tuning method (see Appendix B.3 for further details).

We compare the performance of these ST methods using a notion of *sample-quality per unit cost*. We fix quality across all ST algorithms by fixing a particular value of the confidence interval half-width $\delta > 0$ and level α in Algorithm 4. We measure *cost* via the number of V evaluations. This is an implementation-agnostic proxy of wall-clock time: repeated evaluation of

¹One notable exception is Independence MH (IMH), for which regenerative simulation is possible regardless of the proposal distribution (Mykland et al., 1995, §4.1). But note that we can view IMH as an improperly tuned NRST sampler with $N = 1$, $K_1 = \text{Id}$, and reference given by the proposal. Following the reasoning of Section 5, we would expect that NRST with adaptation and non-trivial exploration kernel to dominate IMH.

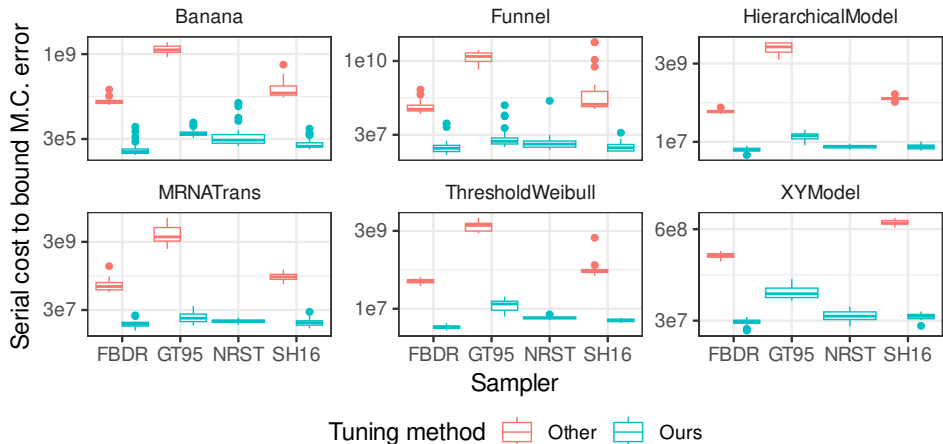


Figure 3: Side-by-side box-plots of serial cost (as defined in Section 7.1) for each simulated tempering algorithm and tuning strategy (color), for 6 selected models (lower is better). Each experiment is replicated 30 times. The number of tours is determined in a quality-consistent approach using Eq. (12) with $\alpha = 0.95$, $\delta = 0.5$, and $\widehat{\text{TE}}$ estimated in a preliminary run. Missing box for GT95 in XYModel is due to all replications exceeding the time budget.

V accounts for the vast majority of the time during our experiments. We define the “parallel cost” as the maximum number of V evaluations across tours, and the “serial cost” as the sum of V evaluations across tours.

For all ST algorithms and all tempering levels, we use slice sampling within Gibbs as the exploration kernel (Neal, 1997, 2003); the natural adaptivity of slice sampling avoids the need to re-adjust exploration kernels at each round of Algorithm 1.

Fig. 3 shows the results of the comparison. We first notice that our automatic adaptation strategy achieves multiple orders of magnitude in cost reduction across all competitors and models. In particular, the worst performing algorithm under the alternative tuning strategy is GT95. This is due to the deterioration of performance that this reversible sampler experiences in the dense grid regime. However, when inspecting the results under our adaptation scheme, we see a much smaller difference between GT95 and the rest. This is because the grids produced by our tuning tend to be sparse, and non-reversibility gains are smaller (although usually still meaningful) on such grids. Lastly, it is interesting that the three non-reversible algorithms become essentially equivalent using our adaptation strategy, although FBDR achieves consistent (if small) gains across examples.

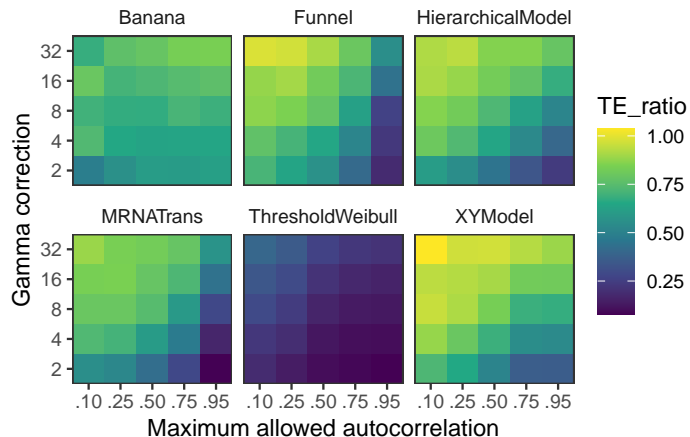


Figure 4: Ratio between the average TE from 30 replications of a given configuration, over the estimated TE^∞ using the same replications. Grid represents different combinations of $\bar{\kappa}$ and γ , with the cost-optimal value represented in the bottom-right corner.

7.2 Tightness of the asymptotic tour effectiveness

In Section 4.3 we showed that, under certain conditions, TE converges to a fixed value TE^∞ as the grid refines. This experiment assesses how close the non-asymptotic TE is to its limiting value, and if it is possible to achieve TE^∞ in certain situations.

Fig. 4 shows the ratio between the mean \widehat{TE} and TE^∞ over 30 repetitions of NRST runs that use a range of combinations of the hyper-parameters $(\gamma, \bar{\kappa})$. The default, cost-optimal values are represented in the bottom-right corner. Notice that these configurations achieve already about 20% of TE^∞ . Also, as either γ increases or $\bar{\kappa}$ decreases, the estimated tour effectiveness approaches the limiting value, validating our analyses. However, convergence is slower for more complex target distributions; e.g., the “ThresholdWeibull” achieves only 40% of TE^∞ . This occurs because estimating the log-partition function for this model is hard, since the distribution of V under $\pi^{(\beta)}$ becomes heavy tailed as $\beta \rightarrow 0$.

8 Regenerative NRST in practice

8.1 Regenerative NRST and Massive Parallelization

In this section, we offer practical advice on deploying NRST for complex problems on massive computing platforms, and how the particular workload

patterns of regenerative MCMC can take advantage of newer architectures for distributed computation. Throughout this section we assume that (1) the model is complex enough that the compute time for a single tour is fairly long; (2) the computing platform dynamically assigns the NRST tours among a pool of concurrent workers of pre-specified size; and (3) that we have already run the adaptation routine in Section 5. Our aim is to devise a strategy to choose the size of the pool to satisfy a time or cost constraint.

We begin with a preliminary run of K_{trial} parallel NRST tours (Algorithm 4). To determine K_{trial} we need an estimate of TE in Eq. (12); we use the mean-energy strategy (see Section 5.1) and estimate TE via the asymptotic formula in Corollary 4.14; i.e., $\widehat{\text{TE}}^\infty := 1/(1 + 2\widehat{\Lambda})$, where $\widehat{\Lambda} = \widehat{\Lambda}(1)$ is the estimated tempering barrier (Eq. (23)) returned by Algorithm 1. The preliminary run provides an estimate of $\widehat{\text{TE}}$ using Eq. (11), which determines the required number of tours K to satisfy the (α, δ) accuracy guarantee. Note that the K_{trial} tours can be used here too, so only the difference $K_{\text{extra}} := K - K_{\text{trial}}$ needs to be executed in the next phase. Given that the asymptotic TE tends to overestimate the true TE (Section 7.2), it is usually the case that K_{extra} is significantly larger than K_{trial} . The preliminary run also provides CPU times incurred by tours; we fit this distribution via a bulk-tail mixture with an 80th percentile threshold, using an empirical distribution for the bulk, and a Weibull density for the tail. This CPU time model enables simulating hypothetical running times and costs for samples of K_{extra} tours.

Fig. 5 displays various simulations that can be used to plan the execution of K_{extra} tours (we fix $K_{\text{extra}} = 2048$ for this example). The top-left panel in Fig. 5 shows the CPU time distribution of K_{extra} tours, highlighting how unbalanced the workload of a typical parallelized run is. The top-right and bottom-left panels display hypothetical usage patterns for worker pools of varying sizes when processing the K_{extra} tours. These figures demonstrate that when few workers are available, doubling the pool size almost halves the runtime; but after a certain point, the longest tour (about 8 hours in this sample) begins to dominate and returns diminish.

This workload pattern has implications for execution on High-Performance Computing (HPC) and Cloud Computing (Cloud) platforms, which have very different characteristics. Jobs submitted to HPC systems often do not incur monetary costs—as they are often owned by the user’s organization—but they are queued until enough resources are free to accommodate them (see Fan et al., 2019). And typically, the scheduler assumes that all workers

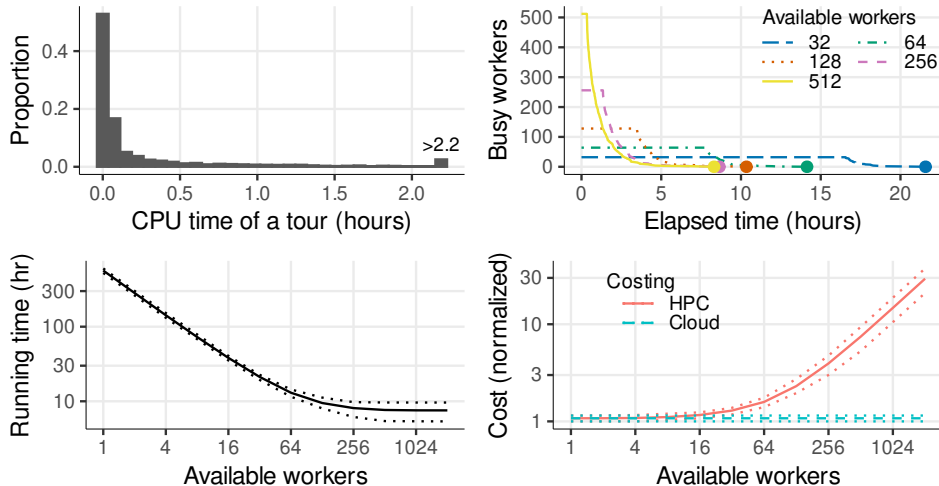


Figure 5: Graphic analysis of a simulation plan to execute 2048 expensive tours in parallel. **Top-left**: histogram of simulated CPU times (truncated at the 97.5-th percentile). **Top-right**: number of active workers at any given time when running 2048 tours using a varying number of available workers, assuming dynamic scheduling of tours. Dots mark the total running time in each case. **Bottom-left**: estimated running time of the algorithm versus number of available workers. Solid line denotes the mean over 30 repetitions, while dotted lines present an 80% confidence interval. **Bottom-right**: estimated cost (normalized so that the minimum is 1) of running the algorithm versus available workers, depending on costing rule. Solid and dashed lines denote the means over 30 repetitions, while dotted envelopes give 80% confidence intervals.

requested will be busy for the duration of the job; i.e.,

$$\text{HPC cost} \propto \text{Running time} \times \text{Pool size}.$$

As we know from the top-right plot in Fig. 5, this is not the case for the usual workloads in regenerative MCMC. Thus, if we requested 2048 workers to execute the running example, the job might wait for an unacceptably long time. A better choice would be 64 workers; when compared to a single worker, this configuration achieves upwards of a 40 fold reduction in runtime while only doubling the cost.

In contrast, Cloud platforms often have little to no scheduling wait time, but do commonly incur monetary cost proportional to the total CPU time,

$$\text{Cloud cost} \propto \sum_{k=1}^{K_{\text{extra}}} (\text{CPU time of the } k^{\text{th}} \text{ tour}). \quad (25)$$

The sum on the right-hand side of Eq. (25) corresponds to the area under the curves in the top-right panel of Fig. 5. Since this sum is invariant to tour allocation, the cost is constant versus pool size. In theory, then, we should always select a pool of size equal to K_{extra} on a Cloud platform. However, Cloud platforms usually have a maximum concurrency limit—for example, Amazon Lambda (Amazon, 2023) currently allows a maximum of 1000 concurrent workers—and if the initialization time of a worker is significant, then it may be better to amortize that time by assigning more than one tour to each worker.

8.2 Regenerative NRST and Probabilistic Programming

Our approach to regenerative MCMC can be easily integrated within many PPLs. In the Bayesian setting, when the prior ϖ is proper and allows i.i.d. simulation, then using ϖ as the reference and setting $V(x) = -\log(L(y|x))$ gives a valid path of distributions to the target posterior density $\pi(x) \propto \varpi(x)L(y|x)$. If this model is coded in a PPL that exposes a minimal set of functions, we can apply regenerative MCMC to the model without any extra user input. The basic required building blocks are 1) a simulator for ϖ , 2) a function that returns $\log(L(y|x))$ for any x , and 3) a method to evaluate $\log(\varpi(x))$ (required for the exploration step). For example, our Julia implementation of NRST² can seamlessly handle models written in DynamicPPL (Tarek et al., 2020), which exposes these three building blocks. More generally, PPLs that compile probabilistic models into graphical models—like WinBUGS and descendants (Lunn et al., 2000)—can in theory provide the type of interface described above (van de Meent et al., 2018, §3).

While the scenario above covers many cases of interest, it fails if the prior is improper or difficult to sample from (e.g., a Markov random field), or if the PPL does not expose the necessary functionality. However, as long as the PPL provides the ability to evaluate $\log(\pi(x))$ for any x —as is the case with Stan (Stan Development Team, 2023)—we can still apply our approach. In particular, we select a parametrized family of references $\mathcal{Q} := \{q_\theta : \theta \in \Theta\}$ such that each q_θ enables i.i.d. sampling and evaluation of $\log(q_\theta(x))$, and then set $V(x) = -\log(\pi(x)/q_\theta(x))$ to obtain a valid path of distributions. The *best* member q_{θ^*} may then be chosen by any automatic variational procedure, e.g., Kucukelbir et al. (2015). This is similar to the approach for NRPT described in the work of Surjanovic et al. (2022).

²<https://github.com/UBC-Stat-ML/NRST.jl>

9 Discussion

In this work we developed the tools necessary to use NRST for automated regenerative MCMC. We derived the TE diagnostic as a key summary of the behavior of ST algorithms, and used its relationship with algorithmic parameters to provide a robust adaptation procedure that facilitates the use of NRST in a wide range of probabilistic models. Our experiments demonstrated that our tuning recommendations produce sizable gains on both reversible and non-reversible ST algorithms.

Future work includes generalizing Theorem 4.4 to arbitrary level distributions. This would allow us to assess the robustness of NRST under imperfect tuning—i.e., when $c_i \neq -\log(\mathcal{Z}(\beta_i))$ —which in practice is how NRST is implemented. A generalized Theorem 4.4 could also provide a better understanding of the median affinity strategy, which in our experiments seems to yield performance gains in settings where there are more workers available than tours to run (see Fig. 6 in Appendix B.2).

Elucidating the connection between TE and the rate of convergence of NRST to its stationary distribution is another potential avenue of future research. One way to approach this would be to leverage Theorem 13.3.1 in Douc et al. (2018), which proves geometric ergodicity for atomic chains when the moment generating function (m.g.f.) of the return time T_1 is analytic at the origin. Under Assumption 4.1, the index process is a finite Markov chain, so the m.g.f. condition holds (see e.g. Nemirovsky, 2013, Prop. 6.1). By linking the radius of convergence of the m.g.f. to the TE diagnostic, we could obtain an expression for the rate of geometric ergodicity in terms of TE.

Annealed importance sampling (AIS, Neal, 2001) is a Monte Carlo algorithm that bears some similarities to ST. It works by sequentially pushing i.i.d. samples from a reference π_0 towards the target π through the tempering path in Eq. (2) using a collection of $\pi^{(\beta)}$ -invariant Markov kernels. Moreover, this process is also embarrassingly parallelizable. On the other hand, AIS is not a proper MCMC method and thus we have excluded it from our experiments. Nevertheless, it would be interesting to establish both theoretical and experimental comparisons between NRST and AIS.

Acknowledgements

We thank Son Luu for his helpful feedback on Theorem 4.4. We also thank an editor and two reviewers for their engaging comments and suggestions.

We further thank one of our reviewers for helping us simplify the proofs of Lemmas C.20 to C.22. ABC and TC acknowledge the support of an NSERC Discovery Grant. We also acknowledge use of the ARC Sockeye computing platform from the University of British Columbia.

References

- Amazon (2023). AWS Lambda developer guide. <https://docs.aws.amazon.com/lambda/latest/dg/welcome.html>. Accessed: 2023-06-29.
- Atchadé, Y. F. and Liu, J. S. (2010). The Wang-Landau algorithm in general state spaces: applications and convergence analysis. *Statistica Sinica*, 20(1):209–233.
- Ballnus, B., Hug, S., Hatz, K., Görlitz, L., Hasenauer, J., and Theis, F. J. (2017). Comprehensive benchmarking of Markov chain Monte Carlo methods for dynamical systems. *BMC Systems Biology*, 11(1).
- Biron-Lattes, M., Surjanovic, N., Syed, S., Campbell, T., and Bouchard-Côté, A. (2023). autoMALA: Locally adaptive Metropolis-adjusted Langevin algorithm. *arXiv e-prints*, page arXiv:2310.16782.
- Brockwell, A. E. and Kadane, J. B. (2005). Identification of regeneration times in MCMC simulation, with application to adaptive schemes. *Journal of Computational and Graphical Statistics*, 14(2):436–458.
- Çınlar, E. (2013). *Introduction to Stochastic Processes*. Dover Books on Mathematics. Dover Publications, reprint edition.
- Chelli, R. (2010). Optimal weights in serial generalized-ensemble simulations. *Journal of Chemical Theory and Computation*, 6(7):1935–1950.
- Chen, F., Lovász, L., and Pak, I. (1999). Lifting Markov chains to speed up mixing. In *ACM symposium on theory of computing*.
- Cheng, R. (2017). *Non-Standard Parametric Statistical Inference*. Oxford University Press.
- Douc, R., Durmus, A., Enfroy, A., and Olsson, J. (2022). Boost your favorite Markov Chain Monte Carlo sampler using Kac’s theorem: the Kick-Kac teleportation algorithm. *arXiv:2201.05002*.

- Douc, R., Moulines, E., Priouret, P., and Soulier, P. (2018). *Markov chains*. Springer International Publishing.
- Dudley, R. M. (2002). *Real analysis and probability*. Cambridge studies in advanced mathematics. Cambridge University Press, 2nd edition.
- Faizi, F., Buigues, P. J., Deligiannidis, G., and Rosta, E. (2020). Simulated tempering with irreversible Gibbs sampling techniques. *The Journal of Chemical Physics*, 153(21):214111.
- Fan, Y., Lan, Z., Rich, P., Allcock, W. E., Papka, M. E., Austin, B., and Paul, D. (2019). Scheduling beyond CPUs for HPC. In *International Symposium on High-Performance Parallel and Distributed Computing*.
- Fishman, G. S. (1983). Accelerated accuracy in the simulation of Markov chains. *Operations Research*, 31(3):466–487.
- Flegal, J., Haran, M., and Jones, G. (2008). Markov chain Monte Carlo: Can we trust the third significant figure? *Statistical Science*, pages 250–260.
- Fourment, M., Magee, A., Whidden, C., Bilge, A., Matsen, F., and Minin, V. (2019). 19 dubious ways to compute the marginal likelihood of a phylogenetic tree topology. *Systematic Biology*, 69(2):209–220.
- Gelman, A. and Meng, X.-L. (1998). Simulating normalizing constants: From importance sampling to bridge sampling to path sampling. *Statistical science*, pages 163–185.
- Geyer, C. J. and Thompson, E. A. (1995). Annealing Markov chain Monte Carlo with applications to ancestral inference. *Journal of the American Statistical Association*, 90(431):909–920.
- Gilks, W. R., Roberts, G. O., and Sahu, S. K. (1998). Adaptive Markov chain Monte Carlo through regeneration. *Journal of the American Statistical Association*, 93(443):1045–1054.
- Glynn, P. W. (2006). Simulation algorithms for regenerative processes. In Henderson, S. G. and Nelson, B. L., editors, *Simulation*, volume 13 of *Handbooks in Operations Research and Management Science*, pages 477–500. Elsevier.
- Gobbo, G. and Leimkuhler, B. J. (2015). Extended hamiltonian approach to continuous tempering. *Phys. Rev. E*, 91:061301.

- Graham, M. M. and Storkey, A. J. (2017). Continuously tempered Hamiltonian Monte Carlo. In *Proceedings of the Conference on Uncertainty in Artificial Intelligence, UAI 2017*. AUAI Press.
- Hasenbusch, M. (2005). The two-dimensional XY model at the transition temperature: a high-precision Monte Carlo study. *Journal of Physics A: Mathematical and General*, 38(26):5869.
- Hobert, J. P., Jones, G. L., Presnell, B., and Rosenthal, J. S. (2002). On the applicability of regenerative simulation in Markov chain Monte Carlo. *Biometrika*, 89(4):731–743.
- Jones, G. L. and Hobert, J. P. (2001). Honest exploration of intractable probability distributions via Markov chain Monte Carlo. *Statistical Science*, 16(4):312–334.
- Kemeny, J. G. and Snell, J. L. (1960). *Finite Markov chains*. Van Nostrand, Princeton, N.J.
- Kucukelbir, A., Ranganath, R., Gelman, A., and Blei, D. M. (2015). Automatic Variational Inference in Stan. *arXiv e-prints*, page arXiv:1506.03431.
- Lan, S., Streets, J., and Shahbaba, B. (2014). Wormhole Hamiltonian Monte Carlo. *Proceedings of the AAAI Conference on Artificial Intelligence*.
- Liu, J. S. and Chen, R. (1995). Blind deconvolution via sequential imputations. *Journal of the American Statistical Association*, 90(430):567–576.
- Lunn, D. J., Thomas, A., Best, N., and Spiegelhalter, D. (2000). WinBUGS – a Bayesian modelling framework: concepts, structure, and extensibility. *Statistics and Computing*, 10(4):325–337.
- Lyubartsev, A. P., Martsinovski, A. A., Shevkunov, S. V., and Vorontsov-Velyaminov, P. N. (1992). New approach to Monte Carlo calculation of the free energy: Method of expanded ensembles. *The Journal of Chemical Physics*, 96(3):1776–1783.
- Marinari, E. and Parisi, G. (1992). Simulated tempering: a new Monte Carlo scheme. *EPL (Europhysics Letters)*, 19(6):451.
- Martinsson, A., Lu, J., Leimkuhler, B., and Vanden-Eijnden, E. (2019). The simulated tempering method in the infinite switch limit with adaptive weight learning. *Journal of Statistical Mechanics: Theory and Experiment*, 2019(1):013207.

- McKimm, H., Wang, A. Q., Pollock, M., Robert, C. P., and Roberts, G. O. (2022). Sampling using Adaptive Regenerative Processes. *arXiv e-prints*, page arXiv:2210.09901.
- Minh, D. L. P., Minh, D. D. L., and Nguyen, A. L. (2012). Regenerative Markov chain Monte Carlo for any distribution. *Communications in Statistics - Simulation and Computation*, 41(9):1745–1760.
- Mitsutake, A. and Okamoto, Y. (2000). Replica-exchange simulated tempering method for simulations of frustrated systems. *Chemical Physics Letters*, 332(1-2):131–138.
- Modi, C., Barnett, A., and Carpenter, B. (2023). Delayed rejection Hamiltonian Monte Carlo for sampling multiscale distributions. *Bayesian Analysis*, pages 1–28.
- Murphy, K. P. (2012). *Machine Learning: A Probabilistic Perspective*. The MIT Press.
- Mykland, P., Tierney, L., and Yu, B. (1995). Regeneration in Markov chain samplers. *Journal of the American Statistical Association*, 90(429):233–241.
- Neal, R. M. (1997). Markov chain Monte Carlo methods based on ‘slicing’ the density function. Technical Report 9722, University of Toronto, Department of Statistics.
- Neal, R. M. (2001). Annealed importance sampling. *Statistics and Computing*, 11:125–139.
- Neal, R. M. (2003). Slice sampling. *The Annals of Statistics*, 31(3):705–767.
- Nemirovsky, D. (2013). Tensor approach to mixed high-order moments of absorbing Markov chains. *Linear Algebra and its Applications*, 438(4):1900–1922.
- Nguyen, A. (2017). Regenerative Markov chain importance sampling. *Communications in Statistics–Simulation and Computation*, 46(5):3892–3906.
- Nguyen, P. H., Okamoto, Y., and Derreumaux, P. (2013). Communication: Simulated tempering with fast on-the-fly weight determination. *The Journal of chemical physics*, 138(6):061102.
- Nummelin, E. (1978). A splitting technique for Harris recurrent Markov chains. *Zeitschrift für Wahrscheinlichkeitstheorie und verwandte Gebiete*, 43(4):309–318.

- Oliver, H. W. (1954). The exact Peano derivative. *Transactions of the American Mathematical Society*, 76(3):444–456.
- Pagani, F., Wiegand, M., and Nadarajah, S. (2022). An n-dimensional Rosenbrock distribution for Markov chain Monte Carlo testing. *Scandinavian Journal of Statistics*, 49(2):657–680.
- Park, S. and Pande, V. S. (2007). Choosing weights for simulated tempering. *Physical Review E*, 76(1):016703.
- Pavliotis, G. and Stuart, A. (2008). *Multiscale methods: averaging and homogenization*. Springer Science & Business Media.
- Predescu, C., Predescu, M., and Ciobanu, C. V. (2004). The incomplete beta function law for parallel tempering sampling of classical canonical systems. *The Journal of Chemical Physics*, 120(9):4119–4128.
- Ripley, B. (1987). *Stochastic simulation*. John Wiley & Sons, Ltd.
- Robert, C. P. and Casella, G. (2004). *Monte Carlo Statistical Methods*. Springer Texts in Statistics. Springer, New York, 2nd edition.
- Rosenthal, J. S. (2006). *A first look at rigorous probability theory*. World Scientific, 2nd edition.
- Rosta, E. and Hummer, G. (2010). Error and efficiency of simulated tempering simulations. *The Journal of Chemical Physics*, 132(3):034102.
- Sahu, S. K. and Zhigljavsky, A. A. (2003). Self-regenerative Markov chain Monte Carlo with adaptation. *Bernoulli*, 9(3):395–422.
- Sakai, Y. and Hukushima, K. (2016a). Irreversible simulated tempering. *Journal of the Physical Society of Japan*, 85(10):104002.
- Sakai, Y. and Hukushima, K. (2016b). Irreversible simulated tempering algorithm with skew detailed balance conditions: a learning method of weight factors in simulated tempering. In *Journal of Physics: Conference Series*, volume 750, page 012013.
- Stan Development Team (2023). Stan modeling language users guide and reference manual, version 2.32. <https://mc-stan.org>. Accessed: 2023-07-05.
- Surjanovic, N., Biron-Lattes, M., Tiede, P., Syed, S., Campbell, T., and Bouchard-Côté, A. (2023). Pigeons.jl: Distributed Sampling From Intractable Distributions. *arXiv:2308.09769*.

- Surjanovic, N., Syed, S., Bouchard-Côté, A., and Campbell, T. (2022). Parallel tempering with a variational reference. In *Advances in Neural Information Processing Systems*, volume 36, pages 565–577.
- Syed, S., Bouchard-Côté, A., Deligiannidis, G., and Doucet, A. (2022). Non-reversible parallel tempering: A scalable highly parallel MCMC scheme. *Journal of the Royal Statistical Society: Series B*, 84(2):321–350.
- Tan, Z. (2017). Optimally adjusted mixture sampling and locally weighted histogram analysis. *Journal of Computational and Graphical Statistics*, 26(1):54–65.
- Tarek, M., Xu, K., Trapp, M., Ge, H., and Ghahramani, Z. (2020). DynamicPPL: Stan-like speed for dynamic probabilistic models. *arXiv:2002.02702*.
- Tierney, L. (1998). A note on Metropolis-Hastings kernels for general state spaces. *The Annals of Applied Probability*, 8(1):1–9.
- Turitsyn, K. S., Chertkov, M., and Vucelja, M. (2011). Irreversible monte carlo algorithms for efficient sampling. *Physica D: Nonlinear Phenomena*, 240(4-5):410–414.
- van de Meent, J.-W., Paige, B., Yang, H., and Wood, F. (2018). An Introduction to Probabilistic Programming. *arXiv:1809.10756*.
- van der Vaart, A. W. (1998). *Asymptotic statistics*. Cambridge series in statistical and probabilistic mathematics. Cambridge University Press.
- Wang, A. Q., Pollock, M., Roberts, G. O., and Steinsaltz, D. (2021). Regeneration-enriched Markov processes with application to Monte Carlo. *The Annals of Applied Probability*, 31(2):703 – 735.
- Wilkinson, D. J. (2005). Parallel Bayesian computation. In Kontoghiorghes, E. J., editor, *Handbook of Parallel Computing and Statistics*, pages 481–512. Marcel Dekker/CRC Press, New York.
- Woodard, D. B., Schmidler, S. C., and Huber, M. (2009). Conditions for rapid mixing of parallel and simulated tempering on multimodal distributions. *The Annals of Applied Probability*, 19(2):617–640.
- Xie, W., Lewis, P. O., Fan, Y., Kuo, L., and Chen, M.-H. (2010). Improving marginal likelihood estimation for Bayesian phylogenetic model selection. *Systematic Biology*, 60(2):150–160.

Yao, Y., Vehtari, A., and Gelman, A. (2022). Stacking for non-mixing bayesian computations: The curse and blessing of multimodal posteriors. *Journal of Machine Learning Research*, 23(79):1–45.

A Implementation details

A.1 Efficient and stable computation of normalizing constants

Here we give a brief description of how the stepping-stone approach can be used to estimate log-normalizing constants. Consider the following importance sampling identity: for any $i < i'$,

$$\frac{\mathcal{Z}(\beta_{i'})}{\mathcal{Z}(\beta_i)} = \mathbb{E}^{(i)} \left[e^{-(\beta_{i'} - \beta_i)V} \right].$$

Building the sample estimate of the above using the samples \mathbf{V} (Section 5) yields

$$\left(\frac{\widehat{\mathcal{Z}(\beta_{i'})}}{\widehat{\mathcal{Z}(\beta_i)}} \right)_{\text{IS}} := \frac{1}{S_i} \sum_{n=1}^{S_i} e^{-(\beta_{i'} - \beta_i)V_n^{(i)}},$$

which is a consistent estimator of the ratio of normalizing constants. Combining these using the telescoping identity

$$\mathcal{Z}(\beta_i) = \prod_{j=1}^i \frac{\mathcal{Z}(\beta_j)}{\mathcal{Z}(\beta_{j-1})}, \quad (26)$$

where we used $\mathcal{Z}(0) = 1$, yields the *forward* stepping-stone estimator

$$\widehat{\mathcal{Z}(\beta_i)}_{\text{SS-F}} := \prod_{j=1}^i \left(\frac{\widehat{\mathcal{Z}(\beta_j)}}{\widehat{\mathcal{Z}(\beta_{j-1})}} \right)_{\text{IS}}.$$

Similarly, the inverted importance sampling identity

$$\frac{\mathcal{Z}(\beta_{i'})}{\mathcal{Z}(\beta_i)} = \mathbb{E}^{(i')} \left[e^{(\beta_{i'} - \beta_i)V} \right]^{-1},$$

admits the estimator

$$\left(\frac{\widehat{\mathcal{Z}(\beta_{i'})}}{\widehat{\mathcal{Z}(\beta_i)}} \right)_{\text{IS-I}} := \left(\frac{1}{S_{i'}} \sum_{n=1}^{S_{i'}} e^{(\beta_{i'} - \beta_i)V_n^{(i')}} \right)^{-1}.$$

Using this in Eq. (26) yields the *backward* stepping-stone estimator

$$\widehat{\mathcal{Z}(\beta_i)}_{\text{SS-B}} := \prod_{j=1}^i \left(\frac{\widehat{\mathcal{Z}(\beta_j)}}{\widehat{\mathcal{Z}(\beta_{j-1})}} \right)_{\text{IS-I}}.$$

Finally, to produce an estimator of the log-normalizing constants we take the simple average of the logarithm of both stepping-stone estimators

$$\log(\widehat{\mathcal{Z}}(\beta_i)) := \frac{1}{2} \left[\log(\widehat{\mathcal{Z}}(\beta_i)_{\text{SS-F}}) + \log(\widehat{\mathcal{Z}}(\beta_i)_{\text{SS-B}}) \right]. \quad (27)$$

Two insights help in efficiently and accurately computing Eq. (27). The first is noting that the calculation can be carried out recursively in one pass over the data \mathbf{V} , since

$$\log(\widehat{\mathcal{Z}}(\beta_i)) = \log(\widehat{\mathcal{Z}}(\beta_{i-1})) + \frac{1}{2} \left[\log\left(\frac{\widehat{\mathcal{Z}}(\beta_i)}{\widehat{\mathcal{Z}}(\beta_{i-1})}\right)_{\text{IS}} + \log\left(\frac{\widehat{\mathcal{Z}}(\beta_i)}{\widehat{\mathcal{Z}}(\beta_{i-1})}\right)_{\text{IS-I}} \right].$$

The second insight is that the logarithms on the right-hand side above should be computed using the log-sum-exp (LSE) trick (Murphy, 2012, §3.5.3)

$$\begin{aligned} \log\left(\frac{\widehat{\mathcal{Z}}(\beta_i)}{\widehat{\mathcal{Z}}(\beta_{i-1})}\right)_{\text{IS}} &= -\log(S_{i-1}) + \text{LSE}(-(\beta_i - \beta_{i-1})V^{(i-1)}) \\ \log\left(\frac{\widehat{\mathcal{Z}}(\beta_i)}{\widehat{\mathcal{Z}}(\beta_{i-1})}\right)_{\text{IS-I}} &= \log(S_i) - \text{LSE}((\beta_i - \beta_{i-1})V^{(i)}). \end{aligned}$$

A.2 Pseudo-code

B Additional experimental details

B.1 Description of the models

In the following we use the convention that $\mathcal{N}(\mu, \sigma^2)$ is a Gaussian distribution with mean μ and variance σ^2 .

Toy multivariate Gaussian This is a toy d -dimensional Bayesian model specified by

$$\begin{aligned} x &\sim \mathcal{N}_d(\mathbf{0}, \sigma_0^2 I) \\ y|x &\sim \mathcal{N}_d(x, I). \end{aligned}$$

By conjugacy, the posterior distribution for x given y is a multivariate Gaussian. In fact, the whole path of distributions $\beta \mapsto \pi^{(\beta)}$ is given by a family of Gaussians. To simplify matters, assume that $y = m\mathbf{1}$ for some $m \in \mathbb{R}$. Then, for all $\beta \in [0, 1]$,

$$\pi^{(\beta)} = \mathcal{N}_d(\mu(\beta)\mathbf{1}, \sigma(\beta)^2 I),$$

Algorithm 2 One step of NRST with fixed grid \mathcal{P} and affinities \mathcal{C} .

```

function NRSTSTEP( $x, i, \epsilon; \mathcal{P}, \mathcal{C}$ )
  # Tempering step
   $i_{\text{prop}} \leftarrow i + \epsilon$  ▷ Propose move
  if  $i_{\text{prop}} = N + 1$  then ▷ Bounce above
     $(i, \epsilon) \leftarrow (N, -1)$ 
  else if  $i_{\text{prop}} = -1$  then ▷ Bounce below
     $(i, \epsilon) \leftarrow (0, +1)$ 
  else ▷ Interior move
     $A \sim \text{Bern}(\alpha_{i, i_{\text{prop}}}(x))$  ▷ Use Eq. (4) with  $\mathcal{P}$  and  $\mathcal{C}$ 
    if  $A = 1$  then
       $i \leftarrow i_{\text{prop}}$ 
    else
       $\epsilon \leftarrow -\epsilon$ 
  # Exploration step
  if  $i > 0$  then
     $x \sim K_i(x, \cdot)$ 
  else
     $x \sim \pi_0$ 
  return  $(x, i, \epsilon)$ 

```

Algorithm 3 Running an NRST tour

```

function NRSTTOUR( $\mathcal{P}, \mathcal{C}$ )
  # Initialize from  $\nu$ 
   $x_0 \sim \pi_0$ 
   $(x, i, \epsilon) \leftarrow (x_0, 0, +1)$ 
   $\mathcal{T} \leftarrow \{(x, i, \epsilon)\}$  ▷ Initialize trace
  # Run NRST until  $\mathcal{A}$  is reached
  while  $i > 0$  or  $\epsilon = +1$  do
     $x, i, \epsilon \leftarrow \text{NRSTSTEP}(x, i, \epsilon; \mathcal{P}, \mathcal{C})$  ▷ Algorithm 2
     $\mathcal{T} \leftarrow \mathcal{T} \cup \{(x, i, \epsilon)\}$  ▷ Update trace
  return  $\mathcal{T}$ 

```

Algorithm 4 Parallelized Regenerative NRST

```

function PARALLELNRSST( $\mathcal{P}, \mathcal{C}, \alpha, \delta, \widehat{\text{TE}}$ )
   $K \leftarrow K_{\min}(\alpha, \delta, \widehat{\text{TE}})$  ▷ Eq. (12)
   $\mathcal{S} \leftarrow \emptyset$  ▷ Initialize storage
  Parallel For  $k \in \{1, \dots, K\}$  do
     $\mathcal{T}_k \leftarrow \text{NRSTTOUR}(\mathcal{P}, \mathcal{C})$  ▷ Algorithm 3
     $\mathcal{S} \leftarrow \mathcal{S} \cup \{\mathcal{T}_k\}$  ▷ Store tour trace
  return  $\mathcal{S}$ 

```

with

$$\mu(\beta) := \beta m \sigma(\beta)^2, \quad \sigma(\beta)^2 := \left(\beta + \frac{1}{\sigma_0^2} \right)^{-1}.$$

For Fig. 1 we use the parameters $d = 3$, $m = 2$, and $\sigma_0 = 2$.

Banana A 2-dimensional target density in the shape of a banana, as described in Equation 1 of [Pagani et al. \(2022\)](#)

$$\begin{aligned} x_1 &\sim \mathcal{N}(1, 10) \\ x_2 | x_1 &\sim \mathcal{N}(x_1^2, 0.1^2). \end{aligned}$$

Using the fact that $\mathbb{E}[x_2^2] = 11$ under this target, we set the reference to be

$$\begin{aligned} x_1 &\sim \mathcal{N}(1, 10) \\ x_2 &\sim \mathcal{N}(11, 10^2). \end{aligned}$$

Funnel A 20-dimensional target density based on Neal’s funnel ([Neal, 2003](#)), using the parametrization in [Modi et al. \(2023\)](#)

$$\begin{aligned} x_1 &\sim \mathcal{N}(0, 3^2) \\ x_i | x_1 &\sim \mathcal{N}(0, e^{x_1}), \quad i \in \{2, \dots, 20\}. \end{aligned}$$

We set the reference distribution to an isotropic Gaussian

$$x_i \stackrel{\text{i.i.d.}}{\sim} \mathcal{N}(0, 3^2), \quad i \in \{1, \dots, 20\}.$$

Hierarchical Model A slightly modified version of the hierarchical model described in [Yao et al. \(2022, §6.3\)](#). It is different only in that our model puts a Cauchy prior on μ instead of the (improper) uniform density on \mathbb{R} . This allows us to obtain a proper prior distribution that can be used as reference

$$\begin{aligned} \mu &\sim \text{Cauchy} \\ \tau^2, \sigma^2 &\stackrel{\text{i.i.d.}}{\sim} \text{InverseGamma}(0.1, 0.1) \\ \theta_j | \mu, \tau^2 &\sim \mathcal{N}(\mu, \tau^2), \quad j \in \{1, \dots, J\} \\ Y_{i,j} | \theta_j, \sigma^2 &\sim \mathcal{N}(\theta_j, \sigma^2), \quad i \in \{1, \dots, M\}, j \in \{1, \dots, J\}. \end{aligned}$$

We generate a dataset \mathbf{Y} with $J = 8$ and $M = 20$ by performing rejection sampling from this model, constraining the output to have a between-group variance 16 times larger than the within-group variance.

mRNA Transfection This is a time series model taken from [Ballnus et al. \(2017\)](#)

$$\begin{aligned} \log_{10}(t_0) &\sim \text{Unif}(-2, 1) \\ \log_{10}(\kappa), \log_{10}(\beta), \log_{10}(\delta) &\stackrel{\text{i.i.d.}}{\sim} \text{Unif}(-5, 5) \\ \log_{10}(\sigma) &\sim \text{Unif}(-2, 5) \\ y_i | t_0, \kappa, \beta, \delta, \sigma &\sim \mathcal{N}(\mu(t_i | t_0, \beta, \delta), \sigma^2), \quad i \in \{1, \dots, n_{\text{obs}}\}, \end{aligned}$$

where

$$\mu(t_i | t_0, \beta, \delta) := \frac{\kappa}{\delta - \beta} [\exp(-\beta(t_i - t_0)) - \exp(-\delta(t_i - t_0))].$$

We use the dataset provided in [Surjanovic et al. \(2022\)](#).

Threshold Weibull This is a 3-parameter Weibull distribution that adds a threshold to the usual 2-parameter family. This creates a likelihood function that is unbounded from above, which usually complicates standard frequentist inference. The likelihood model is taken from [Cheng \(2017, Ch. 8\)](#), and we use the dataset “SteenStickler0” provided there. Finally, we put an uninformative prior to obtain a fully specified Bayesian model

$$\begin{aligned} a &\sim \text{Unif}(0, 200) \\ b &\sim \text{InverseGamma}(0.1, 0.1) \\ c &\sim \text{Unif}(0.1, 10) \\ y_i | a, b, c &\sim \text{Weibull}(a, b, c). \end{aligned}$$

where the 3-parameter Weibull density is

$$p(y | a, b, c) = \mathbb{1}\{y > a\} \frac{c}{b} \left(\frac{y - a}{b}\right)^{c-1} \exp\left[-\left(\frac{y - a}{b}\right)^c\right].$$

XY Model This is a classical 2-dimensional lattice model of statistical mechanics. We focus on the nearest neighbor case with periodic boundaries, using a constant interaction $J = 2$ and no external field. Thus, the potential function can be written as

$$\forall x \in \mathbb{R}^{n^2} : V(x) := -J \sum_{(i,j) \in E} \cos(x_i - x_j),$$

where E is the edge set of the lattice. In our simulations we use a square lattice with sides of length $n = 8$. As reference, we use the uniform distribution

on $[-\pi, \pi]^{n^2}$ (i.e., the microcanonical ensemble). This model is interesting because it induces a phase transition in the path of distributions $\beta \mapsto \pi^{(\beta)}$ (see e.g. [Hasenbusch, 2005](#)).

B.2 Experimentally choosing hyperparameters

Let \mathcal{M} be the collection of models, and furthermore, let \mathcal{S} be a finite set of pseudo-random number generator (PRNG) seeds. To select a *good* default configuration, we first define a fixed sample quality ($\alpha = 0.95, \delta = 0.5$) for Algorithm 4. Then, for each model $m \in \mathcal{M}$ we find the highest cost across seeds produced by every mix of hyper-parameters

$$\text{WorstCost}_m(c', \gamma, \bar{\kappa}) := \max_{s \in \mathcal{S}} \text{Cost}(\text{model} = m, \text{seed} = s; c', \gamma, \bar{\kappa}),$$

where the right-hand side corresponds to a cost measure of running Algorithm 4 with the specified settings and sample quality controlled by the pair (α, δ) . Also, let

$$\forall m \in \mathcal{M} : (c'_m, \gamma_m, \bar{\kappa}_m) = \arg \min_{c', \gamma, \bar{\kappa}} \text{WorstCost}_m(c', \gamma, \bar{\kappa})$$

be the model-specific worst-case-optimal configuration. Then, we choose as default hyper-parameters the triplet that minimizes the highest cost increase across models relative to their own optimal configuration

$$(c'_*, \gamma_*, \bar{\kappa}_*) = \arg \min_{c', \gamma, \bar{\kappa}} \max_{m \in \mathcal{M}} \text{WorstCost}_m(c', \gamma, \bar{\kappa}) - \text{WorstCost}_m(c'_m, \gamma_m, \bar{\kappa}_m).$$

A visualization of the behavior of each model using every combination of the hyper-parameters is available in Fig. 9 at the end of this section. In the following, we give a high-level description of the findings.

Affinity slope function Fig. 6 shows the result of setting the slope function to either of the two possible options—mean or median—while the other parameters are held fixed at their default values. The experiments is run on 6 different models and replicated for 30 seeds. Additionally, the results are evaluated using the two varieties of elapsed-time discussed in Section 7.1: serial (equivalent to total evaluations of V) and fully parallel (considering only the maximum number of evaluations in a tour).

The most relevant aspect of Fig. 6 is the reversal of preferences depending on the cost measure used. Indeed, under the serial run time lens, the box-plots for the mean strategy are in most cases well below the ones for the

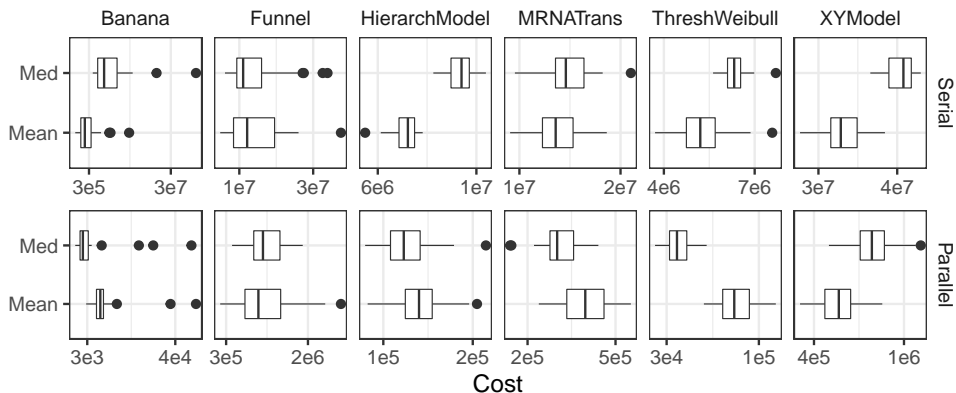


Figure 6: Cost of running Algorithm 4 versus the affinity tuning strategy, for each of 6 selected models. Rows correspond to the two distinct elapsed-time metrics defined in Section 7.1. Each experiment is replicated 30 times. The number of tours is determined in a quality-consistent approach using Eq. (12) with $\alpha = 0.95$, $\delta = 0.5$, and $\widehat{\text{TE}}$ estimated in a preliminary run.

median. The worst-case cost reductions are in the order of 30%, except for the Banana model where it is orders of magnitude lower. On the other hand, when the experiments are evaluated in terms of the running time of a fully parallelized setting, the median strategy generally takes the lead. The largest reduction happens in the “ThresholdWeibull” model, where the median approach has one third of the parallel cost of the mean.

In order to keep the complexity of the rest of the paper manageable, in the following we focus exclusively on the serial cost measure. Since this is an upper bound on the parallelized elapsed-time (for any number of available workers), minimizing serial time still helps in controlling parallel cost. And since the mean-energy strategy performs better in the serial cost metric, we set it as default for the rest of this section.

Autocorrelation limit Fig. 7 shows the summary of the experiments where $\bar{\kappa}$ is varied, while leaving $\gamma = 2$ fixed and using the mean strategy. We also show a control case (“Fix”) where exploration steps are set to 3 in all levels regardless of autocorrelation. We chose this value because it is close to the average number exploration step obtained via autocorrelation tuning. In most cases, fixing is significantly more costly (around 2 times) than tuning the number of exploration steps. The reason is that, in general, most intermediate distributions $\pi^{(\beta)}$ are easy to explore, so that even 1 exploration step is sometimes enough to achieve a low-correlated sample

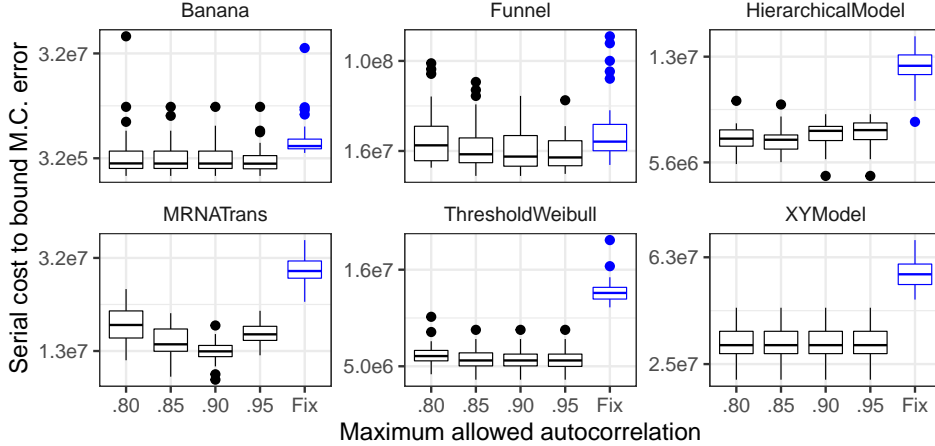


Figure 7: Serial cost (as defined in Section 7.1) versus the maximum allowed correlation parameter $\bar{\kappa}$, for each of 6 selected models. Each experiment is replicated 30 times. The number of tours is determined in a quality-consistent approach using Eq. (12) with $\alpha = 0.95$, $\delta = 0.5$, and $\widehat{\text{TE}}$ estimated in a preliminary run. “Fix” means that exploration steps were not tuned but simply fixed to 3 across all levels.

$V(x)$. Only few intermediate distributions are truly complex and thus require many more than 3 steps to achieve mixing in $V(x)$. Autocorrelation-based tuning can exploit this, concentrating efforts where they are most necessary.

The second thing to notice in Fig. 7 is that varying $\bar{\kappa}$ does not generally produce significantly different cost distributions. The paradigmatic example is the “XYModel”, where using 1 exploration step already gives auto-correlations lower than 0.8. This insensitivity to $\bar{\kappa}$ means that the algorithm is robust to this choice.

Grid size correction In Section 5, we derived a formula for the grid size N that minimizes the expected number of steps taken in a run where the number of tours is determined via $K_{\min}(\alpha, \delta, \text{TE})$ (Eq. (12)). This measure should be a good proxy of the serial running time when the exploration effort at each level is roughly the same.

Fig. 8 shows the serial cost for different values of γ , while fixing $\bar{\kappa} = 0.95$ and using the mean strategy. We can see that the median cost does decrease towards $\gamma = 1$, which supports the derivations from Section 5. However, the worst-case cost does not follow this pattern in at least half the models. The most likely reason is that the quality of the tuning process for the grid and affinities deteriorates as N decreases. Indeed, the interpolation used to set

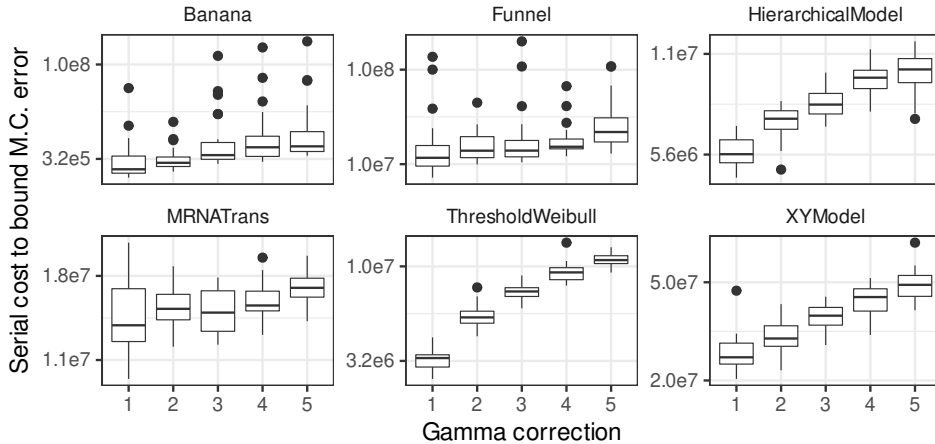


Figure 8: Serial cost (as defined in Section 7.1) versus the correction parameter γ in Section 5.5, for each of 6 selected models. Each experiment is replicated 30 times. The number of tours is determined in a quality-consistent approach using Eq. (12) with $\alpha = 0.95$, $\delta = 0.5$, and $\widehat{\text{TE}}$ estimated in a preliminary run.

grid points and the estimators used in setting affinities worsen as the grid becomes coarser. Thus, though adaptation still works in most cases at $\gamma = 1$, it becomes brittle and susceptible to yielding high-cost configurations. For this reason, we set $\gamma = 2$ as the default value.

B.3 Tuning of competing ST algorithms

In order to quantify the effect of our tuning strategy, for the experiments in Section 7.1 we apply to all samplers both the approach outlined in Section 5 and the tuning schemes recommended by their own authors.

In particular, SH16 uses a uniformly-spaced grid, and estimates $\log(\mathcal{Z}(\beta))$ on-the-fly—i.e., running simulated tempering sequentially with arbitrary affinities and adjusting them at each step by approximating the thermodynamic identity using the trace of $V(x_n)$ —as described in (Sakai and Hukushima, 2016b). FBDR also employs a uniformly-spaced grid, but it uses a simpler approach for setting the affinities described in Park and Pande (2007). The idea is to collect V samples at each level by running the explorers independently. The log normalizing constants are then calculated using the thermodynamic identity. Finally, Geyer and Thompson (1995) propose a more complex tuning method that iteratively adapts both the grid and the affinities. The former is adjusted to promote equi-rejection, targeting an

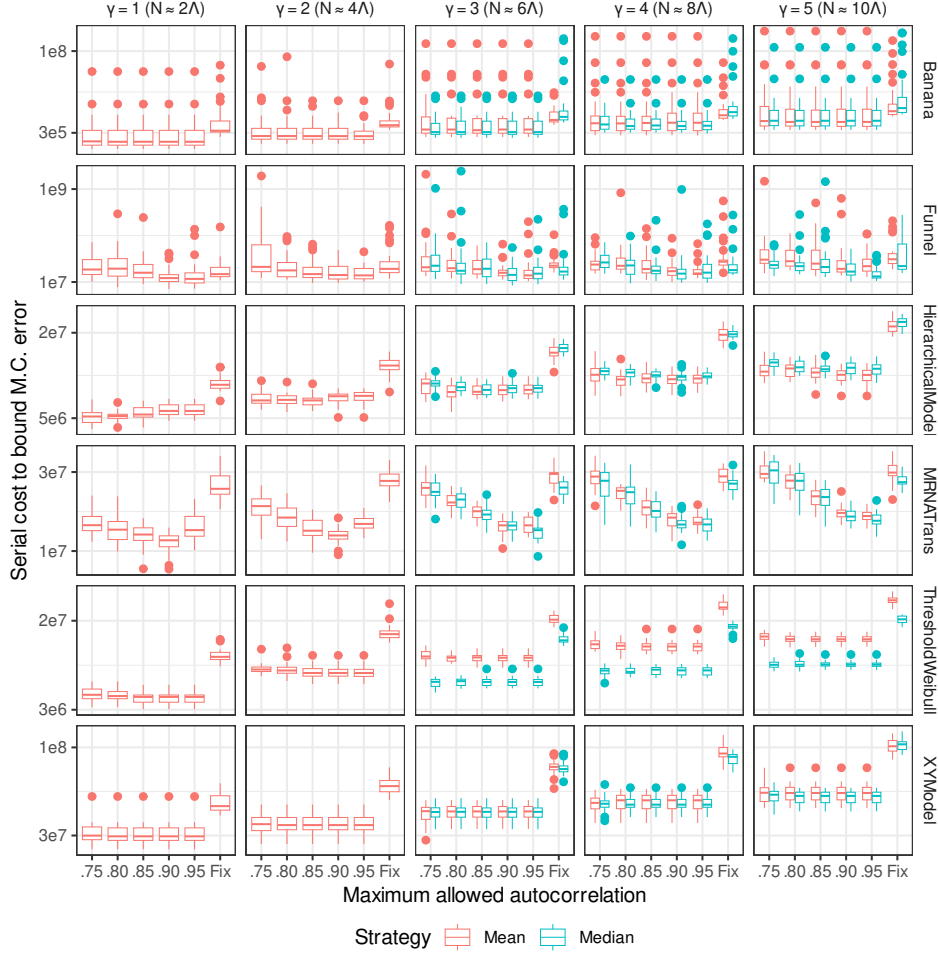


Figure 9: Serial cost (as defined in Section 7.1) by affinity tuning strategy, maximum allowed correlation parameter $\bar{\kappa}$, and grid size parameter γ , for each of 6 selected models. Each combination is replicated 30 times. The number of tours is determined in a quality-consistent approach using Eq. (12) with $\alpha = 0.95$, $\delta = 0.5$, and $\widehat{\text{TE}}$ estimated in a preliminary run. “Fix” means that exploration steps were not tuned but simply fixed to 3 across all levels.

average rejection rate between 20% and 40%. The log-normalizing constants, in turn, are adjusted using a stochastic approximation method. Sadly, this tuning strategy contains model-sensitive hyper-parameters and is not described in enough detail in Geyer and Thompson (1995). Hence, it was impossible for us to replicate robustly, and we opted for tuning GT95 using

the parameters obtained by FBDR.

C Proofs

We begin by stating some basic assumptions, summarizing the notation used so far, and also introducing additional concepts necessary for this section. We assume that the base state space \mathcal{X} is Polish, and let Σ be its associated Borel sigma algebra such that (\mathcal{X}, Σ) is a measurable space. As defined in Section 3, for all $\beta \in [0, 1]$ we let $\mathbb{E}^{(\beta)}$ be the expectation operator associated to the tempered distribution $\pi^{(\beta)}$ on (\mathcal{X}, Σ) .

The fact that \mathcal{X} is Polish implies that $\tilde{\mathcal{X}}$ —the product space for NRST defined in Eq. (6)—is also Polish. Let $\tilde{\Sigma}$ be its Borel sigma algebra—which is identical to the product sigma algebra—so that $(\tilde{\mathcal{X}}, \tilde{\Sigma})$ is a measurable space. Recall that the lifted distribution $\tilde{\pi}$ is defined on $(\tilde{\mathcal{X}}, \tilde{\Sigma})$, and that we use $\tilde{\pi}(f)$ to denote the expectation under $\tilde{\pi}$ of a measurable function $f : \tilde{\mathcal{X}} \rightarrow \mathbb{R}$.

Now, the kernel \mathbf{K} , together with an initial distribution μ on $(\tilde{\mathcal{X}}, \tilde{\Sigma})$, define the NRST Markov chain $\tilde{\mathbf{x}} = \{\tilde{x}_n\}_{n=0}^\infty$ on the path space $(\tilde{\mathcal{X}}^\infty, \tilde{\Sigma}^\infty)$. Let \mathbb{P}_μ denote the law of $\tilde{\mathbf{x}}$ and \mathbb{E}_μ its corresponding expectation operator. In particular, as we did in Section 3, we write \mathbb{P}_ν for the law of the chain initialized from the renewal measure ν (Eq. (7)) associated to the NRST atom \mathcal{A} . When $\mu = \delta_{\tilde{x}}$ for some $\tilde{x} \in \tilde{\mathcal{X}}$, we simply write $\mathbb{P}_{\tilde{x}}$ and $\mathbb{E}_{\tilde{x}}$.

We use $\{\mathcal{F}_n\}_{n=0}^\infty$ to denote the natural filtration of the Markov chain. For $j \in \mathbb{N}$, let $\theta_j : \tilde{\mathcal{X}}^\infty \rightarrow \tilde{\mathcal{X}}^\infty$ denote the shift operator defined by $\theta_j(\{\tilde{x}_n\}_{n=0}^\infty) = \{\tilde{x}_{j+n}\}_{n=0}^\infty$. For any $S \in \tilde{\Sigma}$, define the stopping times

$$\begin{aligned} T_S &:= \inf\{n \geq 0 : \tilde{x}_n \in S\} \\ \sigma_S &:= \inf\{n \geq 1 : \tilde{x}_n \in S\}, \end{aligned} \tag{28}$$

known, respectively, as the first-hitting time and the first-return time of the set S . Furthermore, recursively define the sequences of return times $\{T_S^{(k)}\}_{k \in \mathbb{N}}$ and hitting times $\{\sigma_S^{(k)}\}_{k \in \mathbb{N}}$ by setting $T_S^{(1)} = T_S$, $\sigma_S^{(1)} = \sigma_S$, and for all $k \in \mathbb{N}$,

$$\begin{aligned} T_S^{(k+1)} &:= \inf\{n \geq T_S^{(k)} : \tilde{x}_n \in S\} \\ \sigma_S^{(k+1)} &:= \inf\{n \geq \sigma_S^{(k)} : \tilde{x}_n \in S\}. \end{aligned}$$

In particular, when $S = \mathcal{A}$, we get that $T_{\mathcal{A}}^{(k)} = T_k$ as defined in Section 3.1.

Finally, in the following we assume that for all $i \in \{0, \dots, N\}$, the exploration kernel K_i is π_i -irreducible in addition to π_i -invariant.

C.1 Proofs for Section 3.1

Proposition C.1. *The Markov kernel \mathbf{K} is $\tilde{\pi}$ -invariant.*

Proof. Since the composition of $\tilde{\pi}$ -invariant kernels is $\tilde{\pi}$ -invariant, it suffices to show that both \mathbf{K}_e and \mathbf{K}_t satisfy this property. For the former, note that for all $A \in \Sigma$, $i \in \{0, \dots, N\}$ and $\epsilon \in \{-1, +1\}$

$$\begin{aligned} & [\tilde{\pi}\mathbf{K}_e](A, i, \epsilon) \\ &= \frac{1}{2} \sum_{\epsilon' \in \{-1, +1\}} \sum_{j=0}^N p_j \int \pi_j(dx) K_j(x, A) \mathbb{1}\{j = i\} \mathbb{1}\{\epsilon' = \epsilon\} \\ &= \frac{1}{2} p_i \int \pi_i(dx) K_i(x, A) \\ &= \tilde{\pi}(A, i, \epsilon), \end{aligned}$$

due to K_i being π_i -invariant.

The tempering step can be understood as the composition of two Metropolis steps. Since Metropolis kernels are $\tilde{\pi}$ -reversible, they are $\tilde{\pi}$ -invariant. This shows that the tempering kernel is itself invariant, since it is the composition of invariant kernels. It remains to derive their acceptance probabilities. In the first step we deterministically propose

$$(x_{\text{prop}}, i_{\text{prop}}, \epsilon_{\text{prop}}) = (x, i + \epsilon, -\epsilon).$$

Note that this move is an *involution* (Tierney, 1998, §2); i.e., it is its own inverse, since applying it twice gives

$$(i, \epsilon) \mapsto (i + \epsilon, -\epsilon) \mapsto (i + \epsilon - \epsilon, -(-\epsilon)) = (i, \epsilon).$$

Then, the Metropolis ratio for the first step becomes

$$\frac{\tilde{\pi}(x, i + \epsilon, -\epsilon)}{\tilde{\pi}(x, i, \epsilon)} = \frac{\pi_{i+\epsilon}(x) p_{i+\epsilon}}{\pi_i(x) p_i}.$$

The second move aims to correct the reversal of the velocity that occurs when the tempering step is accepted, which would prevent the sampler from having momentum. To achieve this, we fix x and i , and use the deterministic involutive proposal $\epsilon_{\text{prop}} = -\epsilon$. By definition of $\tilde{\pi}$, this proposal is always accepted, since

$$\frac{\tilde{\pi}(x, i, -\epsilon)}{\tilde{\pi}(x, i, \epsilon)} = \frac{\frac{1}{2}\pi_i(x)p_i}{\frac{1}{2}\pi_i(x)p_i} = 1.$$

It follows that the probability of jointly accepting both sub-steps—and thus the tempering proposal—is precisely the quantity in Eq. (4). \square

Lemma C.2.

1. \mathcal{A} is recurrent.
2. \mathcal{A} is accessible; i.e., $\mathbb{P}_{\tilde{x}_0}(\sigma_{\mathcal{A}} < \infty) > 0$ for $\tilde{\pi}$ -a.e. \tilde{x}_0 .

Proof.

1. Since $\tilde{\pi}(\mathcal{A}) = p_0/2 > 0$, \mathcal{A} is recurrent by Prop. 6.2.8(i) in Douc et al. (2018).

2. Let $\tilde{x}_0 = (x_0, i_0, \epsilon_0) \in \tilde{\mathcal{X}}$. Note that if $\tilde{x}_0 \in \mathcal{A}$, we know that $\mathbb{P}_{\tilde{x}_0}(\tilde{x}_1 \notin \mathcal{A}) = 1$, so by the Markov property

$$\forall \tilde{x}_0 \in \mathcal{A} : \mathbb{P}_{\tilde{x}_0}(\sigma_{\mathcal{A}} < \infty) = \mathbb{E}_{\tilde{x}_0}[\mathbb{P}_{\tilde{x}_1}(\sigma_{\mathcal{A}} < \infty)].$$

The right-hand side is positive if accessibility holds for $\tilde{x}_0 \notin \mathcal{A}$. Let us focus on this case. In particular, when $\epsilon_0 = -1$,

$$\mathbb{P}_{\tilde{x}_0}(\sigma_{\mathcal{A}} < \infty) = \mathbb{P}_{\tilde{x}_0} \left(\bigcup_{n \in \mathbb{N}} \{\tilde{x}_n \in \mathcal{A}\} \right) \geq \mathbb{P}_{\tilde{x}_0}(\tilde{x}_{i_0} \in \mathcal{A}).$$

The bound on the right-hand side is the probability of a perfect return to the atom in exactly i_0 steps, which is positive because

$$\begin{aligned} \mathbb{P}_{\tilde{x}_0}(\tilde{x}_{i_0} \in \mathcal{A}) &= \mathbb{P}_{\tilde{x}_0}(i_1 = i_0 - 1, i_2 = i_0 - 2, \dots, i_{i_0} = 0) \\ &= \alpha_{i_0, i_0-1}(x_0) \prod_{j=1}^{i_0} \int K_{i_0-j}(x_{j-1}, dx_j) \alpha_{i_0-j, i_0-j-1}(x_j) \\ &> 0. \end{aligned}$$

The inequality follows from 1) the fact that for all $i \in \{1, \dots, N\}$, $\alpha_{i, i-1}(x) > 0$ π -a.s.—because $V(x) < \infty$ π -a.s.—and 2) the assumption that the exploration kernels $\{K_i\}_{i=1}^N$ are π_i -invariant and π_i -irreducible.

Finally, to tackle the remaining case $\epsilon_0 = +1$, note that the set

$$\mathcal{N} := \mathcal{X} \times \{0, \dots, N\} \times \{-1\}$$

has $\mathbb{P}_{\tilde{x}_0}(T_{\mathcal{N}} < \infty) = 1$ due to the boundary at $i = N$. Hence

$$\mathbb{P}_{\tilde{x}_0}(\sigma_{\mathcal{A}} < \infty) = \mathbb{E}_{\tilde{x}_0}[\mathbb{P}_{\tilde{x}_{T_{\mathcal{N}}}}(\sigma_{\mathcal{A}} < \infty)] > 0,$$

because $\tilde{x}_{T_{\mathcal{N}}} = (x_{T_{\mathcal{N}}}, i_{T_{\mathcal{N}}}, -1)$ and thus the bound follows from the case $\epsilon_0 = -1$. \square

Lemmas C.3 and C.4 below have the sole purpose of translating results between two conventions: from the atomic Markov chain theory—where tours are started at the atom—to the regenerative simulation approach—where tours begin with a regeneration. With these tools, we can then simply leverage existing results for atomic Markov chains in Lemma C.5 and Theorem 3.1.

Lemma C.3. *For all $\mathcal{S} \in \tilde{\Sigma}$, $k \in \mathbb{N}$, and $\omega \in \tilde{\mathcal{X}}^\infty$: $\sigma_{\mathcal{S}}^{(k)}(\omega) = 1 + [T_{\mathcal{S}}^{(k)} \circ \theta_1](\omega)$.*

Proof. We make the dependence on ω implicit to avoid cluttering the notation. Let us proceed by induction. First, note that

$$\sigma_{\mathcal{S}} = \inf\{n > 0 : \tilde{x}_n \in \mathcal{S}\} = 1 + \inf\{n \geq 0 : \tilde{x}_{n+1} \in \mathcal{S}\} = 1 + T_1 \circ \theta_1.$$

Now, assume $\sigma_{\mathcal{S}}^{(k-1)} = 1 + T_{\mathcal{S}}^{(k-1)} \circ \theta_1$. Then

$$\begin{aligned} \sigma_{\mathcal{S}}^{(k)} &= \inf\{n > \sigma_{\mathcal{S}}^{(k-1)} : \tilde{x}_n \in \mathcal{S}\} \\ &= \inf\{n > 1 + T_{\mathcal{S}}^{(k-1)} \circ \theta_1 : \tilde{x}_n \in \mathcal{S}\} \\ &= 1 + \inf\{n > T_{\mathcal{S}}^{(k-1)} \circ \theta_1 : \tilde{x}_n \circ \theta_1 \in \mathcal{S}\} \\ &= 1 + \inf\{n > T_{\mathcal{S}}^{(k-1)} : \tilde{x}_n \in \mathcal{S}\} \circ \theta_1 \\ &= 1 + T_{\mathcal{S}}^{(k)} \circ \theta_1, \end{aligned}$$

as needed. □

Lemma C.4. *Let $f : \mathcal{X} \rightarrow \mathbb{R}$ be a $\tilde{\Sigma}$ -measurable function. Define*

$$z_1(f) := \sum_{n=1}^{\sigma_{\mathcal{A}}} f(\tilde{x}_n), \quad \forall k \geq 2 : z_k(f) := \sum_{n=\sigma_{\mathcal{A}}^{(k-1)}+1}^{\sigma_{\mathcal{A}}^{(k)}} f(\tilde{x}_n). \quad (29)$$

Then,

1. *for all $k \in \mathbb{N}$ and $\omega \in \tilde{\mathcal{X}}^\infty$, $[z_k(f)](\omega) = [s_k(f) \circ \theta_1](\omega)$, and*
2. *under $\mathbb{P}_{\tilde{x}}$ for $\tilde{x} \in \mathcal{A}$, the real-valued stochastic process $\{z_k(f)\}_{k \in \mathbb{N}}$ has the same finite dimensional distributions as $\{s_k(f)\}_{k \in \mathbb{N}}$ under \mathbb{P}_ν ,*

where $\{s_k(f)\}_{k \in \mathbb{N}}$ are the tour sums of f (see Section 3.1).

Proof.

1. As in previous results, we make the dependence on ω implicit to avoid cluttering the notation. Using Lemma C.3, we see that

$$\sum_{n=1}^{\sigma_{\mathcal{A}}} f(\tilde{x}_n) = \sum_{n=1}^{1+T_1 \circ \theta_1} f(\tilde{x}_n) = \sum_{n=0}^{T_1 \circ \theta_1} f(\tilde{x}_n \circ \theta_1) = s_1(f) \circ \theta_1.$$

Similarly, for $k \geq 2$,

$$\sum_{n=\sigma_{\mathcal{A}}^{(k-1)}+1}^{\sigma_{\mathcal{A}}^{(k)}} f(\tilde{x}_n) = \sum_{n=(1+T_{k-1} \circ \theta_1)+1}^{1+T_k \circ \theta_1} f(\tilde{x}_n) = \sum_{n=T_{k-1} \circ \theta_1+1}^{T_k \circ \theta_1} f(\tilde{x}_n \circ \theta_1) = s_k(f) \circ \theta_1.$$

2. It suffices to show that for all $\tilde{x} \in \mathcal{A}$, $K \in \mathbb{N}$, and any collection of Borel sets $\{A_k\}_{k=1}^K$,

$$\mathbb{P}_{\tilde{x}} \left(\bigcap_{k=1}^K z_k(f) \in A_k \right) = \mathbb{P}_{\nu} \left(\bigcap_{k=1}^K s_k(f) \in A_k \right).$$

Indeed, using part 1., we have by the Markov property

$$\begin{aligned} \mathbb{P}_{\tilde{x}} \left(\bigcap_{k=1}^K s_k(f) \circ \theta_1 \in A_k \right) &= \mathbb{E}_{\tilde{x}} \left[\mathbb{E}_{\tilde{x}} \left[\left(\prod_{k=1}^K \mathbb{1}\{s_k(f) \in A_k\} \right) \circ \theta_1 \middle| \mathcal{F}_1 \right] \right] \\ &= \mathbb{E}_{\tilde{x}} \left[\mathbb{E}_{\tilde{x}_1} \left[\prod_{k=1}^K \mathbb{1}\{s_k(f) \in A_k\} \right] \right] \\ &= \mathbb{P}_{\nu} \left(\bigcap_{k=1}^K s_k(f) \in A_k \right). \end{aligned}$$

□

Lemma C.5. *For any $\tilde{\Sigma}$ -measurable function f , its tour sums $\{s_k(f)\}_{k \in \mathbb{N}}$ —as defined in Section 3.1—are an i.i.d. collection under \mathbb{P}_{ν} .*

Proof. Since \mathcal{A} is recurrent by Lemma C.2, Corollary 6.5.2 in Douc et al. (2018) shows that the random variables $\{z_k(f)\}_{k \in \mathbb{N}}$ defined in Eq. (29) are i.i.d. under $\mathbb{P}_{\tilde{x}}$ for all $\tilde{x} \in \mathcal{A}$. This means that for any K and any collection of Borel sets $\{A_k\}_{k=1}^K$

$$\forall \tilde{x} \in \mathcal{A} : \mathbb{P}_{\tilde{x}} \left(\bigcap_{k=1}^K z_k(f) \in A_k \right) = \prod_{k=1}^K \mathbb{P}_{\tilde{x}}(z_1(f) \in A_k).$$

The above, together with Lemma C.4, imply that

$$\mathbb{P}_{\nu} \left(\bigcap_{k=1}^K s_k(f) \in A_k \right) = \mathbb{P}_{\nu}(s_1(f) \in A_k).$$

We conclude that $\{s_k(f)\}_{n \in \mathbb{N}}$ is i.i.d. under \mathbb{P}_{ν} .

□

Proof of Theorem 3.1. By Lemma C.2, \mathcal{A} is recurrent and accessible. Therefore, Theorem 6.4.2(iii) in Douc et al. (2018) shows that $\tilde{\pi}$ is proportional to the finite measure $\lambda_{\mathcal{A}}$, defined by its action on measurable functions $f : \tilde{\mathcal{X}} \rightarrow \mathbb{R}$

$$\lambda_{\mathcal{A}}(f) := \mathbb{E}_{\tilde{x}}[z_1(f)],$$

where $\tilde{x} \in \mathcal{A}$, and $\{z_k(f)\}_{k \in \mathbb{N}}$ are defined in Eq. (29). By Lemma C.4, the distribution of $z_1(f)$ under $\mathbb{P}_{\tilde{x}}$ when $\tilde{x} \in \mathcal{A}$ is the same as the distribution of $s_1(f)$ under \mathbb{P}_{ν} . Hence,

$$\lambda_{\mathcal{A}}(f) = \mathbb{E}_{\nu}[s_1(f)].$$

Its normalizing constant can be recovered using $f \equiv 1$, so that

$$\tilde{\pi}(f) = \frac{\lambda_{\mathcal{A}}(f)}{\lambda_{\mathcal{A}}(1)} = \frac{\mathbb{E}_{\nu}[s_1(f)]}{\mathbb{E}_{\nu}[\tau_1]}.$$

Thus,

$$\mathbb{E}_{\nu}[s_1(f)] = \tilde{\pi}[f] \mathbb{E}_{\nu}[\tau_1].$$

It follows that $\{s_k\}_{k \in \mathbb{N}}$ is a collection of i.i.d. random variables (Lemma C.5) with common expectation given by the expression above. In particular, using $f = \mathbb{1}_{\mathcal{A}}$, and noting that $s_1(f) = 1$ \mathbb{P}_{ν} -a.s., gives

$$\mathbb{E}_{\nu}[\tau] = \frac{1}{\tilde{\pi}(\mathcal{A})} = \frac{2}{p_0}.$$

Finally, the strong law of large numbers for i.i.d. random variables shows that

$$\lim_{k \rightarrow \infty} \frac{\sum_{n=0}^{T_k} f(\tilde{x}_n)}{\sum_{n=0}^{T_k} g(\tilde{x}_n)} = \lim_{k \rightarrow \infty} \frac{\frac{1}{k} \sum_{j=1}^k s_j(f)}{\frac{1}{k} \sum_{j=1}^k s_j(g)} = \frac{\mathbb{E}_{\nu}[s(f)]}{\mathbb{E}_{\nu}[s(g)]} = \frac{\tilde{\pi}[f]}{\tilde{\pi}[g]}, \quad \mathbb{P}_{\nu}\text{-a.s.}$$

□

Proof of Theorem 3.2. The proof draws from the informal exposition in Ripley (1987, Ch. 6.4). To de-clutter the notation, let

$$\sigma_d^2 := \mathbb{E}_{\nu}[s(\mathbb{1}\{i = N\})(h(x) - \pi(h))^2],$$

and

$$\hbar_k := s_k(h(x) \mathbb{1}\{i = N\}), \quad k \in \mathbb{N}.$$

By Theorem 3.1, for all $k \in \mathbb{N}$

$$\mathbb{E}_\nu[\hat{h}_k] = \mathbb{E}_\nu[v]\pi(h), \quad \mathbb{E}_\nu[v] = \frac{2p_N}{p_0}.$$

On the other hand,

$$\hat{R}_k(h) - \pi(h) = \frac{\sum_{j=1}^k \hat{h}_j}{\sum_{j=1}^k v_j} - \pi(h) = \frac{\sum_{j=1}^k (\hat{h}_j - \pi(h)v_j)}{\sum_{j=1}^k v_j}.$$

Let

$$d_k := \hat{h}_k - \pi(h)v_k = s_k(\mathbf{1}\{i = N\}(h(x) - \pi(h))), \quad k \in \mathbb{N}.$$

By Lemma C.5, $\{d_k\}_{k \in \mathbb{N}}$ is a collection of i.i.d. random variables under \mathbb{P}_ν , with zero mean and variance σ_d^2 . Thus, by the Central Limit Theorem

$$k^{-1/2} \sum_{j=1}^k d_j = k^{1/2} \left(\frac{1}{k} \sum_{j=1}^k d_j \right) \xrightarrow{d} \mathcal{N}(0, \sigma_d^2).$$

Now let us write

$$k^{1/2}(\hat{R}_k(h) - \pi(h)) = \frac{k^{-1/2} \sum_{j=1}^k d_j}{k^{-1} \sum_{j=1}^k v_j} = \frac{a_k}{b_k}.$$

We showed that $a_k \xrightarrow{d} Z$ where $Z \sim \mathcal{N}(0, \sigma_d^2)$, while $b_k \xrightarrow{a.s.} \mathbb{E}_\nu[v]$ by Theorem 3.1. Using Theorem 2.7(v) in van der Vaart (1998), we have that $(a_k, b_k) \xrightarrow{d} (Z, \mathbb{E}_\nu[v])$. Since $\mathbb{E}_\nu[v] = 2p_0/p_N > 0$, by the continuous mapping theorem (van der Vaart, 1998, Thm. 2.3) we conclude that

$$k^{1/2}(\hat{R}_k(h) - \pi(h)) \xrightarrow{d} \mathcal{N} \left(0, \left[\frac{\sigma_d}{\mathbb{E}_\nu[v]} \right]^2 \right).$$

□

C.2 Proofs for Section 4.1

Lemma C.6. *Under Assumption 4.1, for all $i \in \{0, \dots, N\}$ and π -almost every x ,*

$$K_i(x, dv') = \pi_i^{(V)}(dv'),$$

where the right-hand side is the push-forward of π_i under V .

Proof. For $i \in \{1, \dots, N\}$, let

$$K_i(x, dv') = \int_{x'} K_i(x, dx') \delta_{V(x')}(dv'),$$

be the push-forward of $K_i(x, dx')$ under V . By Assumption 4.1, $K_i(x, dv') = q_i(dv')$ for π -almost every x . On the other hand, since K_i is π_i invariant for every $i \in \{1, \dots, N\}$, it follows that $x' \sim \pi_i$ whenever $x \sim \pi_i$. In particular, this means that $v' \sim \pi_i^{(V)}$ whenever $x \sim \pi_i$. The only possible choice for q_i that makes these statements consistent is $q_i = \pi_i^{(V)}$, for all $i \in \{1, \dots, N\}$. \square

Proof of Proposition 4.2. We concentrate on NRST because the proof for ST is identical. Since $\mathcal{X} \times \mathbb{R}$ is a Polish space, for π -almost every x , there exists a regular conditional probability $K_i((x, v'), dx')$ (Dudley, 2002, Theorem 10.2.2) such that the joint distribution of $(x', v' = V(x'))$ conditional on x can be written as

$$K_i(x, dx') \delta_{V(x')}(dv') = K_i(x, dv') K_i((x, v'), dx'),$$

where $K_i(x, dv')$ is the push-forward of $K_i(x, dx')$ under V . By Assumption 4.1 and Lemma C.6,

$$K_i(x, dx') \delta_{V(x')}(dv') = \pi_i^{(V)}(dv') K_i((x, v'), dx'). \quad (30)$$

Hence, for π -almost every x and all (i, ϵ) , the marginal distribution of (i', ϵ')

conditional on (x, i, ϵ) after a full NRST step is

$$\begin{aligned}
& \mathbf{K}((x, i, \epsilon), (\mathcal{X}, i', \epsilon')) \\
&= \int_{x^*} \sum_{i^*, \epsilon^*} \mathbf{K}_e((x, i, \epsilon), (dx^*, i^*, \epsilon^*)) \mathbf{K}_t((x^*, i^*, \epsilon^*), (\mathcal{X}, i', \epsilon')) \\
&= \int_{x^*} K_i(x, dx^*) \mathbf{K}_t((x^*, i, \epsilon), (\mathcal{X}, i', \epsilon')) \\
& \text{(\mathbf{K}_e \text{ only affects the } x \text{ component)} \\
&= \int_{x^*} K_i(x, dx^*) [\alpha_{i, i+\epsilon}(V(x^*)) \mathbf{1}\{i' = i + \epsilon, \epsilon' = \epsilon\} + \rho_{i, i+\epsilon}(V(x^*)) \mathbf{1}\{i' = i, \epsilon' = -\epsilon\}] \\
&= \int_{x^*} K_i(x, dx^*) \int_{v^*} \delta_{V(x^*)}(dv^*) [\alpha_{i, i+\epsilon}(v^*) \mathbf{1}\{i' = i + \epsilon, \epsilon' = \epsilon\} + \rho_{i, i+\epsilon}(v^*) \mathbf{1}\{i' = i, \epsilon' = -\epsilon\}] \\
& \text{(integrate with respect to point mass at } V(x^*)) \\
&= \int_{v^*} \pi_i^{(V)}(dv^*) [\alpha_{i, i+\epsilon}(v^*) \mathbf{1}\{i' = i + \epsilon, \epsilon' = \epsilon\} + \rho_{i, i+\epsilon}(v^*) \mathbf{1}\{i' = i, \epsilon' = -\epsilon\}] \int_{x^*} K_i((x, v^*), dx^*) \\
& \text{(Eq. (30) and Fubini's)} \\
&= \int_{v^*} \pi_i^{(V)}(dv^*) [\alpha_{i, i+\epsilon}(v^*) \mathbf{1}\{i' = i + \epsilon, \epsilon' = \epsilon\} + \rho_{i, i+\epsilon}(v^*) \mathbf{1}\{i' = i, \epsilon' = -\epsilon\}] \\
&= \alpha_{i, i+\epsilon} \mathbf{1}\{i' = i + \epsilon, \epsilon' = \epsilon\} + \rho_{i, i+\epsilon} \mathbf{1}\{i' = i, \epsilon' = -\epsilon\} \\
&= \mathbf{k}((i, \epsilon), (i', \epsilon')).
\end{aligned}$$

Since the right-hand side does not depend on x , we conclude that, for any initial distribution μ on $(\tilde{\mathcal{X}}, \tilde{\Sigma})$, the index process of the NRST chain initialized with μ follows marginally a finite state Markov chain on $\{0, \dots, N\} \times \{-1, +1\}$ with transition kernel \mathbf{k} . Its initial distribution is given by the push-forward of μ under the canonical projection $(x, i, \epsilon) \mapsto (i, \epsilon)$. Moreover, the kernel \mathbf{k} is invariant with respect to $\tilde{\pi}(i, \epsilon)$ because the NRST kernel \mathbf{K} is $\tilde{\pi}$ -invariant (Proposition C.1) and $\tilde{\pi}(i, \epsilon)$ is its marginal. \square

C.3 Proofs for Section 4.2

Before we begin, let us introduce notation specific for the index process. We identify the atom set \mathcal{A} in product space $\tilde{\mathcal{X}}$ with the index process state $(0, -1)$. Thus, we overload the notation for the hitting times of the atom $\{T_k\}_{k \in \mathbb{N}}$ to mean visits of the index process to the state $(0, -1)$. Moreover, define

$$\mathcal{U} := (N, +1),$$

which is the state at the top level of the index process with momentum aiming up. Let us write $T_{\mathcal{U}}$ for the first hitting time (Eq. (28)) of the singleton $\{\mathcal{U}\}$. Then, we can define the *roundtrip time* as

$$T_{\text{RT}} := \inf\{n > T_{\mathcal{U}} : (i, \epsilon) = (0, -1)\} = T_1 \circ \theta_{T_{\mathcal{U}}}. \quad (31)$$

Recall that, under Assumption 4.1, the index process is a finite state Markov chain on $\{0, \dots, N\} \times \{-1, +1\}$ (Proposition 4.2). We use $\mathbb{P}_{(i, \epsilon)}$ to denote the law corresponding to initializing the index process at (i, ϵ) . To simplify the notation further, we write $\mathbb{P}_{(i_0, +)}$ if $\epsilon_0 = +1$, and $\mathbb{P}_{(i_0, -)}$ otherwise. Note that initializing NRST from the regenerative measure ν implies starting the index process from $(0, +1)$.

Lemma C.7. *If $\{p_i\}_{i=0}^N$ is uniform, then $\rho_{i-1, i} = \rho_{i, i-1}$ for all $i \in \{1, \dots, N\}$.*

Proof. Since $\tilde{\pi}(i, \epsilon)$ is constant and non-zero, by the $\tilde{\pi}$ -invariance of the index process

$$\begin{aligned} \tilde{\pi}(i, +1) &= \tilde{\pi}(i, -1)\rho_{i, i-1} + \tilde{\pi}(i-1, +1)(1 - \rho_{i-1, i}) \\ \iff 1 &= \rho_{i, i-1} + 1 - \rho_{i-1, i} \\ \iff \rho_{i, i-1} &= \rho_{i-1, i}. \end{aligned}$$

□

The following result analyzes the probabilities that the index process started at either end of $\{0, \dots, N\}$ is able to reach the opposite end before returning to the initial state. As we shall see in the proof of Theorem 4.4, these are key ingredients for the distribution of the number of visits to level N within a tour—which in turn determines TE (Section 4.2).

Lemma C.8. *For the index process with uniform $\{p_i\}_{i=0}^N$,*

$$\mathbb{P}_{(0, +)}(T_{\mathcal{U}} < T_1) = \mathbb{P}_{(N, -)}(T_{\mathcal{U}} > T_1) = \frac{\mathbb{E}_{(0, +)}[\tau]}{\mathbb{E}_{(0, -)}[T_{\text{RT}}]},$$

where T_{RT} is the roundtrip time (Eq. (31)) and τ is the length of a typical tour (defined in Section 3.1). Consequently, for reversible ST

$$\mathbb{P}_{(0, +)}(T_{\mathcal{U}} < T_1) = \mathbb{P}_{(N, -)}(T_{\mathcal{U}} > T_1) = \frac{1}{2N + 2 \sum_{i=1}^N \frac{\rho_i}{\alpha_i}},$$

whereas for NRST

$$\mathbb{P}_{(0, +)}(T_{\mathcal{U}} < T_1) = \mathbb{P}_{(N, -)}(T_{\mathcal{U}} > T_1) = \frac{1}{1 + \sum_{i=1}^N \frac{\rho_i}{\alpha_i}}.$$

Proof. Define for all $k \in \mathbb{N}$

$$m_k := \mathbb{1}\{0 < s_k(\mathbb{1}\{(i_n, \epsilon_n) = \mathcal{U}\})\} = \mathbb{1}\left\{0 < \sum_{n=T_{k-1}+1}^{T_k} \mathbb{1}\{(i_n, \epsilon_n) = \mathcal{U}\}\right\},$$

which indicates whether the process hit \mathcal{U} at least once during the k -th tour or not. In other words, m_k indicates if the k -th tour is a roundtrip. Note that

$$\mathbb{P}_{(0,+)}(T_{\mathcal{U}} < T_1) = \mathbb{E}_{(0,+)}[m_1],$$

Since the collection $\{m_k\}_{k \in \mathbb{N}}$ is i.i.d., it follows from the strong law of large numbers that

$$\lim_{k \rightarrow \infty} \frac{1}{k} \sum_{j=1}^k m_j = \mathbb{P}_{(0,+)}(T_{\mathcal{U}} < T_1), \quad \mathbb{P}_{(0,+)} - \text{a.s.}$$

Now, let $k(n)$ be the index of the tour occurring at step n ; i.e.,

$$\forall n \in \mathbb{Z}_+ : k(n) := 1 + \sum_{m=0}^n \mathbb{1}\{(i_m, \epsilon_m) = (0, -1)\}.$$

Then, Theorem 3.1 shows that

$$\lim_{n \rightarrow \infty} \frac{n}{k(n)} = \lim_{k \rightarrow \infty} \frac{T_k}{k} = \lim_{k \rightarrow \infty} \frac{1}{k} \sum_{j=1}^k \tau_j = \mathbb{E}_{(0,+)}[\tau], \quad \mathbb{P}_{(0,+)} - \text{a.s.}$$

Under a uniform distribution over levels, Eq. (9) in Theorem 3.1 shows that $\mathbb{E}_{(0,+)}[\tau] = 2(N+1)$ for NRST. A similar identity can be obtained for ST by using the fact that it admits the atom $\mathcal{A}_{\text{ST}} := \mathcal{X} \times \{0\} \times \{-1, +1\}$. This means that for ST, $\mathbb{E}_{(0,+)}[\tau] = N+1$.

On the other hand, let $R(n)$ be the number of roundtrips up to step n ; i.e.,

$$R(n) := \sum_{j=1}^{k(n)} m_j.$$

$\{R_n\}_{n \in \mathbb{Z}_+}$ is a renewal process with i.i.d. holding times that have expectation $\mathbb{E}_{(0,-)}[T_{\text{RT}}]$. By the law of large numbers for renewal processes (Çınlar, 2013, Prop. 9.1.25),

$$\lim_{n \rightarrow \infty} \frac{R(n)}{n} = \frac{1}{\mathbb{E}_{(0,-)}[T_{\text{RT}}]},$$

almost surely. Combining the above two facts gives

$$\begin{aligned}
\mathbb{P}_{(0,+)}(T_U < T_1) &= \lim_{k \rightarrow \infty} \frac{1}{k} \sum_{j=1}^k m_j \\
&= \lim_{n \rightarrow \infty} \frac{n}{k(n)} \frac{R(n)}{n} \\
&= \left[\lim_{n \rightarrow \infty} \frac{n}{k(n)} \right] \left[\lim_{n \rightarrow \infty} \frac{R(n)}{n} \right] \\
&= \frac{\mathbb{E}_{(0,+)}[\tau]}{\mathbb{E}_{(0,-)}[T_{RT}]}.
\end{aligned}$$

Using the expressions from Theorem 1 in Syed et al. (2022) for the expected roundtrip times, together with the values for the expected tour length discussed above, we see that for ST,

$$\mathbb{P}_{(0,+)}(T_U < T_1) = \frac{1}{2N + 2 \sum_{i=1}^N \frac{\rho_i}{\alpha_i}},$$

whereas for NRST

$$\mathbb{P}_{(0,+)}(T_U < T_1) = \frac{1}{1 + \sum_{i=1}^N \frac{\rho_i}{\alpha_i}}.$$

Finally, to see that

$$\mathbb{P}_{(0,+)}(T_U < T_1) = \mathbb{P}_{(N,-)}(T_U > T_1),$$

simply note that we can obtain the right-hand side by re-labelling $i \leftarrow N - i$. But since the quantity $\sum_{i=1}^N \frac{\rho_i}{\alpha_i}$ is invariant under permutations of the indices, the result is identical. \square

Proof of Theorem 4.4. Following the definition of TE, we proceed by describing the distribution of the number of visits to level N within a tour. Under Assumption 4.1, Proposition 4.2 lets us analyze this distribution using only the index process. Now, the probability that the chain hits level N before returning to the atom is $\mathbb{P}_{(0,+)}(T_U < T_1)$. From there, by the strong Markov property, a second visit will occur with probability $\mathbb{P}_{(N,-)}(T_U < T_1)$. If that happens, then—again by the Markov property—a third visit will occur with the same probability. Iterating this argument shows that

$$v \stackrel{d}{=} RUF \tag{32}$$

where R and U are independent random variables with marginal distributions

$$\begin{aligned} R &\sim \text{Bern}(\mathbb{P}_{(0,+)}(T_U < T_1)) \\ U &\sim \text{Geom}_1(\mathbb{P}_{(N,-)}(T_U > T_1)). \end{aligned}$$

$\text{Geom}_1(p)$ refers to a geometric distribution supported on $\mathbb{N} = \{1, 2, \dots\}$, while the constant F is related to the delay in turning back after hitting the boundary at N . For ST, $F = 1$ because this process immediately forgets its current direction. On the other hand, NRST needs $F = 2$ because, after hitting $(N, +)$, it takes an additional step to flip (deterministically) to $(N, -)$. The result now follows directly from Lemma C.8. Indeed, let $p = \mathbb{P}_{(0,+)}(T_U < T_1)$. Then, for NRST we have

$$\mathbb{E}_\nu[v^2] = 4p \left[\frac{1}{p^2} + \frac{1-p}{p^2} \right] = 4 \frac{2-p}{p}.$$

Using this together with $\mathbb{E}_\nu[v] = 2$ (via Eq. (32) or Eq. (9) with $f = \mathbb{1}\{i = N\}$) yields

$$\text{TE} = \frac{p}{2-p} = \frac{1}{2/p-1} = \frac{1}{1+2\sum_{i=1}^N \frac{\rho_i}{\alpha_i}}.$$

Likewise for ST, Eq. (32) gives $\mathbb{E}_\nu[v] = 1$ —we can verify this by modifying Eq. (9) for (reversible) ST as discussed in the proof of Lemma C.8. Finally,

$$\text{TE} = \frac{1}{2/p-1} = \frac{1}{4N-1+4\sum_{i=1}^N \frac{\rho_i}{\alpha_i}}.$$

□

Proof of Theorem 4.3. Applying the triangle inequality twice,

$$|s(\mathbb{1}\{i = N\}[h(x) - \pi(h)])| \leq \sum_{n=0}^{T_1} \mathbb{1}\{i_n = N\} |h(x_n) - \pi(h)| \leq 2v.$$

Therefore,

$$\mathbb{E}_\nu[s(\mathbb{1}\{i = N\}[h(x) - \pi(h)])^2] \leq 4\mathbb{E}_\nu[v^2].$$

Using the definition of $\sigma(h)^2$ and applying the above bound gives

$$\sigma(h)^2 \leq 4 \frac{\mathbb{E}_\nu[v^2]}{\mathbb{E}_\nu[v]^2} = \frac{4}{\text{TE}}.$$

To check that $\text{TE} > 0$, first recall that $\mathbb{E}_\nu[v] = 2p_N/p_0 > 0$ (Theorem 3.1). Secondly, we know that under Assumption 4.1 the index process follows a finite Markov chain on $\{0, \dots, N\} \times \{-1, +1\}$ (Proposition 4.2). Therefore, the number of visits to $i = N$ before absorption into the atom \mathcal{A} —i.e., v —has finite second moment (see e.g. [Kemeny and Snell, 1960](#), Theorem 3.3.3). \square

C.4 Proofs for Section 4.3

Lemma C.9. $\mathcal{Z}(\beta) < \infty$ for all $\beta \in [0, 1]$.

Proof.

$$\mathcal{Z}(\beta) = \mathbb{E}^{(0)}[e^{-\beta V(x)}] \leq \mathbb{E}^{(0)}[e^{-V(x)}]^\beta < \infty.$$

The first bound follows from Jensen's since $u \mapsto u^\beta$ is concave in $[0, \infty)$ when $\beta \in [0, 1]$, and the last one is due to the requirement that $\mathcal{Z} = \mathcal{Z}(1) < \infty$ in Eq. (1). \square

Lemma C.10. For all $\beta \in [0, 1]$ and $\xi \in [-(1 - \beta), \beta]$,

$$\mathcal{M}^{(\beta)}(\xi) := \mathbb{E}^{(\beta)}[e^{\xi V(x)}] < \infty.$$

It follows that for all $\beta \in (0, 1)$, $\mathcal{M}^{(\beta)}(\xi)$ is finite on an open interval around 0. In particular, this implies that for all $a > 0$,

$$\mathbb{E}^{(\beta)}[|V(x)|^a] < \infty.$$

Proof. Note that

$$\mathcal{M}^{(\beta)}(\xi) = \mathbb{E}^{(\beta)}[e^{\xi V(x)}] = \frac{1}{\mathcal{Z}(\beta)} \mathbb{E}^{(0)}[e^{-(\beta - \xi)V(x)}] = \frac{\mathcal{Z}(\beta - \xi)}{\mathcal{Z}(\beta)}.$$

By Lemma C.9, the right-hand side is finite for all $\beta \in [0, 1]$ whenever

$$0 \leq \beta - \xi \leq 1 \iff -(1 - \beta) \leq \xi \leq \beta.$$

For the second statement, note that for $\beta \in (0, 1)$, $\mathcal{M}^{(\beta)}(\xi)$ is finite for all $\xi \in [-(1 - \beta), \beta]$, which is an open interval around 0. The result follows for $a \in \mathbb{N}$ by standard results for moment-generating functions (see e.g. [Rosenthal, 2006](#), Theorem 9.3.3). To extend to $a > 0$, let

$$\lceil a \rceil := \min\{n \in \mathbb{N} : a \leq n\}.$$

Then,

$$\mathbb{E}^{(\beta)}[|V(x)|^a] = \mathbb{E}^{(\beta)} \left[\left(|V(x)|^{|a|} \right)^{\frac{a}{|a|}} \right] \leq \mathbb{E}^{(\beta)} \left[|V(x)|^{|a|} \right]^{\frac{a}{|a|}} < \infty,$$

by Jensen's inequality since $z \mapsto z^{\frac{a}{|a|}}$ is concave. \square

Lemma C.11. $\mathcal{Z}(\beta) \in \mathcal{C}^\infty((0, 1))$, and for all $k \in \mathbb{N}$ and $\beta \in (0, 1)$,

$$\frac{d^k}{d\beta^k} \mathcal{Z}(\beta) = (-1)^k \mathcal{Z}(\beta) \mathbb{E}^{(\beta)}[V^k].$$

Proof. This is a special case of Lemma 4.5 in [van der Vaart \(1998\)](#). \square

Corollary C.12. The function $\beta \mapsto \mathbb{E}^{(\beta)}[V]$ is $\mathcal{C}^\infty((0, 1))$ and monotone non-increasing, with

$$\frac{d\mathbb{E}^{(\beta)}[V]}{d\beta} = -\text{Var}_\beta(V).$$

Additionally,

$$\forall \beta \in [0, 1] : \log(\mathcal{Z}(\beta)) = - \int_0^\beta \mathbb{E}^{(\beta')}[V] d\beta'.$$

Proof. The case $k = 1$ in Lemma C.11 shows that for all $\beta \in (0, 1)$,

$$\mathbb{E}^{(\beta)}[V] = - \frac{\mathcal{Z}'(\beta)}{\mathcal{Z}(\beta)}. \quad (33)$$

Since $\mathcal{Z} \in \mathcal{C}^\infty((0, 1))$, $\mathbb{E}^{(\cdot)}[V]$ is the ratio of two smooth, strictly positive functions. Therefore, $\mathbb{E}^{(\cdot)}[V] \in \mathcal{C}^\infty((0, 1))$ too. Moreover, differentiating Eq. (33) and using Lemma C.11 for $k \in \{1, 2\}$ shows that

$$\frac{d\mathbb{E}^{(\beta)}[V]}{d\beta} = - \frac{\mathcal{Z}''(\beta)}{\mathcal{Z}(\beta)} + \frac{\mathcal{Z}'(\beta)^2}{\mathcal{Z}(\beta)^2} = -\mathbb{E}^{(\beta)}[V^2] + \mathbb{E}^{(\beta)}[V]^2 = -\text{Var}_\beta(V) \leq 0.$$

On the other hand, we can rewrite the right-hand side of Eq. (33) as

$$\mathbb{E}^{(\beta)}[V] = - \frac{d \log(\mathcal{Z}(\beta))}{d\beta}.$$

Integrating on both sides and using $\mathcal{Z}(0) = 1$ gives the last result. \square

Lemma C.13. *If c is differentiable, then for all $\beta, \beta' \in (0, 1)$,*

$$\alpha_{\beta, \beta'} = \frac{\mathbb{E}^{(\bar{\beta})}[\exp(-|\Delta\beta||c'(\check{\beta}) - V|/2)]}{\mathbb{E}^{(\bar{\beta})}[\exp(-\Delta\beta(c'(\check{\beta}) - V)/2)]},$$

where $\Delta\beta = \beta' - \beta$, $\bar{\beta} := (\beta + \beta')/2$, and $\check{\beta} \in (\min\{\beta, \beta'\}, \max\{\beta, \beta'\})$ satisfies the mean value theorem equation

$$c'(\check{\beta}) = \frac{1}{\Delta\beta} (c(\bar{\beta} + \Delta\beta/2) - c(\bar{\beta} - \Delta\beta/2)). \quad (34)$$

Proof. The following is an adaptation of the argument in [Predescu et al. \(2004\)](#) to the simulated tempering case. Consider first the case $\Delta\beta \geq 0$, and note that

$$\begin{aligned} \alpha_{\beta, \beta + \Delta\beta}(x) &= \exp(-\max\{0, \Delta\beta V(x) - [c(\beta + \Delta\beta) - c(\beta)]\}) \\ &= \exp(-\Delta\beta \max\{0, V(x) - [c(\beta + \Delta\beta) - c(\beta)]/\Delta\beta\}) \\ &= \exp(-\Delta\beta \max\{0, V(x) - c'(\check{\beta})\}) && \text{(MVT: } \check{\beta} \in (\beta, \beta')\text{)} \\ &= \exp(\Delta\beta \min\{0, c'(\check{\beta}) - V(x)\}) \\ &= \exp(\Delta\beta[c'(\check{\beta}) - V(x)]/2) \exp(-\Delta\beta|c'(\check{\beta}) - V(x)|/2), \end{aligned}$$

where MVT stands for the mean value theorem. Integrating with respect to $\pi^{(\beta)}$,

$$\begin{aligned} \alpha_{\beta, \beta + \Delta\beta} &= \mathbb{E}^{(\beta)}[\alpha_{\beta, \beta + \Delta\beta}(x)] \\ &= \exp(\Delta\beta c'(\check{\beta})/2) \mathbb{E}^{(\beta)}[\exp(-\Delta\beta V/2) \exp(-\Delta\beta|c'(\check{\beta}) - V|/2)] \\ &= \frac{\exp(\Delta\beta c'(\check{\beta})/2)}{\mathcal{Z}(\beta)} \mathbb{E}^{(0)}[\exp(-\underbrace{(\beta + \Delta\beta/2)}_{\bar{\beta}} V) \exp(-\Delta\beta|c'(\check{\beta}) - V|/2)] \\ &= \frac{\mathcal{Z}(\bar{\beta}) \exp(\Delta\beta c'(\check{\beta})/2)}{\mathcal{Z}(\beta)} \mathbb{E}^{(\bar{\beta})}[\exp(-\Delta\beta|c'(\check{\beta}) - V|/2)]. \end{aligned}$$

On the other hand,

$$\mathcal{Z}(\beta) = \mathbb{E}^{(0)}[e^{-\beta V}] = \mathcal{Z}(\bar{\beta}) \mathbb{E}^{(\bar{\beta})}[e^{\Delta\beta V/2}]. \quad (35)$$

Hence,

$$\alpha_{\beta, \beta + \Delta\beta} = \frac{\mathbb{E}^{(\bar{\beta})}[\exp(-\Delta\beta|c'(\check{\beta}) - V|/2)]}{\mathbb{E}^{(\bar{\beta})}[\exp(-\Delta\beta(c'(\check{\beta}) - V)/2)]}.$$

Similarly for $\Delta\beta < 0$,

$$\begin{aligned}
\alpha_{\beta, \beta - |\Delta\beta|}(x) &= \exp(-\max\{0, -|\Delta\beta|V - [c(\beta - |\Delta\beta|) - c(\beta)]\}) \\
&= \exp(|\Delta\beta| \min\{0, V - [c(\beta) - c(\beta - |\Delta\beta|)]/|\Delta\beta|\}) \\
&= \exp(|\Delta\beta| \min\{0, V - c'(\check{\beta})\}) && \text{(MVT: } \check{\beta} \in (\beta', \beta)) \\
&= \exp(-|\Delta\beta|[c'(\check{\beta}) - V]/2) \exp(-|\Delta\beta|[c'(\check{\beta}) - V]/2)
\end{aligned}$$

Now

$$\begin{aligned}
\alpha_{\beta, \beta - |\Delta\beta|} &= \mathbb{E}^{(\beta)}[\alpha_{\beta, \beta - |\Delta\beta|}(x)] \\
&= \exp(-|\Delta\beta|c'(\check{\beta})) \mathbb{E}^{(\beta)}[\exp(|\Delta\beta|V/2) \exp(-|\Delta\beta|[c'(\check{\beta}) - V]/2)] \\
&= \frac{\exp(-|\Delta\beta|c'(\check{\beta}))}{\mathcal{Z}(\beta)} \mathbb{E}^{(0)}[\exp(-\underbrace{(\beta - |\Delta\beta|/2)}_{\check{\beta}}V) \exp(-|\Delta\beta|[c'(\check{\beta}) - V]/2)] \\
&= \frac{\mathcal{Z}(\bar{\beta}) \exp(-|\Delta\beta|c'(\check{\beta}))}{\mathcal{Z}(\beta)} \mathbb{E}^{(\bar{\beta})}[\exp(-|\Delta\beta|[c'(\check{\beta}) - V]/2)].
\end{aligned}$$

But since $\mathcal{Z}(\beta) = \mathcal{Z}(\bar{\beta}) \mathbb{E}^{(\bar{\beta})}[e^{-|\Delta\beta|V/2}]$, we get

$$\alpha_{\beta, \beta - |\Delta\beta|} = \frac{\mathbb{E}^{(\bar{\beta})}[\exp(-|\Delta\beta|[c'(\check{\beta}) - V]/2)]}{\mathbb{E}^{(\bar{\beta})}[\exp(-\Delta\beta(c'(\check{\beta}) - V)/2)]}$$

as necessary. Note that the right-hand side is also valid for $\Delta\beta \geq 0$. Finally, we can verify that $\alpha_{\beta, \beta'} \leq 1$ because for any $u \in \mathbb{R}$, $e^{-|u|} \leq e^{-u}$. \square

In the last Lemma, the variable $\check{\beta}$ depends on β and β' . Ultimately, we will keep one of the end points, say β , fixed and vary the other end point β' . As a result, in the following we write $\check{\beta}(\Delta\beta)$ to emphasize this dependency.

Lemma C.14. *Under Assumption 4.5, for each $\bar{\beta} \in (0, 1)$, the function $\Delta\beta \mapsto c'(\check{\beta}(\Delta\beta))$ defined by Eq. (34) (Lemma C.13) is $\mathcal{C}^2((-r(\bar{\beta}), r(\bar{\beta})))$, with*

$$r(\bar{\beta}) := 2 \min\{\bar{\beta}, 1 - \bar{\beta}\}, \tag{36}$$

and admits the following second-order Taylor expansion around $\Delta\beta = 0$ with Peano remainder

$$c'(\check{\beta}(\Delta\beta)) = c'(\bar{\beta}) + 0 \cdot \Delta\beta + \frac{1}{24} c'''(\bar{\beta}) \Delta\beta^2 + o(\Delta\beta^2).$$

Proof. Since $c'(\check{\beta}(\cdot))$ is a linear combination of c evaluated at two points, the function is as smooth as c for $\Delta\beta \neq 0$. To understand its behavior at $\Delta\beta = 0$, consider a third order expansion of c around $\bar{\beta}$ with Peano remainder

$$c(\bar{\beta} + \delta) = c(\bar{\beta}) + c'(\bar{\beta})\delta + \frac{1}{2}c''(\bar{\beta})\delta^2 + \frac{1}{6}c'''(\bar{\beta})\delta^3 + h(\delta)\delta^3,$$

with h a function such that $\lim_{\delta \rightarrow 0} h(\delta) = 0$. Substituting δ with $\pm\Delta\beta/2$ and using these approximations in Eq. (34) gives

$$\begin{aligned} & c'(\check{\beta}(\Delta\beta)) \\ &= \frac{1}{\Delta\beta} (c(\bar{\beta} + \Delta\beta/2) - c(\bar{\beta} - \Delta\beta/2)) \\ &= \frac{1}{\Delta\beta} \left(\frac{1}{2}c'(\bar{\beta})[\Delta\beta + \Delta\beta] + \frac{1}{48}c'''(\bar{\beta})[\Delta\beta^3 + \Delta\beta^3] + \underbrace{\frac{1}{8}[h(\Delta\beta/2) - h(-\Delta\beta/2)]\Delta\beta^3}_{:=\tilde{h}(\Delta\beta)} \right) \\ &= c'(\bar{\beta}) + 0 \cdot \Delta\beta + \frac{1}{24}c'''(\bar{\beta})\Delta\beta^2 + \tilde{h}(\Delta\beta)\Delta\beta^2. \end{aligned}$$

This is now a second-order Taylor expansion with Peano remainder for $c'(\check{\beta}(\cdot))$. Since $c \in \mathcal{C}^3((0, 1))$, by Theorem 3 in [Oliver \(1954\)](#) we conclude that $c'(\check{\beta}(\cdot)) \in \mathcal{C}^2((-r(\bar{\beta}), r(\bar{\beta})))$, as required. \square

Lemma C.15. *Suppose Assumption 4.5 holds. Fix $\bar{\beta} \in (0, 1)$ and let $r(\bar{\beta})$ be as in Eq. (36). Then, for $\phi \in \{-1, 1\}$ and $|\Delta\beta| < r(\bar{\beta})$,*

$$\begin{aligned} & \frac{d}{d\Delta\beta} \mathbb{E}^{(\bar{\beta})}[\exp(\phi\Delta\beta(c(\check{\beta}(\Delta\beta)) - V)/2)] \\ &= \frac{\phi}{2} \mathbb{E}^{(\bar{\beta})}[\exp(\phi\Delta\beta(\gamma(\Delta\beta) - V)/2)(\gamma(\Delta\beta) - V + \Delta\beta\gamma'(\Delta\beta))], \\ & \frac{d^2}{d\Delta\beta^2} \mathbb{E}^{(\bar{\beta})}[\exp(\phi\Delta\beta(c(\check{\beta}(\Delta\beta)) - V)/2)] \\ &= \frac{\phi}{2} \mathbb{E}^{(\bar{\beta})}[\exp(\phi\Delta\beta(\gamma(\Delta\beta) - V)/2)(2\gamma'(\Delta\beta) + \Delta\beta\gamma''(\Delta\beta))] \\ & \quad + \frac{1}{4} \mathbb{E}^{(\bar{\beta})}[\exp(\phi\Delta\beta(\gamma(\Delta\beta) - V)/2)(\gamma(\Delta\beta) - V + \Delta\beta\gamma'(\Delta\beta))^2], \end{aligned}$$

where $\gamma(\Delta\beta) := c'(\check{\beta}(\Delta\beta))$. Furthermore, if Assumption 4.6 holds too, then

for all $|\Delta\beta| < r(\bar{\beta})$,

$$\begin{aligned}
& \frac{d}{d\Delta\beta} \mathbb{E}^{(\bar{\beta})}[\exp(-\Delta\beta|c(\check{\beta}(\Delta\beta)) - V|/2)] \\
&= -\frac{1}{2} \mathbb{E}^{(\bar{\beta})}[\exp(-\Delta\beta|\gamma(\Delta\beta) - V|/2)(|\gamma(\Delta\beta) - V| + \Delta\beta\gamma'(\Delta\beta) \operatorname{sgn}(\gamma(\Delta\beta) - V))] \\
& \frac{d^2}{d\Delta\beta^2} \mathbb{E}^{(\bar{\beta})}[\exp(-\Delta\beta|c(\check{\beta}(\Delta\beta)) - V|/2)] \\
&= -\frac{1}{2} \mathbb{E}^{(\bar{\beta})}[\exp(-\Delta\beta|\gamma(\Delta\beta) - V|/2) \operatorname{sgn}(\gamma(\Delta\beta) - V)(2\gamma'(\Delta\beta) + \Delta\beta\gamma''(\Delta\beta))] \\
& \quad + \frac{1}{4} \mathbb{E}^{(\bar{\beta})}[\exp(-\Delta\beta|\gamma(\Delta\beta) - V|/2)(|\gamma(\Delta\beta) - V| + \Delta\beta\gamma'(\Delta\beta) \operatorname{sgn}(\gamma(\Delta\beta) - V))^2].
\end{aligned}$$

Proof. We focus on the case with absolute value and leave the other to the reader since it requires a similar but simpler argument. To simplify the notation, in the following we write z instead of $\Delta\beta$. Now, define

$$F(v, z) := \exp(-z|\gamma(z) - v|/2),$$

and note that $z \mapsto \mathbb{E}^{(\bar{\beta})}[F(V, z)]$ is our function of interest. From Lemma C.14, we know that $\gamma \in \mathcal{C}^2((-r(\bar{\beta}), r(\bar{\beta})))$ under Assumption 4.5. It follows that for each v , the function $F(v, \cdot)$ is absolutely continuous and thus almost everywhere differentiable on $(-r(\bar{\beta}), r(\bar{\beta}))$. Therefore, F admits a well-defined partial derivative on the set

$$A := \{(v, z) : |z| < r(\bar{\beta}), \gamma(z) \neq v\}.$$

Indeed, for $(v, z) \in A$,

$$\frac{\partial F}{\partial z}(v, z) = -\frac{1}{2} \exp(-z|\gamma(z) - v|/2)[|\gamma(z) - v| + z\gamma'(z) \operatorname{sgn}(\gamma(z) - v)].$$

Furthermore, for each v , the function $z \mapsto \frac{\partial F}{\partial z}$ is of bounded variation. Thus, it is almost everywhere differentiable on $(-r(\bar{\beta}), r(\bar{\beta}))$. It follows that $\frac{\partial^2 F}{\partial z^2}$ exists on A too, with

$$\begin{aligned}
\frac{\partial^2 F}{\partial z^2}(v, z) &= -\frac{1}{2} \exp(-z|\gamma(z) - v|/2) \frac{\partial}{\partial z} [|\gamma(z) - v| + z\gamma'(z) \operatorname{sgn}(\gamma(z) - v)] \\
& \quad - [|\gamma(z) - v| + z\gamma'(z) \operatorname{sgn}(\gamma(z) - v)] \frac{\partial}{\partial z} \exp(-z|\gamma(z) - v|/2) \\
&= -\frac{1}{2} \exp(-z|\gamma(z) - v|/2) \operatorname{sgn}(\gamma(z) - v) [2\gamma'(z) + z\gamma''(z)] \\
& \quad + \frac{1}{4} \exp(-z|\gamma(z) - v|/2) [|\gamma(z) - v| + z\gamma'(z) \operatorname{sgn}(\gamma(z) - v)]^2.
\end{aligned}$$

Now, our aim is to show that for $i \in \{1, 2\}$,

$$\frac{d^i}{dz^i} \mathbb{E}^{(\bar{\beta})}[F(V, z)] = \mathbb{E}^{(\bar{\beta})} \left[\frac{\partial^i F}{\partial z^i}(V, z) \right].$$

We will do this only for the second derivative since the first one requires a similar argument. Fix $(v, z) \in A$. Since $\gamma \in \mathcal{C}^2((-r(\bar{\beta}), r(\bar{\beta})))$, there exists $\delta = \delta(v, z)$ with $0 < \delta < r(\bar{\beta})$ such that for all z' with $|z' - z| < \delta$, we have $(v, z') \in A$. Hence, $z' \mapsto \frac{\partial F}{\partial z}(v, z')$ is $\mathcal{C}^1((z - \delta, z + \delta))$ and the MVT implies that

$$\frac{\frac{\partial F}{\partial z}(v, z') - \frac{\partial F}{\partial z}(v, z)}{z' - z} = \frac{\partial^2 F}{\partial z^2}(v, \check{z}), \quad (37)$$

for all $z' \in (z - \delta, z + \delta) \setminus \{z\}$ and some $\check{z} \in (\min\{z, z'\}, \max\{z, z'\})$. On the other hand, for all $(v, z) \in A$,

$$\begin{aligned} \left| \frac{\partial^2 F}{\partial z^2}(v, z) \right| &\leq \frac{1}{2} \exp(-z|\gamma(z) - v|/2) |2\gamma'(z) + z\gamma''(z)| \\ &\quad + \frac{1}{4} \exp(-z|\gamma(z) - v|/2) [|\gamma(z) - v| + z\gamma'(z) \operatorname{sgn}(\gamma(z) - v)]^2 \\ &\leq \frac{1}{2} \exp(-z|\gamma(z) - v|/2) |2\gamma'(z) + z\gamma''(z)| \\ &\quad + \frac{1}{2} \exp(-z|\gamma(z) - v|/2) [(\gamma(z) - v)^2 + (z\gamma'(z))^2]. \end{aligned}$$

Let us call the right-hand side of the above inequality

$$\begin{aligned} G(v, z) &:= \frac{1}{2} \exp(-z|\gamma(z) - v|/2) |2\gamma'(z) + z\gamma''(z)| \\ &\quad + \frac{1}{2} \exp(-z|\gamma(z) - v|/2) [(\gamma(z) - v)^2 + (z\gamma'(z))^2]. \end{aligned}$$

Note that, for each v , the function $G(v, \cdot)$ is continuous for all $|z| < r(\bar{\beta})$. Therefore, $G(v, \cdot)$ achieves its maximum on any compact subset of $(-r(\bar{\beta}), r(\bar{\beta}))$. In particular, for any $0 < \varepsilon < r(\bar{\beta})$,

$$z^*(v) := \arg \max_{z \in [-r(\bar{\beta}) + \varepsilon, r(\bar{\beta}) - \varepsilon]} G(v, z).$$

Let $G(v) := G(v, z^*(v))$. We want to show that this function is integrable. We shall see that $G(\cdot, z)$ is in fact integrable for every $|z| < r(\bar{\beta})$. Indeed, using the bound $e^{|u|} \leq e^u + e^{-u}$, we see that

$$\exp(-z|\gamma(z) - v|/2) \leq e^{-z\gamma(z)/2} e^{zv/2} + e^{z\gamma(z)/2} e^{-zv/2}.$$

It follows that for $p \geq 0$,

$$\begin{aligned}
& \mathbb{E}^{(\bar{\beta})} [|V|^p \exp(-z|\gamma(z) - V|/2)] \\
& \leq e^{z\gamma(z)/2} \mathbb{E}^{(\bar{\beta})} [|V|^p e^{-zV/2}] + e^{-z\gamma(z)/2} \mathbb{E}^{(\bar{\beta})} [|V|^p e^{zV/2}] \\
& = \frac{e^{z\gamma(z)/2} \mathcal{Z}(\bar{\beta} - z/2)}{\mathcal{Z}(\bar{\beta})} \mathbb{E}^{(\bar{\beta}-z/2)} [|V|^p] + \frac{e^{-z\gamma(z)/2} \mathcal{Z}(\bar{\beta} + z/2)}{\mathcal{Z}(\bar{\beta})} \mathbb{E}^{(\bar{\beta}+z/2)} [|V|^p],
\end{aligned} \tag{38}$$

and the right-hand side is finite for $|z| < r(\bar{\beta})$ by Lemmas C.9 and C.10. Hence, for $|z| < r(\bar{\beta})$,

$$\begin{aligned}
\mathbb{E}^{(\bar{\beta})} [G(V, z)] & \leq \frac{1}{2} (|2\gamma'(z) + z\gamma''(z)| + (z\gamma'(z))^2) \mathbb{E}^{(\bar{\beta})} [\exp(-z|\gamma(z) - V|/2)] \\
& \quad + \frac{1}{2} \mathbb{E}^{(\bar{\beta})} [\exp(-z|\gamma(z) - V|/2) (\gamma(z) - V)^2] \\
& \leq \frac{1}{2} (|2\gamma'(z) + z\gamma''(z)| + (z\gamma'(z))^2 + 2\gamma(z)^2) \mathbb{E}^{(\bar{\beta})} [\exp(-z|\gamma(z) - V|/2)] \\
& \quad + \mathbb{E}^{(\bar{\beta})} [V^2 \exp(-z|\gamma(z) - V|/2)],
\end{aligned}$$

and the right-hand side is finite by Eq. (38). Since $|z^*(v)| < r(\bar{\beta})$, we conclude that $G(v) := G(v, z^*(v))$ is integrable. And since this function maximizes the right-hand side of Eq. (37), we see that for all v and $|z| < r(\bar{\beta}) - \varepsilon$,

$$\left| \frac{\mathbb{1}\{\gamma(z') \neq v\} \frac{\partial F}{\partial z}(v, z') - \mathbb{1}\{\gamma(z) \neq v\} \frac{\partial F}{\partial z}(v, z)}{z' - z} \right| \leq G(v),$$

Furthermore, since $(v, z) \in A$ implies $(v, z') \in A$ when $|z' - z| < \delta$,

$$\begin{aligned}
& \lim_{z' \rightarrow z} \frac{\mathbb{1}\{\gamma(z') \neq v\} \frac{\partial F}{\partial z}(v, z') - \mathbb{1}\{\gamma(z) \neq v\} \frac{\partial F}{\partial z}(v, z)}{z' - z} \\
& = \lim_{z' \rightarrow z} \frac{\mathbb{1}\{\gamma(z) \neq v\} \frac{\partial F}{\partial z}(v, z') - \mathbb{1}\{\gamma(z) \neq v\} \frac{\partial F}{\partial z}(v, z)}{z' - z} \\
& = \mathbb{1}\{\gamma(z) \neq v\} \lim_{z' \rightarrow z} \frac{\frac{\partial F}{\partial z}(v, z') - \frac{\partial F}{\partial z}(v, z)}{z' - z} \\
& = \mathbb{1}\{\gamma(z) \neq v\} \frac{\partial^2 F}{\partial z^2}(v, z).
\end{aligned}$$

Finally, since for each z , the set $\{v : \gamma(z) = v\}$ is π_0 -null by Assumption 4.6—and therefore it is $\pi^{(\bar{\beta})}$ -null—the dominated convergence theorem shows that

for all $|z| < r(\bar{\beta}) - \varepsilon$,

$$\begin{aligned}
\frac{d^2}{dz^2} \mathbb{E}^{(\bar{\beta})} [F(V, z)] &= \frac{d}{dz} \mathbb{E}^{(\bar{\beta})} \left[\frac{\partial F}{\partial z}(V, z) \right] \\
&= \lim_{z' \rightarrow z} \frac{\mathbb{E}^{(\bar{\beta})} \left[\frac{\partial F}{\partial z}(V, z') - \frac{\partial F}{\partial z}(V, z) \right]}{z' - z} \\
&= \lim_{z' \rightarrow z} \frac{\mathbb{E}^{(\bar{\beta})} \left[\mathbf{1}\{\gamma(z') \neq V\} \frac{\partial F}{\partial z}(V, z') - \mathbf{1}\{\gamma(z) \neq V\} \frac{\partial F}{\partial z}(V, z) \right]}{z' - z} \\
&= \lim_{z' \rightarrow z} \mathbb{E}^{(\bar{\beta})} \left[\frac{\mathbf{1}\{\gamma(z') \neq V\} \frac{\partial F}{\partial z}(V, z') - \mathbf{1}\{\gamma(z) \neq V\} \frac{\partial F}{\partial z}(V, z)}{z' - z} \right] \\
&= \mathbb{E}^{(\bar{\beta})} \left[\lim_{z' \rightarrow z} \frac{\mathbf{1}\{\gamma(z') \neq V\} \frac{\partial F}{\partial z}(V, z') - \mathbf{1}\{\gamma(z) \neq V\} \frac{\partial F}{\partial z}(V, z)}{z' - z} \right] \\
&= \mathbb{E}^{(\bar{\beta})} \left[\mathbf{1}\{\gamma(z) \neq V\} \frac{\partial^2 F}{\partial z^2}(V, z) \right] \\
&= \mathbb{E}^{(\bar{\beta})} \left[\frac{\partial^2 F}{\partial z^2}(V, z) \right],
\end{aligned}$$

as required. And since the result holds for any $\varepsilon > 0$, we conclude that the derivative exists for all $|z| < r(\bar{\beta})$. \square

Lemma C.16. *Let $x : \mathcal{O} \rightarrow \mathbb{R}_+$, $y : \mathcal{O} \rightarrow (0, \infty)$, with $x, y \in \mathcal{C}^2(\mathcal{O})$ for some open set $\mathcal{O} \subset \mathbb{R}$. Consider*

$$f(z) := \frac{x(z)}{y(z)}.$$

Then,

$$\begin{aligned}
\frac{df}{dz}(z) &= \frac{1}{y(z)^2} (y(z)x'(z) - x(z)y'(z)) \\
\frac{d^2f}{dz^2}(z) &= \frac{1}{y(z)^3} (y(z)^2x''(z) - y(z)(2x'(z)y'(z) + x(z)y''(z)) + 2x(z)y'(z)^2).
\end{aligned}$$

Furthermore, if $z_0 \in \mathcal{O}$ is such that $x(z_0) = y(z_0) = 1$ and $x''(z_0) = y''(z_0)$, then

$$\begin{aligned}
f(z) &= 1 + (x'(z_0) - y'(z_0))(z - z_0) - y'(z_0)(x'(z_0) - y'(z_0))(z - z_0)^2 \\
&\quad + o((z - z_0)^2).
\end{aligned}$$

Proof. The expressions for the derivatives can be directly obtained via standard calculus. Now, a second order Taylor expansion of f around z_0 with Peano remainder gives

$$\begin{aligned}
f(z) &= \frac{x(z_0)}{y(z_0)} + \frac{1}{y(z_0)^2}(y(z_0)x'(z_0) - x(z_0)y'(z_0))(z - z_0) \\
&\quad + \frac{1}{2y(z_0)^3}(y(z_0)^2x''(z_0) - y(z_0)(2x'(z_0)y'(z_0) + x(z_0)y''(z_0)) + 2x(z_0)y'(z_0)^2)(z - z_0)^2 \\
&\quad + o((z - z_0)^2) \\
&= 1 + (x'(z_0) - y'(z_0))(z - z_0) \\
&\quad + \frac{1}{2}(x''(z_0) - 2x'(z_0)y'(z_0) - y''(z_0) + 2y'(z_0)^2)(z - z_0)^2 + o((z - z_0)^2) \\
&= 1 + (x'(z_0) - y'(z_0))(z - z_0) - y'(z_0)(x'(z_0) - y'(z_0))(z - z_0)^2 + o((z - z_0)^2),
\end{aligned}$$

as required. \square

Proof of Theorem 4.7. The idea is to re-parametrize $(\beta, \beta') \mapsto (\bar{\beta}, \Delta\beta)$, then fix $\bar{\beta}$ and analyze the asymptotics on $\Delta\beta$. In turn, we do this by applying Lemma C.16 to the ratio expressions for the jump probabilities in Lemma C.13. When separating upwards and downwards jump, these expressions become

$$\begin{aligned}
\alpha_{\beta, \beta'} &= \frac{\mathbb{E}^{(\bar{\beta})}[\exp(-\Delta\beta|c'(\check{\beta}) - V|/2)]}{\mathbb{E}^{(\bar{\beta})}[\exp(-\Delta\beta(c'(\check{\beta}) - V)/2)]} \\
\alpha_{\beta', \beta} &= \frac{\mathbb{E}^{(\bar{\beta})}[\exp(-\Delta\beta|c'(\check{\beta}) - V|/2)]}{\mathbb{E}^{(\bar{\beta})}[\exp(\Delta\beta(c'(\check{\beta}) - V)/2)]}.
\end{aligned} \tag{39}$$

Now, applying Lemma C.16 requires obtaining the derivatives of numerators and denominators in Eq. (39) evaluated at $\Delta\beta = 0$. Under the assumptions considered, Lemma C.15 shows that the common numerator satisfies,

$$\begin{aligned}
\frac{d}{d\Delta\beta}\mathbb{E}^{(\bar{\beta})}[\exp(-\Delta\beta|c'(\check{\beta}) - V|/2)]_{\Delta\beta=0} &= -\frac{1}{2}\mathbb{E}^{(\bar{\beta})}[|c'(\bar{\beta}) - V|] \\
\frac{d^2}{d\Delta\beta^2}\mathbb{E}^{(\bar{\beta})}[\exp(-\Delta\beta|c'(\check{\beta}) - V|/2)]_{\Delta\beta=0} &= \frac{1}{4}\mathbb{E}^{(\bar{\beta})}[(c'(\bar{\beta}) - V)^2],
\end{aligned}$$

where we used the fact that the derivative of $\Delta\beta \mapsto c'(\check{\beta}(\Delta\beta))$ is zero at $\Delta\beta = 0$ (Lemma C.14). Similarly, for the denominator in the upward jump

probability we get

$$\begin{aligned}\frac{d}{d\Delta\beta}\mathbb{E}^{(\bar{\beta})}[\exp(-\Delta\beta(c'(\bar{\beta}) - V)/2)]_{\Delta\beta=0} &= -\frac{1}{2}\mathbb{E}^{(\bar{\beta})}[c'(\bar{\beta}) - V] \\ \frac{d^2}{d\Delta\beta^2}\mathbb{E}^{(\bar{\beta})}[\exp(-\Delta\beta(c'(\bar{\beta}) - V)/2)]_{\Delta\beta=0} &= \frac{1}{4}\mathbb{E}^{(\bar{\beta})}[(c'(\bar{\beta}) - V)^2],\end{aligned}$$

while the denominator for the downward jump yields

$$\begin{aligned}\frac{d}{d\Delta\beta}\mathbb{E}^{(\bar{\beta})}[\exp(\Delta\beta(c'(\bar{\beta}) - V)/2)]_{\Delta\beta=0} &= \frac{1}{2}\mathbb{E}^{(\bar{\beta})}[c'(\bar{\beta}) - V] \\ \frac{d^2}{d\Delta\beta^2}\mathbb{E}^{(\bar{\beta})}[\exp(\Delta\beta(c'(\bar{\beta}) - V)/2)]_{\Delta\beta=0} &= \frac{1}{4}\mathbb{E}^{(\bar{\beta})}[(c'(\bar{\beta}) - V)^2].\end{aligned}$$

Since the second derivatives match for numerators and denominators on both expressions in Eq. (39), we can now apply Lemma C.16. The upward jump probability can be expanded as

$$\begin{aligned}\alpha_{\beta,\beta'} &= 1 - \frac{1}{2}\mathbb{E}^{(\bar{\beta})}[|c'(\bar{\beta}) - V| - (c'(\bar{\beta}) - V)]\Delta\beta \\ &\quad - \frac{1}{4}\mathbb{E}^{(\bar{\beta})}[c'(\bar{\beta}) - V]\mathbb{E}^{(\bar{\beta})}[|c'(\bar{\beta}) - V| - (c'(\bar{\beta}) - V)]\Delta\beta^2 + O(\Delta\beta^3) \\ &= 1 - \mathbb{E}^{(\bar{\beta})}[\max\{0, V - c'(\bar{\beta})\}]\Delta\beta \\ &\quad + \frac{1}{2}\mathbb{E}^{(\bar{\beta})}[V - c'(\bar{\beta})]\mathbb{E}^{(\bar{\beta})}[\max\{0, V - c'(\bar{\beta})\}]\Delta\beta^2 + o(\Delta\beta^2).\end{aligned}$$

The downward jump probability can be similarly expanded as

$$\begin{aligned}\alpha_{\beta',\beta} &= 1 - \frac{1}{2}\mathbb{E}^{(\bar{\beta})}[|c'(\bar{\beta}) - V| + (c'(\bar{\beta}) - V)]\Delta\beta \\ &\quad + \frac{1}{4}\mathbb{E}^{(\bar{\beta})}[c'(\bar{\beta}) - V]\mathbb{E}^{(\bar{\beta})}[|c'(\bar{\beta}) - V| + (c'(\bar{\beta}) - V)]\Delta\beta^2 + o(\Delta\beta^2) \\ &= 1 + \mathbb{E}^{(\bar{\beta})}[\min\{0, V - c'(\bar{\beta})\}]\Delta\beta \\ &\quad + \frac{1}{2}\mathbb{E}^{(\bar{\beta})}[V - c'(\bar{\beta})]\mathbb{E}^{(\bar{\beta})}[\min\{0, V - c'(\bar{\beta})\}]\Delta\beta^2 + o(\Delta\beta^2).\end{aligned}$$

The expressions for the rejection probabilities then follow immediately. \square

Proof of Corollary 4.8. This is direct from Theorem 4.7, since

$$\begin{aligned}\frac{\rho_{\beta,\beta'}}{\Delta\beta} &= \mathbb{E}^{(\bar{\beta})}[\max\{0, V - c'(\bar{\beta})\}] + O(\Delta\beta) \\ \frac{\rho_{\beta',\beta}}{\Delta\beta} &= -\mathbb{E}^{(\bar{\beta})}[\min\{0, V - c'(\bar{\beta})\}] + O(\Delta\beta).\end{aligned}$$

Taking the limit $\Delta\beta \rightarrow 0$ gives the expressions for the directional rates, since $\beta = \bar{\beta} = \beta'$ in the limit. The expressions in Eqs. (17) and (16) can be obtained by applying the identities

$$\max\{0, v\} = \frac{v + |v|}{2}, \quad \min\{0, v\} = \frac{v - |v|}{2}.$$

□

Lemma C.17. *For all $\beta \in [0, 1]$,*

$$\mathbb{E}^{(\beta)}[|V - \mathbb{E}^{(\beta)}[V]|] \leq \mathbb{E}^{(\beta)}[|V - V'|] \leq 2\mathbb{E}^{(\beta)}[|V - \mathbb{E}^{(\beta)}[V]|].$$

Proof. Since $V' \stackrel{d}{=} V$, it holds that

$$\begin{aligned} \mathbb{E}^{(\beta)}[|V - \mathbb{E}^{(\beta)}[V]|] &= \int \pi^{(\beta)}(dv) \left| v - \int \pi^{(\beta)}(dv')v' \right| \\ &= \int \pi^{(\beta)}(dv) \left| \int \pi^{(\beta)}(dv')(v - v') \right| \\ &\leq \int \pi^{(\beta)}(dv) \int \pi^{(\beta)}(dv')|v - v'| \quad (\text{Triangle ineq.}) \\ &= \int \int \pi^{(\beta)}(dv)\pi^{(\beta)}(dv')|v - v'| \quad (\text{Fubini's}) \\ &= \mathbb{E}^{(\beta)}[|V - V'|]. \end{aligned}$$

On the other hand,

$$\begin{aligned} \mathbb{E}^{(\beta)}[|V - V'|] &= \mathbb{E}^{(\beta)}[|(V - \mathbb{E}^{(\beta)}[V]) - (V' - \mathbb{E}^{(\beta)}[V])|] \\ &\leq 2\mathbb{E}^{(\beta)}[|V - \mathbb{E}^{(\beta)}[V]|]. \end{aligned}$$

□

Lemma C.18. *Let $f : \mathbb{R} \rightarrow \mathbb{R}_+$ be a non-negative function such that $f(V)$ is integrable under both π_0 and π . Then, for all $\beta \in [0, 1]$,*

$$\mathcal{Z}(\beta)\mathbb{E}^{(\beta)}[f(V)] \leq \beta\mathcal{Z}(1)\mathbb{E}^{(1)}[f(V)] + (1 - \beta)\mathbb{E}^{(0)}[f(V)]. \quad (40)$$

Consequently, under Assumption 4.11,

- There exist constants $\mathcal{Z}_{min}, \mathcal{Z}_{max}$ such that for all $\beta \in [0, 1]$,

$$0 < \mathcal{Z}_{min} \leq \mathcal{Z}(\beta) \leq \mathcal{Z}_{max} < \infty.$$

- For $p \in [0, 2]$ and all $\beta \in [0, 1]$,

$$\mathbb{E}^{(\beta)}[|V|^p] \leq M_p := \frac{1}{\mathcal{Z}_{\min}} \max \left\{ \mathcal{Z}(1)\mathbb{E}^{(1)}[|V|^p], \mathbb{E}^{(0)}[|V|^p] \right\}.$$

Proof. Note that we can trivially write βV as a convex combination

$$\beta V = \beta V + (1 - \beta) \cdot 0.$$

And because $x \mapsto e^{-x}$ is convex,

$$e^{-\beta V} \leq \beta e^{-V} + (1 - \beta)$$

Hence,

$$\begin{aligned} \mathcal{Z}(\beta)\mathbb{E}^{(\beta)}[f(V)] &= \mathbb{E}^{(0)}[f(V)e^{-\beta V}] \\ &\leq \beta\mathbb{E}^{(0)}[f(V)e^{-V}] + (1 - \beta)\mathbb{E}^{(0)}[f(V)] \\ &= \beta\mathcal{Z}(1)\mathbb{E}^{(1)}[f(V)] + (1 - \beta)\mathbb{E}^{(0)}[f(V)]. \end{aligned}$$

We can now tackle the second set of statements. The existence of \mathcal{Z}_{\max} follows from Lemma C.9 and Eq. (40) with $f \equiv 1$. Let us now suppose Assumption 4.11 is in place. By the convexity of $x \mapsto e^{-\beta x}$,

$$\mathcal{Z}(\beta) = \mathbb{E}^{(0)}[e^{-\beta V}] \geq e^{-\beta\mathbb{E}^{(0)}[V]} \geq e^{-\mathbb{E}^{(0)}[V]\mathbf{1}_{\{\mathbb{E}^{(0)}[V]>0\}}} =: \mathcal{Z}_{\min} > 0.$$

Now, for $f_p(v) = |v|^p$ with $p \in [0, 2]$, Assumption 4.11 means f_p is integrable under both π_0 and π . Hence,

$$\begin{aligned} \mathbb{E}^{(\beta)}[|V|^p] &\leq \frac{1}{\mathcal{Z}(\beta)} \left(\beta\mathcal{Z}(1)\mathbb{E}^{(1)}[|V|^p] + (1 - \beta)\mathbb{E}^{(0)}[|V|^p] \right) \\ &\leq \frac{1}{\mathcal{Z}_{\min}} \left(\beta\mathcal{Z}(1)\mathbb{E}^{(1)}[|V|^p] + (1 - \beta)\mathbb{E}^{(0)}[|V|^p] \right) \\ &\leq \frac{1}{\mathcal{Z}_{\min}} \max \left\{ \mathcal{Z}(1)\mathbb{E}^{(1)}[|V|^p], \mathbb{E}^{(0)}[|V|^p] \right\}, \end{aligned}$$

as required. \square

Lemma C.19. *Under Assumptions 4.5, 4.6, 4.11 and 4.12, there exist functions b_1 and b_2 such that for any partition \mathcal{P} ,*

$$\left| \frac{\partial \rho_i}{\partial \Delta \beta}(\bar{\beta}_i, \Delta \beta_i) \right| \leq b_1(\|\mathcal{P}\|) \quad \left| \frac{\partial^2 \rho_i}{\partial \Delta \beta^2}(\bar{\beta}_i, \Delta \beta_i) \right| \leq b_2(\|\mathcal{P}\|)$$

uniformly on $i \in \{1, \dots, N\}$, and b_1, b_2 have finite limits for $\|\mathcal{P}\| \rightarrow 0$.

Proof. From the definition of $\bar{\rho}$ (Eq. (45)) follows that for $i \in \{1, 2\}$,

$$\left| \frac{\partial^i}{\partial \Delta \beta^i} \bar{\rho}_{\beta, \beta'} \right| \leq \frac{1}{2} \left(\left| \frac{\partial^i}{\partial \Delta \beta^i} \alpha_{\beta, \beta'} \right| + \left| \frac{\partial^i}{\partial \Delta \beta^i} \alpha_{\beta', \beta} \right| \right).$$

Thus, it suffices to bound both terms on the right. By symmetry, we can focus only on the ones for the forward jump. Now, recall from Lemma C.13 that the acceptance probabilities can be expressed as ratios of functions,

$$\alpha_{\beta, \beta'} = \frac{\mathbb{E}^{(\bar{\beta})}[\exp(-\Delta\beta|c'(\check{\beta}) - V|/2)]}{\mathbb{E}^{(\bar{\beta})}[\exp(-\Delta\beta(c'(\check{\beta}) - V)/2)]} = \frac{x(z)}{y(z)},$$

where, for clarity of exposition, we have written $z = \Delta\beta$ and made the dependence on $\bar{\beta}$ implicit. By Lemma C.16,

$$\frac{\partial \alpha_{\beta, \beta'}}{\partial \Delta \beta} = \frac{1}{y(z)^2} (y(z)x'(z) - x(z)y'(z)) \quad (41)$$

$$\frac{\partial^2 \alpha_{\beta, \beta'}}{\partial \Delta \beta^2} = \frac{1}{y(z)^3} (y(z)^2 x''(z) - y(z)(2x'(z)y'(z) + x(z)y''(z)) + 2x(z)y'(z)^2).$$

To prove that these derivatives are uniformly bounded, we will first show that the denominator $y(z)$ is uniformly bounded away from zero. Indeed, from Eq. (35) in Lemma C.13, we know that

$$\begin{aligned} y(z) &= \mathbb{E}^{(\bar{\beta})}[\exp(-\Delta\beta(c'(\check{\beta}) - V)/2)] = \frac{\mathcal{Z}(\bar{\beta} - \Delta\beta/2)}{\mathcal{Z}(\bar{\beta})} e^{-c'(\check{\beta})\Delta\beta/2} \quad (42) \\ &\geq \frac{\mathcal{Z}_{\min}}{\mathcal{Z}_{\max}} e^{-|c'(\check{\beta})|\Delta\beta/2} \\ &\geq \frac{\mathcal{Z}_{\min}}{\mathcal{Z}_{\max}} e^{-c_1 \|\mathcal{P}\|/2}, \end{aligned}$$

where the first bound follows from Lemma C.18, while the second uses Assumption 4.12 and the definition of $\|\mathcal{P}\|$.

To continue, note that the numerators on the right-hand side of Eq. (41) are, respectively, first and second order polynomials on the functions (x, y) and their derivatives (x', x'', y', y'') . Hence, we proceed by showing that the absolute value of each of these functions is uniformly bounded under the assumptions given. Indeed, note that

$$\begin{aligned} 0 < x(z) &= \mathbb{E}^{(\bar{\beta})}[\exp(-\Delta\beta|c'(\check{\beta}) - V|/2)] \\ &\leq \mathbb{E}^{(\bar{\beta})}[\exp(-\Delta\beta(c'(\check{\beta}) - V)/2)] \\ &= y(z) \\ &\leq \frac{\mathcal{Z}_{\max}}{\mathcal{Z}_{\min}} e^{c_1 \|\mathcal{P}\|/2}, \end{aligned}$$

where we used an argument similar to the one for Eq. (42). To continue with the derivatives, recall the expressions given by Lemma C.15

$$\begin{aligned} x'(z) &= -\frac{1}{2}\mathbb{E}^{(\bar{\beta})}[\exp(-\Delta\beta|\gamma(\Delta\beta) - V|/2)(|\gamma(\Delta\beta) - V| + \Delta\beta\gamma'(\Delta\beta) \operatorname{sgn}(\gamma(\Delta\beta) - V))] \\ y'(z) &= -\frac{1}{2}\mathbb{E}^{(\bar{\beta})}[\exp(-\Delta\beta(\gamma(\Delta\beta) - V)/2)(\gamma(\Delta\beta) - V + \Delta\beta\gamma'(\Delta\beta))], \end{aligned}$$

where $\gamma(\Delta\beta) := c'(\check{\beta}(\Delta\beta))$. Now,

$$\begin{aligned} |x'(z)| &\leq \frac{1}{2}\mathbb{E}^{(\bar{\beta})}[\exp(-\Delta\beta|\gamma(\Delta\beta) - V|/2)(|\gamma(\Delta\beta) - V| + \Delta\beta\gamma'(\Delta\beta) \operatorname{sgn}(\gamma(\Delta\beta) - V))] \\ &\leq \frac{1}{2}\mathbb{E}^{(\bar{\beta})}[\exp(-\Delta\beta(\gamma(\Delta\beta) - V)/2)(|\gamma(\Delta\beta) - V| + \Delta\beta\gamma'(\Delta\beta) \operatorname{sgn}(\gamma(\Delta\beta) - V))] \\ &\leq \frac{1}{2}\mathbb{E}^{(\bar{\beta})}[\exp(-\Delta\beta(\gamma(\Delta\beta) - V)/2)(|\gamma(\Delta\beta) - V| + \Delta\beta|\gamma'(\Delta\beta)|)]. \end{aligned}$$

Note that $|y'|$ admits the same bound,

$$\begin{aligned} |y'(z)| &\leq \frac{1}{2}\mathbb{E}^{(\bar{\beta})}[\exp(-\Delta\beta(\gamma(\Delta\beta) - V)/2)|\gamma(\Delta\beta) - V + \Delta\beta\gamma'(\Delta\beta)|] \\ &\leq \frac{1}{2}\mathbb{E}^{(\bar{\beta})}[\exp(-\Delta\beta(\gamma(\Delta\beta) - V)/2)(|\gamma(\Delta\beta) - V| + \Delta\beta|\gamma'(\Delta\beta)|)]. \end{aligned}$$

Moreover,

$$\begin{aligned} &\mathbb{E}^{(\bar{\beta})}[\exp(-\Delta\beta(\gamma(\Delta\beta) - V)/2)(|\gamma(\Delta\beta) - V| + \Delta\beta|\gamma'(\Delta\beta)|)] \quad (43) \\ &\leq (|\gamma(\Delta\beta)| + \Delta\beta|\gamma'(\Delta\beta)|)y(\Delta\beta) + \mathbb{E}^{(\bar{\beta})}[|V| \exp(-\Delta\beta(\gamma(\Delta\beta) - V)/2)] \\ &\leq (c_1 + c_2\|\mathcal{P}\|)\frac{\mathcal{Z}_{\max}}{\mathcal{Z}_{\min}}e^{c_1\|\mathcal{P}\|/2} + \mathbb{E}^{(\bar{\beta})}[|V| \exp(-\Delta\beta(\gamma(\Delta\beta) - V)/2)]. \end{aligned}$$

Before searching for a uniform bound for the second term on the right-hand side, let us show that $|x''|$ and $|y''|$ allow for a bound of the same form.

Indeed, from the expressions in Lemma C.15

$$\begin{aligned}
|x''(z)| &= \frac{1}{2} \left| \mathbb{E}^{(\bar{\beta})} [\exp(-\Delta\beta|\gamma(\Delta\beta) - V|/2) \operatorname{sgn}(\gamma(\Delta\beta) - V)(2\gamma'(\Delta\beta) + \Delta\beta\gamma''(\Delta\beta))] \right. \\
&\quad \left. + \frac{1}{4} \mathbb{E}^{(\bar{\beta})} [\exp(-\Delta\beta|\gamma(\Delta\beta) - V|/2)(|\gamma(\Delta\beta) - V| + \Delta\beta\gamma'(\Delta\beta) \operatorname{sgn}(\gamma(\Delta\beta) - V))^2] \right| \\
&\leq \frac{1}{2} (2|\gamma'(\Delta\beta)| + \Delta\beta|\gamma''(\Delta\beta)|) \mathbb{E}^{(\bar{\beta})} [\exp(-\Delta\beta|\gamma(\Delta\beta) - V|/2)] \\
&\quad + \frac{1}{2} \mathbb{E}^{(\bar{\beta})} [\exp(-\Delta\beta|\gamma(\Delta\beta) - V|/2)((\gamma(\Delta\beta) - V)^2 + \Delta\beta^2\gamma'(\Delta\beta)^2)] \\
&= \frac{1}{2} (2|\gamma'(\Delta\beta)| + \Delta\beta|\gamma''(\Delta\beta)| + \Delta\beta^2\gamma'(\Delta\beta)^2) \mathbb{E}^{(\bar{\beta})} [\exp(-\Delta\beta|\gamma(\Delta\beta) - V|/2)] \\
&\quad + \frac{1}{2} \mathbb{E}^{(\bar{\beta})} [\exp(-\Delta\beta|\gamma(\Delta\beta) - V|/2)(\gamma(\Delta\beta) - V)^2] \\
&\leq \frac{1}{2} (2|\gamma'(\Delta\beta)| + \Delta\beta|\gamma''(\Delta\beta)| + \Delta\beta^2\gamma'(\Delta\beta)^2) \mathbb{E}^{(\bar{\beta})} [\exp(-\Delta\beta(\gamma(\Delta\beta) - V)/2)] \\
&\quad + \frac{1}{2} \mathbb{E}^{(\bar{\beta})} [\exp(-\Delta\beta(\gamma(\Delta\beta) - V)/2)(\gamma(\Delta\beta) - V)^2].
\end{aligned}$$

Similarly,

$$\begin{aligned}
|y''(z)| &\leq \frac{1}{2} (2|\gamma'(\Delta\beta)| + \Delta\beta|\gamma''(\Delta\beta)|) \mathbb{E}^{(\bar{\beta})} [\exp(-\Delta\beta(\gamma(\Delta\beta) - V)/2)] \quad (44) \\
&\quad + \frac{1}{4} \mathbb{E}^{(\bar{\beta})} [\exp(-\Delta\beta(\gamma(\Delta\beta) - V)/2)(\gamma(\Delta\beta) - V + \Delta\beta\gamma'(\Delta\beta))^2] \\
&\leq \frac{1}{2} (2|\gamma'(\Delta\beta)| + \Delta\beta|\gamma''(\Delta\beta)| + \Delta\beta^2\gamma'(\Delta\beta)^2) \mathbb{E}^{(\bar{\beta})} [\exp(-\Delta\beta(\gamma(\Delta\beta) - V)/2)] \\
&\quad + \frac{1}{2} \mathbb{E}^{(\bar{\beta})} [\exp(-\Delta\beta(\gamma(\Delta\beta) - V)/2)(\gamma(\Delta\beta) - V)^2] \\
&\leq \frac{1}{2} (2|\gamma'(\Delta\beta)| + \Delta\beta|\gamma''(\Delta\beta)| + \Delta\beta^2\gamma'(\Delta\beta)^2 + 2\gamma(\Delta\beta)^2) \mathbb{E}^{(\bar{\beta})} [\exp(-\Delta\beta(\gamma(\Delta\beta) - V)/2)] \\
&\quad + \mathbb{E}^{(\bar{\beta})} [V^2 \exp(-\Delta\beta(\gamma(\Delta\beta) - V)/2)].
\end{aligned}$$

Thus, both functions admit the same bound. Furthermore,

$$\begin{aligned}
&(2|\gamma'(\Delta\beta)| + \Delta\beta|\gamma''(\Delta\beta)| + \Delta\beta^2\gamma'(\Delta\beta)^2 + 2\gamma(\Delta\beta)^2) \mathbb{E}^{(\bar{\beta})} [\exp(-\Delta\beta(\gamma(\Delta\beta) - V)/2)] \\
&\leq (2c_2 + \|\mathcal{P}\|c_3 + \|\mathcal{P}\|^2[c_2^2 + 2c_1^2]) \frac{Z_{\max}}{Z_{\min}} e^{c_1\|\mathcal{P}\|/2}.
\end{aligned}$$

It remains to bound the second term on the right-hand sides of Eqs. (43)

and (44). Note that for $p \geq 0$,

$$\begin{aligned} & \mathbb{E}^{(\bar{\beta})}[|V|^p \exp(-\Delta\beta(\gamma(\Delta\beta) - V)/2)] \\ &= \frac{e^{\Delta\beta\gamma(\Delta\beta)/2} \mathcal{Z}(\bar{\beta} - \Delta\beta/2)}{\mathcal{Z}(\bar{\beta})} \mathbb{E}^{(\bar{\beta} - \Delta\beta/2)}[|V|^p] \\ &\leq \frac{\mathcal{Z}_{\max}}{\mathcal{Z}_{\min}} e^{c_1 \|\mathcal{P}\|/2} M_p. \end{aligned}$$

where M_p is the uniform p -moment bound from Lemma C.18. We conclude by noting that all the bounds have finite limits for $\|\mathcal{P}\| \rightarrow 0$, as required. \square

Proof of Proposition 4.13. Let us begin by showing that

$$\lim_{\|\mathcal{P}\| \rightarrow 0} \sum_{i=1}^{\ell(\beta)} \rho_i = \Lambda(\beta).$$

To this end, let us extend the definition of symmetrized rejection probability ρ_i to arbitrary pairs $\beta < \beta'$ via

$$\bar{\rho}_{\beta, \beta'} := 1 - \frac{\alpha_{\beta, \beta'} + \alpha_{\beta', \beta}}{2}, \quad (45)$$

so that $\rho_i = \bar{\rho}_{\beta_{i-1}, \beta_i}$ for all $i \in \{1, \dots, N\}$. Now, consider a first-order Taylor expansion of $\bar{\rho}_{\beta, \beta'}$ around $\Delta\beta = 0$ and fixed $\bar{\beta} = (\beta + \beta')/2$, with Lagrange remainder

$$\bar{\rho}_{\beta, \beta'} = \rho'(\bar{\beta})\Delta\beta + \frac{1}{2} \frac{\partial^2 \bar{\rho}_{\beta, \beta'}}{\partial \Delta\beta^2}(z)\Delta\beta^2,$$

for some $z \in [0, \Delta\beta]$ and all $\Delta\beta \leq r(\bar{\beta})$, with $r(\bar{\beta})$ as in Eq. (36). Let us write $\bar{\beta}_i := (\beta_{i-1} + \beta_i)/2$ and $\Delta\beta_i := \beta_i - \beta_{i-1}$. Since $\beta_i \in [0, 1]$, we see that

$$\Delta\beta_i = \beta_i - \beta_{i-1} = 2\bar{\beta}_i - 2\beta_{i-1} \leq 2\bar{\beta}_i,$$

and

$$\Delta\beta_i = 2(\beta_i - \bar{\beta}_i) \leq 2(1 - \bar{\beta}_i).$$

So the restriction $\Delta\beta_i \leq r(\bar{\beta}_i)$ is satisfied for all $i \in \{1, \dots, N\}$ and for any partition $\mathcal{P} \subset [0, 1]$. Hence,

$$\rho_i = \rho'(\bar{\beta}_i)\Delta\beta_i + \frac{1}{2} \frac{\partial^2 \bar{\rho}_{\beta, \beta'}}{\partial \Delta\beta^2}(z_i)\Delta\beta_i^2.$$

for some $z_i \in [0, \Delta\beta_i]$. Summing these expansions over $i \in \{1, \dots, \ell(\beta)\}$ yields

$$\sum_{i=1}^{\ell(\beta)} \rho_i = \sum_{i=1}^{\ell(\beta)} \rho'(\bar{\beta}_i) \Delta\beta_i + \frac{1}{2} \sum_{i=1}^{\ell(\beta)} \frac{\partial^2 \bar{\rho}_{\beta, \beta'}}{\partial \Delta\beta^2}(z_i) \Delta\beta_i^2$$

The first term on the right-hand side is a Riemann sum that converges to $\Lambda(\beta)$. We must show that the second sum vanishes in the limit. Indeed, by Lemma C.19,

$$\left| \sum_{i=1}^{\ell(\beta)} \frac{\partial^2 \bar{\rho}_{\beta, \beta'}}{\partial \Delta\beta^2}(z_i) \Delta\beta_i^2 \right| \leq b_2(\|\mathcal{P}\|) \sum_{i=1}^{\ell(\beta)} \Delta\beta_i^2 \leq b_2(\|\mathcal{P}\|) \|\mathcal{P}\| \sum_{i=1}^{\ell(\beta)} \Delta\beta_i \leq b_2(\|\mathcal{P}\|) \|\mathcal{P}\| \beta,$$

and the right-hand side goes to 0 as $\|\mathcal{P}\| \rightarrow 0$.

We now turn to proving that

$$\lim_{\|\mathcal{P}\| \rightarrow 0} \sum_{i=1}^{\ell(\beta)} \frac{\rho_i}{\alpha_i} = \lim_{\|\mathcal{P}\| \rightarrow 0} \sum_{i=1}^{\ell(\beta)} \frac{\rho_i}{1 - \rho_i} = \Lambda(\beta).$$

To this end, consider the function

$$f(z) = \frac{x(z)}{1 - x(z)}.$$

Its first and second derivatives are

$$f'(z) = \frac{x'(z)}{(1 - x(z))^2}$$

and

$$f''(z) = \frac{x''(z)}{(1 - x(z))^2} + 2 \frac{(x'(z))^2}{(1 - x(z))^3}.$$

We want to use these expressions with $z \leftarrow \Delta\beta$ and $x(z) \leftarrow \bar{\rho}_{\beta, \beta'}$. Note that if we can bound uniformly (on i) the second derivative $f''(\Delta\beta)$, then the same proof technique used for the first series yields the result. Indeed, ρ_i and $\rho_i/(1 - \rho_i)$ are first-order identical, since $f(0) = 0$ and $f'(0) = \rho'(\bar{\beta})$. Now, recall that

$$\bar{\rho}_{\beta, \beta'} = \rho'(\bar{\beta}) \Delta\beta + \frac{1}{2} \frac{\partial^2 \bar{\rho}_{\beta, \beta'}}{\partial \Delta\beta^2}(z) \Delta\beta^2.$$

Since $\rho'(\bar{\beta}) = \frac{\partial \bar{\rho}_{\beta, \beta'}}{\partial \Delta \beta}(0)$, Lemma C.19 shows that both derivatives in the above display are uniformly bounded. Hence, $\bar{\rho}_{\beta, \beta'} = O(\|\mathcal{P}\|)$. And since we are concerned with the limit $\|\mathcal{P}\| \rightarrow 0$, for any $\varepsilon \in (0, 1)$, we may only consider fine enough partitions \mathcal{P} such that $\rho_i \leq \varepsilon$ for all $i \in \{1, \dots, N\}$. Under this scenario, we have

$$|f''(\Delta\beta)| \leq \frac{\left| \frac{\partial^2 \bar{\rho}_{\beta, \beta'}}{\partial \Delta \beta^2} \right|}{(1-\varepsilon)^2} + 2 \frac{\left(\frac{\partial \bar{\rho}_{\beta, \beta'}}{\partial \Delta \beta} \right)^2}{(1-\varepsilon)^3}.$$

Again, the two derivatives appearing in the right-hand side are uniformly bounded by Lemma C.19, which concludes the proof. \square

C.5 Proofs for Section 5

Lemma C.20. *For convex $f : \mathbb{R} \rightarrow \mathbb{R}$ and $c \in \mathbb{R}$, the optimization problem*

$$\min_{x \in \mathbb{R}^N} \sum_{i=1}^N f(x_i) \quad \text{s.t.} \quad \sum_{i=1}^N x_i = c$$

has a unique solution given by $x_i^ = \frac{c}{N}$ for all $i \in \{1, \dots, N\}$.*

Proof. By Jensen's inequality,

$$\sum_{i=1}^N f(x_i) = N \frac{1}{N} \sum_{i=1}^N f(x_i) \geq N f\left(\frac{1}{N} \sum_{i=1}^N x_i\right) = N f\left(\frac{c}{N}\right),$$

and the bound on the right-hand side is achieved whenever $x_i^* = \frac{c}{N}$ for all $i \in \{1, \dots, N\}$. \square

Lemma C.21. *Let $\alpha, \beta, \gamma \in \mathbb{R}$ such that $\alpha \leq \gamma$ and $\beta \leq \gamma$. Consider the function $\psi : [\gamma, \infty) \rightarrow (0, \infty)$ given by*

$$\psi(t) := \frac{t - \gamma}{(t - \alpha)(t - \beta)}.$$

Then ψ has a unique maximizer at

$$t^* := \gamma + \sqrt{(\gamma - \alpha)(\gamma - \beta)}.$$

Proof. Consider the change of variable

$$t(s) := \gamma + e^s \sqrt{(\gamma - \alpha)(\gamma - \beta)}.$$

Then,

$$\begin{aligned}
\psi(t(s)) &= \frac{e^s \sqrt{(\gamma - \alpha)(\gamma - \beta)}}{(\gamma - \alpha)(\gamma - \beta) + e^{2s}(\gamma - \alpha)(\gamma - \beta) + e^s(\gamma - \alpha + \gamma - \beta)\sqrt{(\gamma - \alpha)(\gamma - \beta)}} \\
&= \frac{1}{e^{-s} \sqrt{(\gamma - \alpha)(\gamma - \beta)} + e^s \sqrt{(\gamma - \alpha)(\gamma - \beta)} + (2\gamma - \alpha - \beta)} \\
&= \frac{1}{2 \cosh(s) \sqrt{(\gamma - \alpha)(\gamma - \beta)} + (2\gamma - \alpha - \beta)} \\
&= \phi(\cosh(s)),
\end{aligned}$$

where

$$\phi(u) := \frac{1}{2u \sqrt{(\gamma - \alpha)(\gamma - \beta)} + (2\gamma - \alpha - \beta)}$$

is strictly decreasing. It follows that $\psi(t(s))$ is maximized when $\cosh(s)$ is minimized; i.e., for $s^* = 0$. Translating this back to the original scale gives

$$t^* = \gamma + \sqrt{(\gamma - \alpha)(\gamma - \beta)},$$

as required. \square

Lemma C.22. *Let $\Lambda > 0$. The function $F : (\Lambda, \infty) \rightarrow \mathbb{R}_+$ given by*

$$F(t) = \frac{t - \Lambda}{(t + 1)(t(1 + 2\Lambda) - \Lambda)},$$

has a unique maximizer

$$t^* = \Lambda \left(1 + \sqrt{1 + \frac{1}{1 + 2\Lambda}} \right).$$

Proof. Note that

$$F(t) = \frac{1}{1 + 2\Lambda} \left(\frac{t - \Lambda}{(t + 1)(t - \frac{\Lambda}{1 + 2\Lambda})} \right).$$

Therefore, we can apply Lemma C.21 with $\gamma := \Lambda$, $\alpha := -1 < \gamma$, and $\beta := \frac{\Lambda}{1 + 2\Lambda} < \gamma$ to obtain

$$t^* = \Lambda + \sqrt{(\Lambda + 1) \left(\Lambda - \frac{\Lambda}{1 + 2\Lambda} \right)} = \Lambda \left(1 + \sqrt{1 + \frac{1}{1 + 2\Lambda}} \right),$$

as required. \square